# Investigation of *cpeb1* transcript regulation and potential functions of CPEB1 in germline development in *X. laevis*

Doctoral Thesis

Dissertation for the award of the degree

"Doctor of Philosophy"

in the GGNB Program Molecular Biology

at the Georg-August-University Göttingen

**submitted by**

**Anita Smarandache**

**born in Craiova, Romania**

Göttingen, 2016

**Thesis Committee Members**

Prof. Dr. Tomas Pieler (Reviewer and Thesis Supervisor)

Department of Developmental Biochemistry, University Medical Center, Georg-August-University Göttingen

PD Dr. Halyna Shcherbata (reviewer)

Gene Expression and Signaling, Max Planck Institute for Biophysical Chemistry Göttingen

Prof. Dr. Michael Kessel

Developmental Biology, Max Planck Institute for Biophysical Chemistry Göttingen

**Members of the Extended Examination Board**

Prof. Dr. Matthias Dobbelstein

Institute for Molecular Oncology, University Medical Center, Georg-August-University, Göttingen

Prof. Dr. Gregor Bucher

Department of Evolutionary Developmental Genetics, Georg-August-University, Göttingen

Prof. Dr. Ahmed Mansouri

Molecular Developmental Genetics, Max Planck Institute for Biophysical Chemistry, Göttingen

Prof. Dr. Markus Bohnsack

Institute for Molecular Oncology, University Medical Center, Georg-August-University, Göttingen

**Date of the oral examination: 16th November 2016**

**Affidavit**

Herewith I declare that I prepared the Doctoral thesis

“Investigation of *cpeb1* transcript regulation and potential functions of CPEB1 in germline development in *X. laevis*”

on my own and with no other sources and aids than quoted.

Anita Smarandache

Göttingen, September 30th, 2016

# Table of Contents

## ACKNOWLEDGMENTS

I am deeply grateful to Professor Pieler for offering me careful guidance, constant support and the opportunity to work in a stimulating scientific environment.

I would like to acknowledge Maike Claussen for her supervision, patient guidance and constructive criticism during the planning and development of this project. I want to thank all lab and department members for creating a nice environment for fruitful and creative scientific discussion, and I want to especially acknowledge the constant help and advice from Julianne Pfennig, Diana Obermann, Aliaksandr Dzementsei and Julianne Melchert, Marion Dornwell and Katja Ditter. Assistance provided by Tomas Lügner and Prof. Olaf Jahn was valuable for the analysis of mass-spectrometry data. Excellent technical assistance was provided by Marion Dornwell and Katja Ditter, with whom I have tied close friendships in the course of this project.

Warm thanks to Kerstin Güninger and Steffen Burckhardt for around the clock availability and help.

I would like to thank the Dorothea Schlözer Program and the Ph.D. program Molecular Biology International Max Planck Research School at the Georg August University Göttingen for the financial support provided for the entire length of the project.

Last but not least, profound gratitude goes to my family and friends for offering me support, patience and love in good and bad times.

**ABSTRACT**

Germline specification represents the first functional segregation between two cell populations in the embryo. The germ cell lineage is the source of genetic variation and is essential for the continuity of the species. In *X. laevis*, primordial germ cells (PGCs) inherit distinct maternal determinants present in the germ plasm. They are required for the specification and maintenance of germline identity during early embryogenesis. Intriguingly, during the maternal to zygotic transition, which represents the most profound change in the life of an embryo as the maternally contributed factors are cleared and the zygotic genome is activated, transcripts provided in the germplasm are efficiently depleted in the soma, nevertheless circumvent degradation in the germline. In a genome-wide RNA sequencing analysis performed in our lab to determine the overlap and the distinctions between the transcript pools of primordial germ cells with their somatic neighbors, *cpeb1* was identified as germline specific. *Cpeb1* transcripts are depleted at MZT, yet upon inhibition of miRNA maturation, *cpeb1* mRNA levels increase substantially in gastrulating embryos. Therefore, somatic degradation of *cpeb1* probably occurs via miRNA-mediated decay, a key player during MZT.

In the present study I addressed the mechanisms regulating the restriction of *cpeb1* transcripts to PGCs and the potential role the encoded protein could exert in the formation of the germline. Initially, I identified a minimal regulatory region in the *cpeb1* 3'UTR by analyzing the distribution of exogenous chimeric reporter constructs in the germline and surrounding somatic tissues. By using two complementary approaches for identifying miRNA-mRNA pairs I attempted to determine which miRNAs are responsible for the depletion of *cpeb1*. The results suggest that a 25bp region in the proximal 3'UTR sequence is involved in transcript regulation. Nevertheless, the identity of the miRNAs remains to be determined. CPEB1 is involved in oocyte maturation by regulating the timing and extent of translation for bound transcripts, a mechanism described in minute detail. Nonetheless, little is known about what role CPEB1 could play in germline development. To address this, I overexpressed dominant negative mutants lacking the N-terminus and flag-tagged CPEB1, which lead to a decrease in germ cell numbers. To determine how this effect is induced, I identified candidate interaction partners by mass spectrometry analysis. The functional diversity of potential interactions suggests that CPEB1 may be involved in a complex array of cellular processes.

## 1. INTRODUCTION

The continuity of the species relies on the segregation of a small, specialized population of cells that have a differentiation program that preserves the capacity for totipotency, the primordial germ cells. Therefore, addressing how distinctions between somatic and germ cells are initiated and maintained and understanding the mechanisms of germline formation as well as the factors involved in this process is of notable significance for understanding development.

### 1.1 GERM CELL SPECIFICATION

Primordial germ cells (PGCs) together with somatic cells form the gonads. PGCs are precursors to the highly specialized gametes (spermatozoa and ova) which upon fusion form the zygote capable of generating an entire new organism. Gametes are set aside from somatic tissues early during development (Seydoux and Braun, 2006; Johnson and Alberio, 2015). During evolution at least two modes of germline segregation have emerged, with epigenesis and preformation being the best described (Extavour and Akam, 2003; Seydoux and Braun, 2006). Possibly ancestral and most widespread across metazoa including mammals, epigenesis describes the mechanism of *de novo* germ cell formation in response to inductive signals from neighboring tissues. Preformation is conserved in the several model organisms studied in developmental biology, such as *C. elegans*, *D. melanogaster*, *D. rerio* and *X. laevis*. A small population of germline cells emerges following the inheritance of germ plasm composed of localized maternally derived determinants (Extavour and Akam, 2003; Swartz and Wessel, 2015).

Regardless of the specification mechanism, in many organisms migration to the future gonad is an essential aspect of the germline lifecycle (Molyneaux and Wylie, 2004; Richardson and Lehmann, 2010). Primordial germ cells have to maintain their undifferentiated state also during the migratory phase to prevent converting to a somatic cell fate. Notably, several processes contributing to germline identity preservation are conserved (Seydoux and Brown, 2006). An important role in germline development is held by transcriptional silencing. Generally, it occurs by blocking the transcriptional elongation step due to a lack of phosphorylation of Serine 2 on the C-terminal domain (CTD) of RNA polymerase II (Seydoux and Brown, 2006; Nakamura and Seydoux, 2008; Lai and King 2013). Epigenetic regulation also contributes to specific transcriptional silencing by chromatin modification (Surani et al., 2007; Cinalli et al., 2008). In addition to transcriptional regulation, the repression of somatic gene expression in the germline falls under the control of translational regulation for exact temporal and spatial gene expression (Seydoux and Brown, 2006; Sengupta and Boang, 2012). For example in *Drosophila*, pole cell formation is

dependent on *hunchback* repression at the posterior pole, mediated by a ternary complex composed of Pumilio, Nanos and Brat that prevents initiation by disrupting the closed loop structure essential for translation (Lai and King 2013; Marlow, 2015). A regulatory mechanism that makes use of miRNAs for post-transcriptional regulation is essential for somatic depletion of transcripts that become germline specific (Koebernick et al., 2010; Yamaguchi et al., 2014; Yartseva and Giraldez 2015).

## 1.2. GERM CELL DEVELOPMENT IN *X. LAEVIS*

The vertebrate model organism *X. laevis* is extensively used in developmental biology and molecular biology. There are various advantages the *X. laevis* system provides, namely the availability of large numbers of externally developing embryos that provide substantial quantities of material for biochemical analyses (Pearl et al., 2012). Furthermore, the large size of the oocytes and eggs facilitate embryo manipulations such as microinjection. Thereby this organism is a suitable system for monitoring gene activity, mRNA localization and translational regulation (Dawid and Sargent, 1988; Yasuo and Lemaire, 2001; Pearl et al., 2012). Investigations in *X. laevis* have brought major contributions to the study of oocyte maturation, germ layer determination, germline segregation and morphogenesis (Heasman et al., 1984; Dawid and Sargent, 1988; Yasuo and Lemaire, 2001; Pearl et al., 2012).

### 1.2.1 THE IMPORTANCE OF VEGETAL TRANSCRIPT LOCALIZATION FOR GERMLINE DEVELOPMENT

In *X. laevis* the stage is set for germline segregation and germ layer formation from the very beginning of oogenesis (Mowry and Cote, 1999). In the course of six stages spanning several months, the *Xenopus* oocyte grows and matures, preparing for fertilization and coordination of early development (Heasman et al., 1984). It becomes a polarized structure as early as the first stage of oogenesis as a set of factors important for germline development form a distinct membrane free organelle at one side of the germinal vesicle, the Balbiani body (Billet and Adam, 1976; Heasman et al., 1984; Mowry and Cote, 1999; Kloc et al., 2014). Also referred to as the mitochondrial cloud (MC), it is composed of clusters of mitochondria, specific transcripts, proteins and unique electron dense organelles termed germinal granules embedded in a fibrillar matrix (Heasman et al., 1984). During stages I-II of oogenesis it translocates to the future vegetal side, where it is anchored to the most distal cortical region, defining the first coordinate for polarity (Kloc and Etkin, 1995). The heterogeneity of the oocyte is further built upon during the following stages of oogenesis, characterized by localized storage of mRNAs and proteins, both maternally provided and produced in the oocyte. An illustrative example is that of yolk platelets, which

predominantly occupy the vegetal hemisphere, their size and volume decreasing towards the animal hemisphere, which also harbours the nucleus (Mowry and Cote 1999).

The asymmetry occurring at a macromolecular level is recapitulated at the molecular level, playing an essential role specifying the reference axes regulating early maternally driven development (Mowry and Cote, 1999). Differential transcript distribution relies on two main mechanisms active at sequential oogenesis stages, the early METRO (**me**ssenger **tr**ansport **o**rganizer) pathway and the late transport pathways (Kloc and Etkin, 1995; Zhou and King 1996; Choo et al., 2005; Claussen et al., 2004; Wilk et al., 2005).

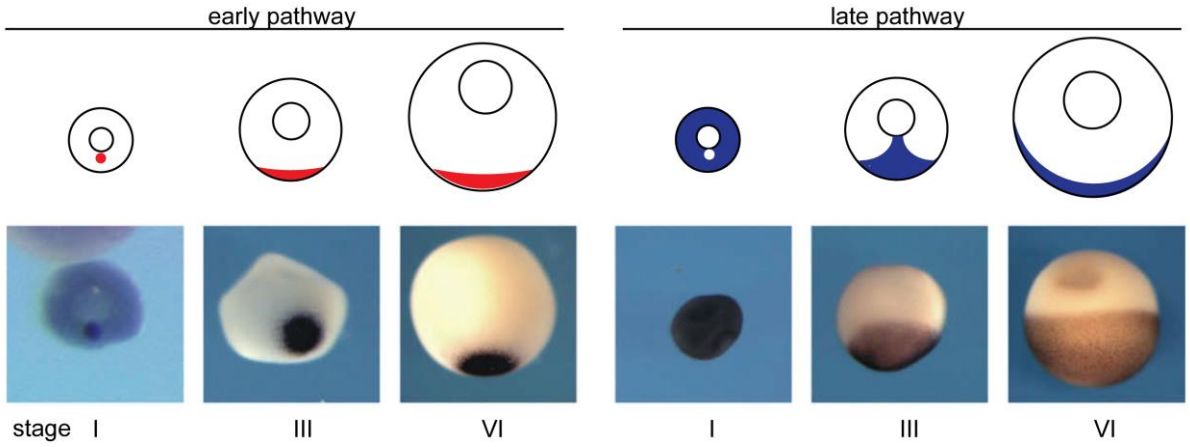


**Figure 1.1 Localization to the vegetal cortex during *X. laevis* oogenesis is mediated by two main pathways, the early and late pathways. Endogenous *pgat* and *gdf1* are detected by w**hole mount *in situ* hybridization at the indicated stages of development. A schematic representation of the two pathways is depicted above. Early localizing transcripts such as *pgat* are associated with the mitochondrial cloud (MC) in stage I oocytes and after the disassembly of the MC they become localized at the vegetal cortex where they remain until the end of oogenesis (VI-VI). Late pathway mRNAs such as *gdf1* are distributed throughout the cytoplasm of stage I oocytes. At the end of stage II/beginning of stage III they are localized in a wedge shaped region below the oocyte nucleus and start to accumulate at the vegetal cortex, which they cover by the end of oogenesis (VI). From Claußen and Pieler, 2010.

The early pathway is active at stages I-II and is responsible for anchoring the MC together with specific germ plasm determinants, such as *Xlsirts*, *nanos1* (formerly *xcat2*), *dazl*, *pgat*, *ddx25* (known as *XDead South*), at the tip of the vegetal cortex (Kloc and Etkin, 1995; Kloc et al., 1998; Mowry and Cote, 1999; Claussen et al., 2004; Zhou and King, 2004; Cuykendall and Houston 2010; Kloc et al., 2014).

The late pathway operates only after MC anchorage and relies on the cytoskeleton for directional, motor–driven transport of germ layer determinants like *gdf1* (known as vg1), *vegt*, *tgfb* and *bicc1* (known as *XBic-C*) to the vegetal cortex (Kloc and Etkin, 1995; Mowry and Cote, 1999; Claussen et al., 2004). Experimental evidence supports the hypothesis that nucleation of transport RNPs

initiates in the nucleus and remodeling occurs after transport to the cytoplasm (Kress et al., 2004; Lewis et al., 2008; Bauermeister et al., 2014).

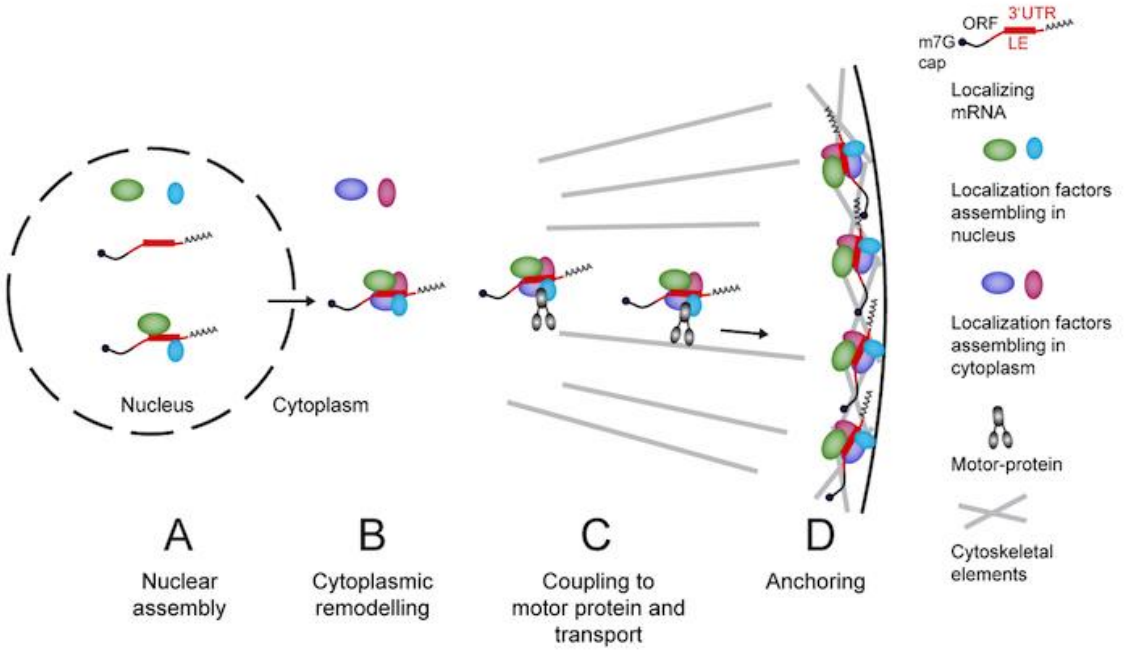


**Figure 1.2 Schematic view of sequential steps in motor-dependent mRNA localization.** A. Initiation of mRNA localization depends on the interaction between nuclear localization factors with the RNA localization element in the nucleus. B. After cytoplasmic export, RNPs are remodeled and cytoplasmic localization factors join the complex. C. Localization RNPs associate with motor proteins and are actively transported along cytoskeletal elements. D. Localization RNPs are anchored at their final destination. From Bauermeister et al., 2014.

For instance, the *gdf1* and *vegt* transcripts are bound in the nucleus by transport complex proteins, such as Igf2bp3 and Ptbp1 (Kress et al., 2004). After export to the cytosol additional factors such as Stau1 and Prrp, two proteins with important roles in vegetal RNA localization, associate with the already existing RNP (Kress et al., 2004; Cote et al., 1999). Consequently, the late localized mRNAs occupy a distinct and broader area overlapping with that of the germ plasm (Claussen et al., 2004). As a consequence, the vegetal pole becomes the anlage for determinants required for germ layer and germline specification (Kloc and Etkin, 1995; Zhou and King 2004). Therefore, subcellular localization is a key posttranscriptional regulatory mechanism for establishing regional cellular fates essential for normal embryonic development.

### 1.2.2 GERM CELL SEGREGATION DURING EARLY EMBRYOGENESIS

Immature oocytes are loaded with an ensemble of factors required for early development, including those crucial for primordial germ cell segregation (Kloc and Etkin, 1995; Kloc et al., 1998;

Mowry and Cote, 1999; Claussen et al., 2004; Zhou and King, 2004; Kloc et al., 2014). Cytoplasmic germ plasm at this point in time is localized to the vegetal subcortex in small islets (Kloc and Etkin, 1995). Following fertilization they fuse end-to-end to form larger patches, decreasing the area of the egg occupied by germ plasm. As a result, four patches are distinguishable, one in each blastomere of a 4-cell stage embryo (Ressom and Dixon 1988; Taguchi et al., 2012). The distribution of germ plasm changes essentially due to three factors (1) a microtubule based mechanism that acts after egg activation results in coalescence of the islets; (2) cytoplasmic streaming is responsible for the ingression of germ plasm, positioning the patches towards the internal part of the cleavage furrows; (3) the mitotic spindle formed after fertilization maintains the germ plasm islands in position in the vegetal hemisphere (Ressom and Dixon 1988).

Interestingly, quantitative studies show that until blastula stage, only four cells inherit germline determinants (Taguchi et al., 2012). During initial cleavage cycles germ plasm is associated with only one of the spindle poles to effect asymmetric distribution to the daughter cells (Yamaguchi et al., 2013). Between gastrula and tailbud stages, germ cell numbers increase due to the relocation of the germ plasm to a perinuclear position so that during mitotic division it is distributed to both daughter cells (Whitington and Dixon, 1975) Taguchi et al., 2012; Yamaguchi et al., 2013).

Primordial germ cells are often specified in a location distant from the future gonads, creating a requirement for passive and/or active migration. This is the case in *Xenopus* as well, as germ-plasm bearing cells formed in the vegetal hemisphere will become PGCs (Cuykendall and Houston 2010; Kloc et al., 2014). During gastrulation involution collectively relocates germline and surrounding somatic cells to the prospective endoderm within the embryo (Whitington and Dixon 1975; Taguchi et al., 2012). At the end of gastrulation, between 4 and 7 PGCs lie in the floor of the archenteron (Whitington and Dixon 1975; Nishiumi et al., 2005). Early tailbud embryos contain clustered germ cells deep within the endoderm. From stage 24 onwards the migratory phase begins (Nishiumi et al., 2005; Dzementsei et al., 2013). Cells disperse and migrate individually within a cohort through the endodermal cell mass, first laterally then dorsally and anteriorly. By tailbud stage 33, PGCs are scattered mostly in the dorsal half, closer to the endodermal wall. They reach the dorsal crest around stage 38-39 at the top of the endoderm (Terayama et al., 2013). At subsequent stages, germ cells incorporate into the dorsal mesentery, translocate laterally, associate with somatic cells that will form the germinal cuboidal epithelium, and by stage 49 gonadal ridges are observed (Wylie and Heasman 1976; Wylie et al., 1976).

### 1.2.3 ESTABLISHED FUNDAMENTAL FACTORS FOR GERMLINE DEVELOPMENT

Generation of functional germ cells is dependent on the germ plasm. Tada and colleagues have shown that EGFP-labeled germ plasm transplantation into the endoderm of DsRed2 transgenic hosts resulted in functional PGCs capable of migrating to and populating germinal gonads, generating healthy progeny (Tada et al., 2012). This report among many others underscores the involvement of germ plasm in the formation of the germline (Smith, 1966; Buehr and Blackler, 1970; Wakahara, 1977; Wakahara, 1978).

Germ plasm is characterized by an abundance of mitochondria, electron dense germinal material and specific transcripts and proteins (Billet and Adam, 1976; Heasman et al., 1984; Mowry and Cote, 1999; Kloc et al., 2014). Its formation is thought to be dependent on Pgat, a protein with no conserved domains and a major component of the germ plasm. Exogenous Pgat is capable of aggregating mitochondria-rich structures similar to germ plasm islands (Machado et al., 2005). In early oogenesis and throughout the following oocyte stages its mRNA is strictly associated with the MC, whereas from early embryogenesis up to stage 40 the *pgat* mRNA (formerly known as *xpat*) is associated with the germ plasm. Additionally, localization to the MC requires the 3'UTR (Hudson and Woodland 1998).

Transcripts associated with the germ plasm are translationally silent indicating that post-transcriptional regulation is a fundamental mechanism for germline survival (Sengupta and Boang 2012). Many of the mRNAs localizing with the MC have been found to encode for RNA-binding proteins, such as Nanos1 (Xcat2) and Deleted in azoospermia-like (Dazl; Lai et al 2011; Houston and King 2000).

Nanos1 is an illustrative example of the interplay between different mechanisms that ensure the formation of the germline. Its depletion prevents germ cell migration from the endoderm, followed by apoptosis. The underlying cause seems to be precocious zygotic genome activation during gastrulation resulting from early phosphorylation of the C-terminal domain of RNA polymerase II (RNAPII; Lai et al., 2012; Lai and King 2013). Normally, RNAPII is transcriptionally blocked before the elongation step by a delay in Serine2 phosphorylation in the germline. Hence, somatic determinants partitioned to germ cells by chance, such as *vegt*, are silenced until the neurula stage (Venkatarama et al., 2010). In addition, *vegt* was shown to be a bona-fide target transcript of the Nanos1/Pumilio translational repressing complex, resulting in the suppression of endodermal VegT downstream gene expression, allowing completion of PGC segregation at gastrulation (Lai et al., 2012; Lai and King 2013).

The Dazl protein binds RNA and is essential for correct germline determination. It functions as a translational regulator of germ cell specific transcripts and cooperation between multiple Dazl proteins enhances translation (Collier et al., 2005; Martins et al., 2016). Moreover, it also has a role in the oocyte, where it binds *Ringo/Spy* mRNA as part of a repressing translational complex together with Pumilio2 and embryonic poly(A) binding protein (ePABP). During meiotic activation, Pumilio exits the complex and ePABP can recruit eIF4G to enhance translation (Collier et al., 2005; Houston and King 2000a).

*Dnd1* is the first example of a germ plasm specific transcript localized via the late transport pathway (Horvay et al., 2006). Localization requires the binding of transport proteins to an element in the 3'UTR termed the localization element (LE; Horvay et al., 2006). Intriguingly, the same element is targeted for somatic degradation via miR-18 targeted miRNA-mediated decay during the maternal-to-zygotic transition (Koebernick et al., 2010). Degradation of *dnd1* is counteracted in the germline by ElrB1, a component of the vegetal localization complex, as it is bound to the transcript together with the Dnd1 protein (Koebernick et al., 2010). The latter is a RNA binding protein shown to play a role in PGC development. Its knock-down leads to aberrant migration and a severe reduction in germ cell number at tadpole stage (Horvay et al., 2006).

Taken together, several mechanisms are responsible for specifying and maintaining the identity of the germline, localization, transcriptional and translational regulation and miRNA mediated degradation. Up to this point the known factors involved in how a certain population of cells acquires and maintains its identity were described. Therefore, it is time to focus on early embryonic development to define processes that are essential for both the germline and the somatic lineage.

## 1.3 INITIATING EMBRYONIC DEVELOPMENT

### 1.3.1 OOCYTE MATURATION

Immature oocytes are arrested in the first meiotic prophase. In *Xenopus*, oocyte maturation is triggered by progesterone, a canonical steroid hormone produced by follicular cells. The meiotic cell cycle is resumed and oocytes progress through the first meiotic division (meiosis I), extruding the first polar body. They then continue through the second meiotic cell division (meiosis II) up to metaphase II when they pause awaiting fertilization (Ferrell 1999).

At a molecular level, progesterone signaling leads to a reduction in cAMP, resulting in reducing the pool of active PKA (protein kinase A), which in turn inactivates Cdc25B phosphatase and

activates Wee1/Myt1 kinase, two cyclin-dependent-kinase 1 (CDK1/Cdc2) regulators. Consequently, the activated CDK1 associates with Cyclin B to form the maturation promoting factor (MPF). During maturation, MPF facilitates entry into meiosis I and germinal vesicle breakdown (GWBD). After first polar body extrusion, MPF levels drop and increase once more, being maintained high until fertilization by the action of cytostatic factor (CSF), a downstream factor of the Mos-MAPK pathway. Upon release from prophase I arrest, the Mos-MAPK pathway is activated through *de novo* protein synthesis and in turn enables new protein synthesis important for meiotic progression. Moreover, the Mos-MAPK pathway contributes to the proper organization of chromosomes on the mitotic spindles essential for the first meiotic cycle (Karaiskou et al., 2001; Sato 2014).

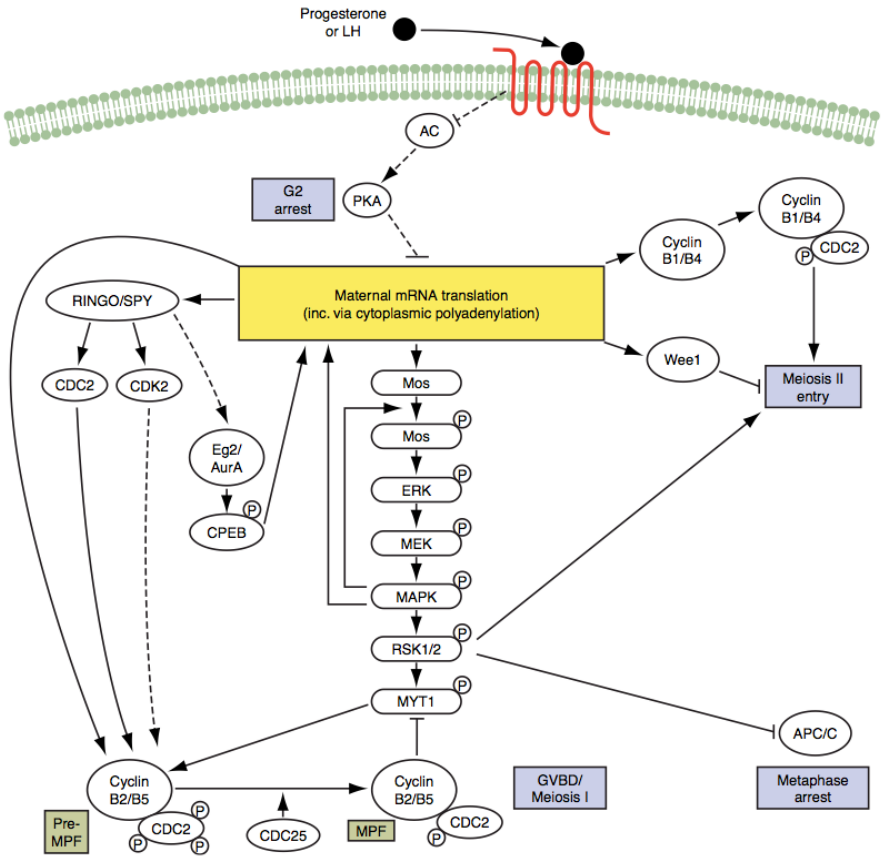


**Figure 1.3 Scheme major signaling and gene expression events regulating vertebrate oocyte maturation.** Exposure to hormones initiates cascades of kinase/phosphatase activity and translationally regulated gene expression. Progesterone in *X. laevis* (luteinizing hormone in mammals) signaling causes inhibition of adenylate cyclase (AC) activity and subsequent decline in cAMP levels, leading to a reduction in protein kinase A (PKA) levels. Consequently, in *X. laevis*, rapid inducer of G2/M progression in oocytes (RINGO)/speedy (SPY) mRNA translation is activated resulting in the activation of CDK2, AurkA and additional factors (not depicted). This results in translational upregulation of mRNAs encoding key meiotic factors, such as Mos, which promotes the MAPK pathway. Subsequently, a large subset of mRNAs is translationally activated, a process in which CPEB1 plays a major role. In *X. laevis*, Mos is necessary for the complete activation of MPF and cytostatic factor activity, both being required for maintaining meiosis II

metaphase arrest. AC: adenylate cyclase, APC: anaphase promoting complex; AurA: AuroraA; CF: cytostatic factor; CPEB: CPE-binding protein; GVDB: germinal vesicle breakdown; MAPK: mitogen activated protein kinase; MPF: maturation promoting factor; PKA: protein kinase A; RINGO/SPY: rapid inducer od G2/M progression in oocytes/speedy. Dotted arrows indicate events in which an as of yet unindentified factor may play a role. From Brook et al., 2009.

In the immature oocyte a large fraction of the maternal pool of transcripts is non-polysomal. Injection of mRNAs leads to their recruitment onto polysomes by proteins derived from rough endoplasmic reticulum indicating the potential of stored proteins to effect translation. In a seminal study, Richter and Smith have identified proteins that preferentially bind to messenger RNAs over other types of RNA (Richter and Smith 1983). In the initial phases of uncovering the mechanisms underlying oocyte maturation, it was discovered that cytoplasmic polyadenylation is required for meiotic progression. One of the first examples was that of *mos* entering translation only at maturation (Sagata et al., 1988). Following this discovery, efforts were made to discover what originates translational initiation during oocyte maturation. A *cis*-sequence element present in the 3'UTR of the *bud31* mRNA, which is recruited for translation at this time was discovered to be essential for polysomal recruitment. This is a U-rich element located 5' to the AAAUAA hexanucleotide required for end-processing of the transcript (McGrew et al., 1989; Fox et al., 1989). The sequence of this element, referred to as the "cytoplasmic-polyadenylation element" (CPE) was further characterized by identifying its sequence, with a consensus of UUUUUAU, and binding *trans*-element, the cytoplasmic polyadenylation binding protein (CPEB1; McGrew and Richter 1990; Hake and Richter 1994).

Later studies have shown that indeed cytoplasmic polyadenylation is involved in oocyte maturation, a revealing example being the CPE-dependent activation of *mos* and *cyclinB* translation (Hake and Richter 1994; Mendez et al., 2000a, 2000b). Cell cycle re-entry has been described to depend also on Musashi–directed and translation dependent activation of the MAPK signaling cascade (Arumugam et al., 2012).

### 1.3.2 EARLY DEVELOPMENT

#### 1.3.2.1 Fertilization

Fertilization promotes the exit from meiosis II metaphase arrest and activates calcium/calmodulin-dependent kinase II (CaMKII). CaMKII and polo-like kinase inactivate Emi2, cancelling the inhibition of Cdc20, an activator of the anaphase promoting complex (APC/C). Active APC/C induces the degradation of Cyclin B, which decreases MPF activity required for metaphase MII arrest. Hence meiosis II proceeds, the second polar body is extruded and the first cleavage starts (Liu et al., 2006; Madgwick and Jones 2007).

#### 1.3.2.2 Early development is coordinated by the maternal program

The first embryonic cleavage lasts approximately 90 minutes to accommodate for an array of specialized events. The second meiotic division of the female genome is permitted and accompanied by the extrusion of the second polar body. Subsequently, the sperm nucleus is adjusted to support embryonic development by breakdown of its nuclear envelope and replacement of nuclear protamines by somatic histones. This allows chromosomal decondensation of both egg and sperm nuclei, which results in the formation of the heterokaryon (Newport and Kirschner 1982a; Hörmanseder et al., 2013).

The following 11 rapid and synchronous rounds of division are driven exclusively by the maternal developmental program, each lasting half an hour (Newport and Kirschner 1982a). These specialized cell cycles occur in the absence of transcription, demonstrated by the continuation of division upon application of transcription inhibitors. They involve only the DNA-replication (S) and mitosis (M) phases of the cell cycle. The duration of subsequent cell cleavage cycles lengthens to encompass the gap phases G1 and G2, and the synchrony of division is lost (Newport and Kirschner 1982a, 1982b; Philpott and Yew 2008).

This change in cell cycle marks the mid-blastula transition (MBT), a crucial point in development characterized by the initiation of embryonic reorganization. Rearrangements ensue both at the molecular level, as the zygotic genome assumes command of ongoing developmental processes and at the macromolecular level as cells become susceptible to apoptosis and acquire the potential for mobility, allowing the onset of gastrulation (Newport and Kirschner 1982a; Tadros and Lipshitz 2009).

#### 1.3.2.3 The zygotic genome takes control at the Maternal to Zygotic Transition (MZT)

Whereas the MBT occurs at a defined point in time during development, the maternal to zygotic transition (MZT) is an overlapping event that extends over a longer overlapping developmental period. Maternal to zygotic transition has profound implications for the life of an embryo. MZT involves remodeling at many levels, being defined by the carefully regulated interplay between the clearance of maternal determinants and the activation of the zygotic genome. Remodeling serves to clear the inherited oocyte genetic program in order to allow transitioning to a transiently totipotent zygotic state (Yartseva and Giraldez 2015).

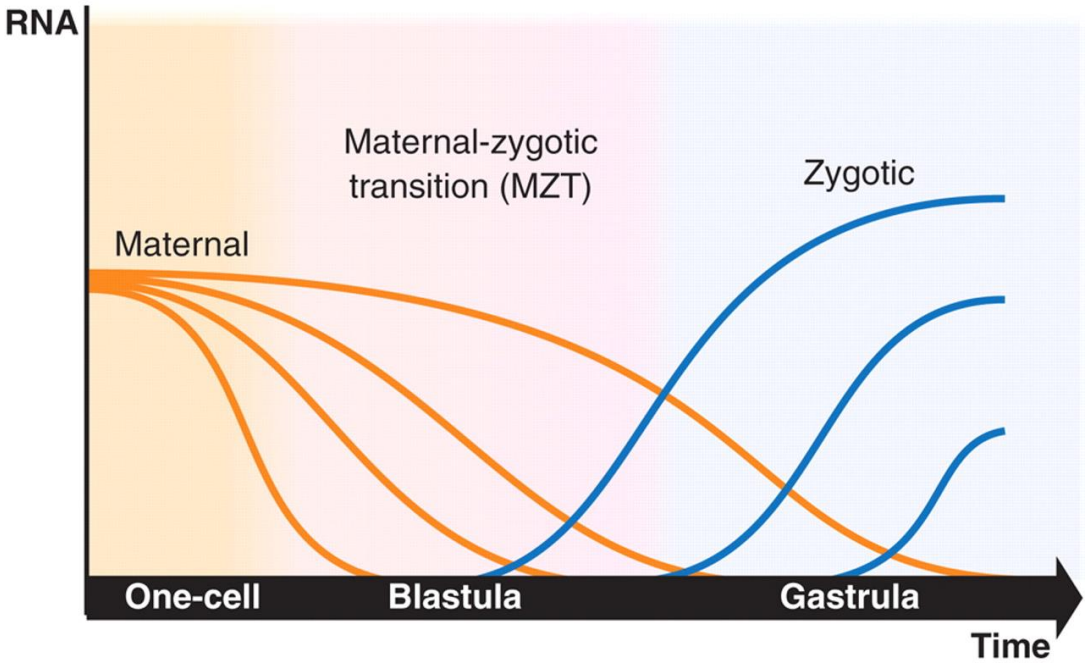


**Figure 1.4 Maternal to zygotic transition.** During maternal to zygotic transition maternal mRNAs are degraded at different stages of embryogenesis including blastula and gastrula, while coincidentally the zygotic genome is activated. From Schier 2007.

Maternal transcript destabilization is essential for three possible reasons: preventing abnormal mRNA and protein dosage in the embryo ensuing zygotic transcriptional activation, permitting patterned gene expression by eliminating ubiquitously distributed mRNAs, and allowing for the gradual lengthening of the cell cycle required for cellular differentiation (Tadros and Lipshitz 2009). Remodeling the transcriptional landscape is enacted by the cooperative action of two degradation activities: one "maternal", composed exclusively of maternally derived products and the other "zygotic", which require zygotic genome activation (Bashirullah et al., 1999). The joint action of these pathways leads to the elimination of 30-40% and the destabilization of 60% of maternally derived transcripts. The stability of an mRNA is influenced by three main transcript features: the mRNA sequence also considering codon usage, the 7-methylguanylate ($m^7G$) cap at the 5'end and the poly(A) tail length at the 3' end (Tadros and Lipshitz 2009).

Mechanistically, maternal gene products are targeted for degradation either by RNA-binding proteins (RBPs) and/or by the microRNA-induced silencing complex (RISC). For both of the named *trans*-factors, destabilization and decay of the targeted transcript occurs through either of the following three mechanisms: endonucleolytic cleavage followed by XRN1 and Exosome-complex mediated hydrolysis from both the 3' and 5'mRNA ends, recruitment of deadenylases such as PARN or the CCR4-NOT1 complex to shorten the poly(A) tail, or by the hydrolysis of the 5'cap via DCP2 which allows hydrolysis from the 5'end (Yartseva and Giraldez 2015).

Deadenylation is a common regulation mechanism involved in translational silencing and transcript destabilization. Poly(A) tail shortening is also a convergence point for RBP and RISC mediated degradation pathways. For example on the RBP level in *Xenopus*, the embryonic deadenylation element (EDEN) is bound by EDEN-binding proteins (EDEN-BP/CELF1), involved in the degradation of a select group of 158 maternal mRNAs accountable for cell cycle and oocyte maturation (Graindorge et al., 2008). On the small RNA level, miR-427 and miR-18, which share the 5'-proximal seed sequence AAGUGC trigger deadenylation of several maternal transcripts. miR-427 acts in the degradation of *cyclin A1* and *cyclin B2*, and miR-18 in that of inefficiently localized germ-plasm transcripts such as *XDE*, described above (Lund et al., 2009, 2011; Koebernick et al., 2010). Interestingly, miR-427 is the ortholog of the *Zebrafish* miR-430, which acts during MZT in the degradation of several hundred maternal transcripts (Giraldez et al., 2006).

The second player in MZT is the initiation of *en masse* zygotic transcription. There is extensive variability in the timing and dynamics of zygotic gene expression across species, yet universally, zygotic transcription commences following a period of quiescence. Several models have emerged during the last few decades, an integrative picture involving the cooperative activity of at least three mechanisms. First, in accordance with the nucleocytoplasmic ratio model, the zygotic genome is released from a repressed state by epigenetic remodeling. Subsequently, the accumulation of the correct repertoire of transcription factors is accomplished by translation of maternal transcripts and DNA becomes compatible with transcription after a particular time post-fertilization according to the "molecular clock" model (Langley et al., 2014).

An additional tier of complexity is given by the regulation of maternal transcript degradation on the spatial level. Notably, a subset of destabilized mRNAs is eliminated in somatic tissues but not in the germline. Spatial control can be achieved either by selective degradation in the soma as for *hsp83* mRNA in *Drosophila* or by interfering with the activity of the destabilization-inducing factor on the target transcript. To elaborate on this latter mechanism, it was shown that the RNA binding proteins Dnd1 and DAZL have a stabilizing effect in the *Zebrafish* germline. Dnd1 prevents miRNAs from binding to their target site, whereas DAZL recruits a poly(A) polymerase, counteracting deadenylation induced by the bound RISC complex (Kedde et al., 2007; Takeda et al., 2009).

#### 1.3.2.4 miRNA biogenesis

The gathered knowledge suggests an essential role of miRNA involvement in spatial regulation of maternal determinants. This is further supported by experimental evidence in *Zebrafish* and *X. laevis* suggesting that the inhibition of miRNA maturation leads to developmental defects during

gastrulation (Giraldez et al., 2006; Lund et al., 2011). Considering the essential role miRNAs exert during MZT, it is essential to have a quick overview on their biogenesis.

A large fraction of miRNA genes are mainly located within intragenic regions, predominantly introns of protein-coding genes, with a few located in pre-mRNA exons and others in intergenic regions (Tang and Maxwell 2008). Similarly to mRNAs, miRNAs are transcribed mainly by RNA polymerase II (RNAPII) and require further processing to reach their mature form (Lee et al., 2004). Their primary transcripts (pri-miRNA) possess a 5' cap and a 3' poly(A) tail and form secondary stem-loop structures recognized by the microprocessor complex containing the two core components Drosha and *Di George Syndrome critical region gene 8* (DGCR 8; Lee et al., 2003; Lee et al., 2004). DGCR8 binds the base of the stem-loop and positions the RNase III enzyme Drosha such that it cuts the pri-miRNA 11 nucleotides from the base, generating a RNA duplex with a two-nucleotide overhang at the 3' end, the precursor miRNA (pre-miRNA; Lee et al., 2003). Exportin 5 exports the pre-miRNAs to the cytoplasm, where they are further processed by Dicer, also a RNase III enzyme, to give rise to the mature miRNA which is then incorporated into the RISC complex (Lee et al., 2003; Yi et al., 2003; Lund et al., 2004; Bohnsack et al., 2004; Treiber et al., 2012; Kim et al., 2016).

## 1.4 CPEB1 IN *X. LAEVIS*

### 1.4.1 CPEB1 GENE STRUCTURE AND HOMOLOGUES IN OTHER SPECIES

Homologues of the *cpeb1* gene have been identified both in invertebrates (two genes) and vertebrates (four genes). The encoded proteins bind RNA in a sequence specific manner, by recognizing the cytoplasmic polyadenylation elements (CPEs) in the 3'UTR of target transcripts (Paris et al., 1991; Hake and Richter 1994). From the founding member of the family CPEB1 two protein families have diverged one encompassing CPEB1 alone and the other family CPEB2, CPEB3 and CPEB4. The two families have been shown to bind overlapping populations of transcripts, despite their preferences for slightly different motifs from that preferred by CPEB1 (Richter 2007; Mendez and Richter 2001).

*X. laevis* is an allotetraploid organism, many genes being present in two copies, one on the short and one on the long chromosome (Uno et al., 2013). There are two homologues for *cpeb1*, denoted *cpeb1_s* and *cpeb1_l* for the short and long chromosomes respectively, with high sequence similarity (94% identities *cpeb1_s/1_l*, 0 gaps; blastn; XB-GENEPAGE-946166).

CPEB1 is a highly conserved 63.5 kDa protein measuring 568 amino acids in length. Structurally it is comprised of two main regions, a more variable N-terminal domain and a conserved C-terminal domain, as indicated by structural homology analysis (Gebauer and Richter 1996). The amino-terminus is mainly responsible for posttranslational regulation and protein-protein interaction as it contains a PEST domain important for its degradation, several phosphorylation sites and mapped microtubule interaction sites. The RNA-binding capacity is provided by two RNA recognition motifs (RRMs) and one zinc-finger (Zif) harbored in the carboxi-terminal domain (Hake et al., 1998).

CPEB1 binds U-rich CPEs with motifs as diverse as UUUAU and UUUUAACA, with a consensus of UUUUUAU (McGrew and Richter 1990). The exact binding mechanism was recently investigated, and the amino acids essential for RNA binding were determined (Afroz et al., 2014). The number of CPEs and their positioning in respect to other elements is relevant for the regulation of the bound transcripts (see CPEB1 function, Stebbins-Boaz et al., 1996). Individual translational activation patterns depend on the CPE localization respective to other elements, such as the *hex* element, musashi binding element (MBE), pumillio binding element (PBE), DAZL binding elements and recently miRNA binding sites (Charlesworth et al., 2006; Piqué et al. 2008; Martins et al., 2016; Wilczynska et al., 2016). Representative examples are those of *mos* and *Cyclin B1*. *Mos* contains one single CPE and is translationally activated early after progesterone maturation induction. *Cyclin B1* has two regulatory CPEs and is robustly translated only after partial CPEB1 destruction. This is effected by the later phosphorylation events leading to a change in CPEB1:CPE ratio which is important for oocyte entry into metaphase II arrest (Mendez et al., 2002).

#### 1.4.2 CPEB REGULATION AND EXPRESSION

In early stage oocytes, the *cpeb1* mRNA and the encoded protein were reported to be ubiquitously distributed. During late oogenesis (stages V-VI), CPEB1 is enriched five fold in the animal as compared to the vegetal hemisphere. During progesterone induced oocyte maturation, 75% of the protein is degraded (Mendez et al 2002). Besides, detectable levels of CPEB1 were observed only in animally derived explants in eggs and embryos (Groisman et al., 2000). Furthermore, expression analysis of embryos at sequential embryonic stages indicates that the protein and mRNA are detected only until gastrula (Hake and Richter 1994). In addition to these observations, the *cpeb1* transcript has been specifically detected in the germline in *X. laevis,* in a screen aiming at characterizing the mRNA pools specific to PGCs in comparison to endodermal somatic cells (Dzementsei, 2013). These observations suggest strict regulation at the posttranscriptional and posttranslational levels.

Several experimental results suggest that *cpeb1* is a target of miRNA mediated decay. Burns et al reported in 2011 that the *cpeb1* transcript harbors two actively regulated microRNA-122 (miR-122) target sites in its 3'UTR in mouse embryo fibroblasts and human foreskin fibroblasts. Stabilization of miR-122 by the addition of a single non-template adenylate residue by Papd4 (Gld2) leads to targeting *cpeb1*, which is then destabilized or translationally inhibited. CPEB1 modulates the posttranscriptional regulation of *p53* by the recruitment of a poly(A) polymerase, Gld4. Hence, the downregulation of CPEB1 expression results in lower levels of p53 due to lower polyadenylation rates, preventing senescence (Burns et al., 2011). Another key experiment indicating that *cpeb1* is targeted by miRNA mediated decay comes from our lab. The maturation of miRNAs was prevented by overexpression of an siRNA which saturated the pool of Dicer protein, responsible for miRNA processing. In this scenario, the levels of miRNA regulated mRNAs would increase, as was indeed the case for *cpeb1* (Pfennig, 2014).

At the protein level, the first regulation event occurs during oocyte maturation. Progesterone stimulation triggers the release of AurkA, a member of the Aurora family of Serine/Threonine kinases, from GSK3 inhibition. Within 30 minutes since induction, AurkA (Eg2) phosphorylates CPEB1 serine 174 (S174). This residue is found in the LSDR motif observed in all vertebrate CPEBs, varying to LDTR or LDSH which could be functionally similar (Mendez et al. 2000a). Later during maturation Cdk1 catalyzes subsequent phosphorylation events on six serine residues resulting in the recruitment of a third kinase, polo-like kinase 1 (Plx1) which phosphorylates S191. This last phosphorylation is required for the recognition by the E3-ubiquitin ligase $SCF^{\beta\text{-}TRCP}$ which targets CPEB1 to the 26S proteasome for degradation (Reverte et al. 2001; Mendez and Richter 2002; Setoyama et al. 2007). A PEST domain is important for Pin1 interaction, which is also involved in targeting CPEB1 for degradation (Nechama et al., 2013).

An additional posttranslational mechanism completes the regulatory picture. In order to maintain the CPE:CPEB1 ratio and to have an immediate modulation of CPEB1 levels in the cell the RRMs can function as interaction platforms for dimerization. Therefore, surplus protein is maintained inactive in immature oocytes. During maturation, only monomers are observed. Dimers are readily degraded due to their preferential association with the kinase Plx1 and the F-box protein $SCF^{\beta\text{-}TRCP}$. Interestingly, CPEB1 dimers also bind members of the polyadenylation machinery, suggesting that upon meiotic maturation and dimer degradation, associated factors are released into the cytoplasm facilitating translational regulation on CPEB1 bound transcripts. There are two advantages to this mechanism: there is no genetic burden and the inactive extra protein would be readily available in the cytoplasm when required (Lin et al. 2012).

### 1.4.3 CPEB1 FUNCTION IN *X. LAEVIS* OOCYTE MATURATION

The best characterized system where the role of CPEB1 was described is the late stage *X. laevis* oocyte. Its essential function in oocyte maturation was uncovered by neutralizing CPEB1 with a specific antibody, a treatment that significantly reduced the proportion of oocytes that underwent maturation (Stebbins-Boaz et al., 1996). Progesterone or insulin stimulation initiate a non-transcriptional cascade of events ultimately leading to oocyte maturation. One relevant outcome is the phosphorylation of CPEB1 on S174 by Aurk A (Eg 2) kinase (Mendez et al., 2000a). Following phosphorylation translation of several transcripts ensues, one being that of *mos* encoding for Mos, a mitogen-activated protein kinase kinase kinase (MAPKKK) essential for inducing the MAP kinase cascade which culminates with the activation of maturation promoting factor (MPF). MPF is a heterodimer of Cyclin B and cdc2 and initiates oocyte maturation (Mendez et al., 2000a; de Moor et al., 1997). Furthermore, Mos is a component of cytostatic factor (CSF) which prevents parthenogenetic oocyte division by arresting maturation at metaphase II (Mendez and Richter 2001). Early on, CPEB1 was also shown to bind CPEs in *hist1h4d* (histone H4), *bud31* (*G10*), *cdk2* and *ccna1* (*cyclin a1*), *ccnb1* (*cyclin b1*) and *ccnb2* (*cyclin B2*) mRNAs in a temporally regulated manner, depending on the number of CPEs present in their 3'UTR (Stebbins-Boaz et al., 1996). Moreover, the effect of the AurkA mediated phosphorylation extends its effects on the protein-protein interactions CPEB1 holds. For example, the interaction between CPEB1 and the cytoplasmic form of cleavage and polyadenylation specificity factor (CPSF), more specifically its 160kDa subunit, is strengthened four fold after progesterone stimulation (Mendez et al., 2000b). This correlates with cytoplasmic polyadenylation requirements. Two 3'UTR elements must be present in order for polyadenylation to occur, the hexanucleotide AAUAAA recognized by CPSF (Dickson et al., 1999) and the CPE bound by CPEB1 (Hake and Richter 1994). Barnard et al., show that symplekin and xGLD-2 also reside in a cytoplasmic polyadenylation complex with CPEB1, symplekin and xGLD-2 being in direct contact with both CPSF and CPEB1. Moreover, when the complex formed by these four proteins is tested for its polyadenylation capacity, the mRNAs are provided with tails exceeding 1000 bases, indicating that a regulator of poly(A) tail length is missing (Barnard et al., 2004). This regulator was discovered to be the embryonic poly(A)-binding protein (ePAB), which is transiently associated with the polyadenylation complex by being tethered to CPEB1. ePAB dissociates from CPEB1 following the second round of six phosphorylations mediated by the RINGO-activated cdk1. Then the free ePAB can bind the newly elongated poly(A)-tail of target transcripts, restricting the homopolymer length to approximately 200 nucleotides, protecting it from nuclease attack, and promoting translation initiation by associating with eIF4G, component of the 43S ribosomal complex (Kim et al., 2007).

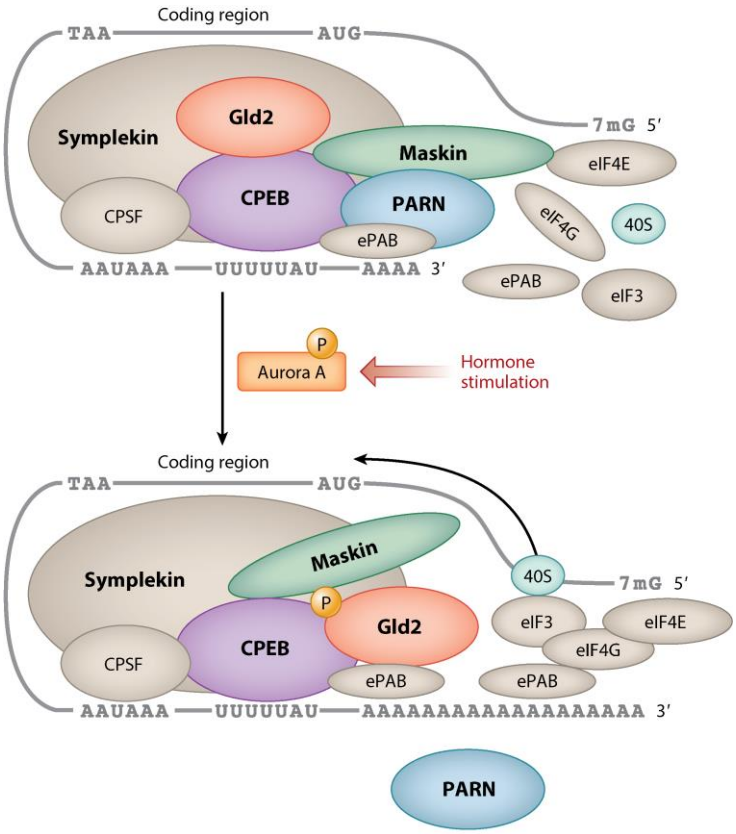


**Figure 1.5 Cytoplasmic polyadenylation during oocyte maturation in *X. laevis*.** In immature oocytes, RNP complexes composed of CPE-containing transcripts as well as CPEB1, Symplekin, Papd4 (Gld2), Pabpc1l (ePAB), Tacc3 (Maskin), Parn, Cpsf2 are translationally silent. Following hormone stimulation, AurkA phosphorylate CPEB1, an event that leads to PARN being excluded from the complex. This allows Papd4 to polyadenylate the mRNA. Consequently, Pabpc1l binds the newly elongated poly(A) tail and eIF4G1 (eIF4G), together displacing Tacc3, which enables translational initiation. From Ivshina et al., 2014.

In immature oocytes, CPEB1 bound mRNAs undergo deadenylation following export to the cytoplasm and are retained in a translationally inactive form (Paris and Richter 1990). Silencing is mediated by Tacc3 (Tacc3), a protein which directly binds CPEB1 and the 5' 7-methylguanosine cap associated – eIF4E. Under translationally permissive circumstances, the poly(A) binding proteins (Pabpc1, previously knows as the poly-A binding protein PABP) associated with the poly(A) tail interact with eIF4G. The PABP-eIF4G pair enables association of the small ribosomal subunit to the transcript by replacing Tacc3 (Stebbins-Boaz et al., 1999; Cao and Richter 2002). Furthermore, polyadenylation regulation also depends on xGLD-2, a member of a nucleotidyl-transferase family, and a poly(A) specific ribonuclease PARN. The two enzymes form direct interactions with each other and CPEB1 (Kim and Richter 2006). In immature oocytes, the deadenylating activity of PARN is more efficient than polyadenylation exerted by xGLD-2, keeping poly(A) tails of CPE-containing transcripts short. During maturation, PARN is expelled from the complex permitting xGLD-2 adenosine addition (Kim and Richter 2006).

The molecular mechanism of translational silencing has been dissected over many years being put together piece by piece into the present-day picture. CPEB1 is a key translational regulator, being responsible for maintaining target transcripts silenced in immature oocytes and then alleviating their translation during oocyte maturation by regulating polyadenylation.

#### 1.4.4 CPEB1 ROLES IN DIFFERENT MODEL SYSTEMS AND KNOWN INTERACTION PARTNERS

The discussion on CPEB1 function has been focused on oocyte maturation. Nevertheless CPEB1 was found to play diverse roles in different model systems and several examples are described next.

During early *X. laevis* embryogenesis, CPEB1 together with Tacc3 were shown to directly interact with microtubules and to be implicated in translational control of Cyclin B1 at the mitotic spindle. The protein motif in CPEB1 responsible for this interaction was mapped to the PEST and LDSR domains (Groisman et al., 2000).

Lin et al. investigated the potential shuttling of CPEB1 between nucleus and cytoplasm in the *Xenopus* oocyte. CPEB1 associated with transcriptionally active chromosomes and several RNA-processing factors, as Tacc3, Symplekin, CPSF73, RNAse Polymerase II and eIF4A3 were successfully co-precipitated from stage VI oocyte nuclei. Their findings indicate that translational silencing of transcripts may start in the nucleus (Lin et al., 2010).

A recent study on the posttranscriptional regulation of *cyclin E1* during *X. laevis* oocyte maturation revealed for the first time a surprising cooperation between CPEB1 and a miRNA family, miR-15/16. Firefly luciferase assays showed that polyadenylation of Cyclin E1 is dependent on the two CPEs and that the miR-15/16 sequences are functional. In addition, CPEB1 and miR-15/16 co-precipitate and there is evidence suggesting that CPEB1 and Ago2 interact directly. Interestingly, inhibiting miR-15/16 with LNA oligos causes premature polyadenylation and premature meiotic maturation (Wilczynska et al., 2016).

Another recent report brings to light the synergistic activity of CPEB1 and miR-15b/RISC in the posttranscriptional regulation of the cell-cycle regulator Wee1 in the human Hela cell line. Once more, the potential interaction between Ago2 belonging to the RISC complex and CPEB1 was tested. In contrast to what was observed in Xenopus (Wilczynska et al., 2016), the CPEB1 and Ago2 cross-precipitation was dependent on the RNA scaffold, without a direct interaction. Intriguingly the coordinated action of the two complexes is cell cycle dependent. The CPE and miR-15b sites having an inhibitory effect during G1 and S phases and an activating effect, requiring the functionality of both elements, in the G2/M transition (Kratassiouk et al., 2016).

In mouse oocyte maturation, CPEB1 and DAZL collaborate in coordinating the translational regulation of a maternal transcript population containing CPEs and DAZL binding sites. Interestingly, deleting DAZL binding sites affects the efficiency of CPEB1-mediated translational activation. Immunoprecipitation experiments show the presence of CPEB1 and DAZL on the same transcript, but no direct interaction was observed. Moreover, depletion of either CPEB1 or DAZL leads to reduced translational activation during meiotic progression, yet the most substantial effect is obtained upon depletion of both, indicating that CPEB1 and DAZL act synergistically. Bioinformatic analysis supports this conclusion as transcripts containing three or more DAZL binding sites in combination with a CPE are predicted to be recruited to polysomes more efficiently than those with only DAZL binding elements (Martins et al., 2016).

In cultured rat hippocampal neurons CPEB1 resides with the anterograde kinesin and retrograde dynein molecular motors in ribonucleoprotein (RNP) particles. Immunoprecipitation experiments indicate that the two molecular motors interact directly with CPEB1. Once more, Tacc3 was detected in the RNPs, suggesting that the transported mRNAs are translationally dormant (Huang et al., 2004).

In rat glioma cells, CPEB1 is important for regulating the mRNA encoding metadherin (MTDH/AEG-1), which may coordinate several signaling pathways involved in tumor progression. Using a dominant negative (DN) mutant of CPEB1 lacking the phosphorylation site required for activation, yet retaining the ability to bind mRNA, the authors show that glioblastoma growth is inhibited *in vivo*. In addition, CPEB1 is not only involved in CPE dependent MTDH localization to the periphery of migrating astrocytes, but also shuttling the transcript between the nucleus and cytoplasm. Moreover, migration assays indicate a role of CPEB1 in directional migratory behavior (Kochanek and Wells 2013).

Interestingly in the human Glioblastoma Multiforme (HGM) the protein expression of CPEB1 is significantly reduced. This is associated with an enhanced capacity of malignant cells to promote invasion and angiogenesis, increased nutritional stress resistance and epithelial-to-mesenchymal transition. An established prognostic marker, the cyclin-dependent-kinase inhibitor $p27^{Kip1}$,was shown to be directly regulated by CPEB1 as it counteracts the destabilizing activity of miR-221/222. The miRNA target site partially overlaps that of CPEB1, therefore by its binding CPEB1 prevents the degradation of the $p27^{Kip1}$ and it also enhances translation by inducing polyadenylation. Higher $p27^{Kip1}$ levels inhibit cell proliferation thus inversely correlating with carcinogenesis (Galardi et al., 2016).

In addition to translational silencing, other mechanisms of regulation in the nuclear space are alternative exon usage and alternative polyadenylation sites. In CPEB1 knock out (KO) mouse embryonic fibroblasts (MEFs) and tissues derived from CPEB KO mice collagen 9 encoding transcripts are differentially spliced. Furthermore, CPEB was shown to interfere with the recruitment of U2AF65 to alternative splice sites, thence generating different isoforms from the same transcript. This novel function is coordinated with regulation of mRNA translation through its dual nuclear and cytoplasmic functions (Bava et al., 2013).

#### 1.4.5 CPEB1 IN GERMLINE DEVELOPMENT

The *Drosophila* homolog of CPEB1 is ORB (Hake and Richter, 1994; Thompson et al., 2005). Similarly to *Xenopus* CPEB1, ORB functions in the regulation of translation and localization of transcripts such as *oskar*, *gurken*, as well as *orb* itself. Furthermore, in case of ORB loss-of-function (LOF) mutation, oocytes failed to differentiate properly and the formation of oocyte-nurse complex was impaired (Lanz et al., 1994). Another recently described function of Orb is controlling autophagy by regulating the translation of mRNAs encoding Atg proteins (Rojas-Rios et al., 2015).

In *C. elegans*, the CPEB1 homologue Fog-1 is important for promoting early germline proliferation. In addition, Fog-1 expression levels dictate the sperm-oocyte decision, higher doses leading to the sperm cell fate (Thompson et al., 2006).

CPEB1 was found to be specifically expressed in the mouse ovary and testis. Knocking out CPEB1 leads to abnormal development of the female and male gonads (Gebauer and Richter, 1996; Tay and Richter, 2001).

Altogether, CPEB1 is involved in recruiting factors important for multiple cellular processes centered around mRNA processing. Through its different interaction partners, it exerts functions ranging from translational regulation, mRNA splicing and differential use of polyadenylation sites to RNA subcellular localization.

## 1.5 THESIS AIMS

PGCs remain developmentally naïve by being unresponsive to differentiation cues intended for somatic cells. Germline cells have diverse interlocking systems for acquiring and maintaining germ cell identity. Consequently identifying and characterizing participating factors is profoundly important for understanding germ cell development. One factor lying at the intersection point of several processes is *cpeb1*. Consequently this project has two lines of investigation: deciphering the regulation of *cpeb1* transcripts in the embryo and identifying a potential role for CPEB1 in *X. laevis* germline development.

The regulation of *cpeb1* required to confer germline specificity is almost certainly based on an interplay of multiple mechanisms. It will be interesting to determine whether the transcript is zygotically transcribed and if so to examine the onset of zygotic transcription. Additionally, identifying minimal regions in the 3'UTR and addressing the identity of individual miRNAs responsible for somatic depletion will be instrumental in dissecting the posttranscriptional regulation governing the restriction of *cpeb1* to the germline.

On the protein level, different strategies for modulating CPEB1 levels in the developing embryo will be employed to observe germline related phenotypes. Furthermore, for a comparative characterization of the CPEB1 interactome in the oocyte and embryo, immunoprecipitation experiments coupled with mass spectrometry will be performed. This may reveal the cellular processes where CPEB1 may play a role and may offer a glimpse of the protein-protein interaction landscape and its dynamics in the oocyte to embryo transition.

## 2. MATERIALS AND METHODS

### 2.1 MODEL ORGANISM

Adult *X. laevis* frogs were purchased from Nasco (Fort Atkinson, Wisconsin, USA). Embryos and oocytes were used for *in vivo* experimental procedures. *X. laevis* embryos were staged according to the NF system (Nieuwkoop and Faber, 1994) and *X. laevis* oocytes according to Dumont (Dumont, 1972).

### 2.2 BACTERIA STRAINS

*Escherichia coli (E. coli)* strains:
XL1-Blue: RecA1, endA1, gyrA96, thi-1, hsdR17, supE44, relA1, lac[F'proAB, lacIqZΔM15, Tn10(Tet$^r$)]$^{c.}$ for cloning procedures (Stratagene).
BL21 (DE3): *E.coli* B F$^-$, ompT, hsdS(rB-mB-), dcm+, Tetr, gal λ(DE3) endA Hte [argU proLCamr] [argU ileY leuW Strep/Specr] for protein expression.

### 2.3 CHEMICALS

Chemicals were purchased from: Roth (Karlsruhe), Sigma-Aldrich Chemie (Taufkirchen), Applichem (Darmstadt), Biochrom (Berlin), Life Technologies GmbH (Darmstadt), Roche (Mannheim), Thermo Fisher Scientific/Fermentas - Germany GmbH (Schwerte).

### 2.4 BUFFERS AND MEDIA

The listed media and buffers used for investigations in this study were prepared using Millipore double distilled water (MiliQ dd$H_2O$) and were autoclaved if required. Unless indicated differently, percentages represent volume/volume (v/v) ratios.

**Table 2.1 Buffers and media**

| Buffer/Media name | Composition |
|---|---|
| Alkaline phosphatase buffer (APB) | 100 mM Tris, 50 mM $MgCl_2$, 100 mM NaCl, 0.1 % Tween-20; pH 9.0 |
| Acidic glycine buffer | 100 mM Glycine, pH 2.5 with HCl |
| Bleaching solution | 5 % Formamide, 0,5 % $H_2O_2$, 0,5x SSC |
| Blocking solution (WB) | 5 % nonfat dry milk (w/v) in 1x TBST |
| Blocking solution (WMISH) | 1x MAB, 2 % Boehringer Mannheim Blocking reagent (BMB), 20 % horse |

| | |
|---|---|
| | serum (HS) |
| Blocking solution (IF) solution 1 | 1x PBS, 2 % BSA, 2 % HS, 0,1 % Triton X-100 |
| Blocking solution (IF) solution 2 | 1x TBST, 2 % BSA, 10 % HS |
| Blotting buffer | 48 mM Tris, 39 mM glycine, 0.037 % SDS, 20 % methanol, pH 8.0 |
| Collagenase-buffer | 82.5 mM NaCl, 2 mM KCl, 1 mM $MgCl_2$, 5 mM HEPES; pH 7.5 |
| Color reaction solution (WMISH) | 87.5 µg/ml NBT, 175 µg/ml BCIP in APB; pH 9.0 |
| Coomassie Destaining solution | 1 % acetic acid |
| Coomassie Staining (stock solution) | 0.1% (w/v) Coomassie Brilliant Blue G-250, 2 % (w/v) ortho-phosphoric acid 10% (w/v) ammonium sulfate |
| Coomassie Staining (working solution) | 80 % Coomassie stock solution, 20 % methanol |
| Cysteine solution | 2 % L-Cysteine hydrochloride, pH 7.8 – 8 |
| Dent's fix | 80 % methanol, 20 % DMSO |
| Gel fixing solution | 40 % ethanol, 10 % acetic acid |
| Glyoxal fixation solution (IF) | 20 % ethanol, 8 % glyoxal (available as a 40 % solution from Sigma), 0,75 % acetic acid, pH 4 |
| Hybridization Mix (Hyb Mix) | 50 % Formamide, 5x SSC, 1 mg/ml Torula-RNA, 100 µg/ml Heparin, 1x Denhards, 0.1 % Tween-20, 0.1 % (w/v) CHAPS, 10 mM EDTA |
| Injection buffer | 1 % Ficoll, 1x MBS |
| IPP145 buffer (10x stock solution) | 100 mM Tris (pH 8), 1450 mM NaCl, 1 % NP40 (v/v) |
| IPP145 buffer (1x) | 1x IPP145 buffer, 5 % Glycerol, Complete protease inhibitor cocktail – EDTA free (1 tablet per 50 ml of buffer, Roche), PhosphoStop Phosphatase inhibitors cocktail (1 tablet per 50mL buffer, Roche) |
| L15 oocyte culture medium | 50 % L-15 medium, 1 mM L-glutamine, 1 µg/ml insulin, 15 mM HEPES pH 7.8, 100 µg/ml gentamycine, 50 µg/ml tetracycline, 50 units/ml nystatin, 2.5 mg/ml vitellogenin (isolated from frog blood) |
| Laemmli running buffer (1x) | 25 mM Tris, 192 mM Glycine, 0.1 % SDS |
| Laemmli loading buffer (2x) | 65 mM Tris pH 6.8, 2% (w/v) SDS, 10% glycerin, 0,02% (w/v) Bromphenol blue |
| Luria-Bertani (LB)-Agar | 1.5 % (w/v) agar in liquid LB-medium |
| Luria-Bertani (LB)-Medium | 1 % (w/v) Bacto-Trypton, 0.5 % (w/v) yeast extract, 1 % (w/v) NaCl, pH |

| | |
|---|---|
| | 7.5. The medium was supplemented with Ampicillin (50 µg/ml), Kanamycin (50 µg/ml), Tetracycline (20 µg/ml). |
| MAB (1x) | 100 mM maleic acid, 150 mM NaCl; pH 7.5 |
| MBSH (5x) | 88 mM NaCl, 1 mM KCl, 0.82 mM $MgSO_4$, 10 mM Hepes pH 7.5, 2.4 mM $NaHCO_3$, 0.41 mM $CaCl_2$, 0.66 mM $KNO_3$ |
| MEM (10x) | 1 M MOPS, 20 mM EGTA, 10 mM $MgSO_4$; pH 7.4 |
| MEMFA (1x) | 1 x MEM, 4 % formaldehyde |
| PBS (10x) | 1.75 M NaCl, 1 M KCl, 65 mM $Na_2HPO_4$, 18 mM $KH_2PO_4$; pH 7.4 |
| PBT | 1x PBS, 0,1 % Tween-20 |
| PBT (IF) | 1x PBS pH 7.4, 0.2% BSA, 0.1 % Triton X-100 |
| Ponceau S solution | 2 g Ponceau S, 30 g trichloroacetic acid, 30 g sulfosalicylic acid per 100 ml |
| Proteinase K solution (IF) | 100 mM Tris-HCl pH 7.5, 10 mM EDTA, 50 µg Proteinase K |
| PTw | 0.1 % Tween-20 in 1 x PBS |
| SDS loading buffer (2x) | 62,5 mM 0.5 M Tris (pH 6.8), 2 % SDS (w/v), 10% glycerol, 700 mM β-mercaptoethanol, 0.05 % (w/v) bromphenol blue |
| SSC (20x) | 3 M NaCl, 0.3 M Sodium citrate; pH 7.4 |
| TAE (Tris/Acetate/EDTA) | 40 mM Tris-Acetate (pH 8.5), 2 mM EDTA |
| TBS (Tris/Boric acid/EDTA) (IF) | 150 mM NaCl, 10 mM Tris pH 7.5 |
| TBST (Tris buffered saline with Tween-20) | 50 mM Tris, 150 mM NaCl, 0.1 % TWEEN-20; pH 7.5 |
| TE (Tris/EDTA) | 100 mM Tris-HCl pH 7.5, 10 mM EDTA |
| Tris-HCl | 1 M Tris, pH adjusted with 37 % HCl |

### 2.5 OLIGONUCLEOTIDES

Oligonucleotides were purchased from Sigma-Aldrich Chemie. The indicated volume of MilliQ dd$H_2O$ was used to dissolve the lyophilized product to obtain a primer stock concentration of 100 µM (stored at –20 °C). The working oligonucleotide concentration of 10 µM was used for DNA amplification.

**Table 2.2 Sequencing oligonucleotides**

| Name | Sequence 5' – 3' |
|---|---|
| SP6 | TTAGGTGACACTATAGAATAC |
| T7 (pCS2+) | TCTACGTAATACGACTCACTATAG |
| T7 (pGEM-T easy) | TAATACGACTCACTATAGGGCGA |
| M13 rev | AGCGGATAACAATTTCACAC |
| pSP64 rev - 1 | GAGCGGATAACAATTTCTCTC |
| pSP64 rev - 1 | CACAGGAAACAGCTATGACATG |
| pSP64(A)_uptrMCS_1 | CAGTAAGCCAGATGCTACAC |
| GFP fw - 1 | CATGGTCCTTCTTGAGTTTG |
| mmGFP5_rev_118 | CGTATGTTGCATCACCTTCAC |
| mmGFP5_rev_163 | CAGGTAGTTTTCCAGTAGTGC |

**Table 2.3 Oligonucleotides* for preparation of WMISH asRNA probes**

| Name | Sequence 5' – 3' |
|---|---|
| CPEB_1a_up1 | ATGGCCTTCCCACTGAAAG |
| CPEB_1a_low1 | TGGTATCTGGAAGGCCGC |
| CPEB_1a_up2 | ATGACTTGTGCCTTGGTC |
| CPEB_1a_low2 | TCAGAAGGGCTGCTGGAGC |
| CPEB_1a_up3 | CCTCCGCTGCATTTCCTCC |
| CPEB_1a_low3 | TAGGGGGCAGCTGCCCAC |
| CPEB_1a_up4 | AATCCTGTGTATTCCTGC |
| CPEB_1a_low4 | TTGAAGTAGTGTTCACTCAG |
| CPEB_1a_up5 | TGCAAGGAGGTGCAGGTC |
| CPEB_1a_low5 | AGAGTCTTCCAAATACGG |

*Oligonucleotides designed by Dr. Maike Claußen.

**Table 2.4 Oligonucleotides for protein cloning**

| Name | Sequence 5' – 3' |
|---|---|
| CPEB_1a_begin ORF_EcoRI_fw | CGGAATTC **ATG**GCCTTCCCACTGAAAGATG |
| CPEB_1a_1st_half_Xba I_rev | GCTCTAGA**TTA**TGGGTCCTCTGCAGAATCCAG |
| CPEB_1a_2nd_half_EcoRI_fw | CGGAATTC**ATG**CTAGGTATTGGCTCAAGGCTAG |
| CPEB1a_ORF_N-terminus_XbaI_rev | GCTCTAGA**TTA**TGCAGAATCCAGCAGATCCCAGG |
| CPEB1a_ORF_C-terminus_EcoRI_fw | CGGAATTC**ATG**TCTGCAGAGGACCCATTTAGC |
| CPEB_1a_endORF_XbaI_rev | GCTCTAGA**TTA**GCTGGAGTCACGACTTTTC |

The underlined sequences correspond to the enzymatic cleavage sites and the trinucleotides in bold to introduced start (ATG) and stop (TTA) codons respectively.

**Table 2.5 Oligonucleotides for 3'UTR fragmentation analysis**

| Name | Sequence 5' – 3' |
|---|---|
| Primer_1_fw_Xho I | CTCGAG ACATTGGAACAACATTGGTC |
| Primer_1_rev_Not I | GCGGCCGC GCAATTAAGTCCTGAGAAG |
| Primer_2_fw_Xho I | CTCGAG CTCACACTAGTGCACACTTG |
| Primer_2_rev_Not I | GCGGCCGC GTTTATGTAGTTCAGATGGGAC |
| Primer_3_fw_Xho I | CTCGAG CTTCCCATGTTTTGCTGTTGC |

| | |
|---|---|
| Primer_3_rev_Not I | GCGGCCGC CTCTACCATCCCCTTAAGTGC |
| Primer_4_fw_Xho I | CTCGAG GATTATGACAGTGTGTGTG |
| Primer_4_rev_Not I | GCGGCCGC GGGTCTTTGGCACAGAGCTTAC |
| Primer_5_fw_Xho I | CTCGAG GGAATAAGTGCCCATGCTCTG |
| Primer_5_rev_Not I | GCGGCCGC CCATAGATTAAGTGCATCTTCTGC |
| Primer_5_rev_Not I_2 | GCGGCCGC CTGCTTCAACGTGTTTATTTTGTG |

The underlined sequences correspond to the enzymatic cleavage sites.

**Table 2.6 Oligonucleotides for 3'UTR Fragment 1 analysis**

| Name | Sequence 5' – 3' |
|---|---|
| Fr_1_fw_Xho I | CCG CTCGAG ACATTGGAACAACATTGGTC |
| Fr_1_rev_Not I | ATAAGAAT GCGGCCGC GCAATTAAGTCCTGAGAAG |
| Fr 1_208_rev_Not I | ATAAGAAT GCGGCCGC GCACTAGTGTGAGAAAACTACCAC |
| Fr 1_95_rev_Not I | ATAAGAAT GCGGCCGC GTGCTTCCAGTGCTAGAGGGAG |
| Fr 1_74_fw_Xho I | CCG CTCGAG CTCCCTCTAGCACTGGAAGCAC |
| Fr 1_139_fw_Xho I | CCG CTC GAG GGATTGTGGGGAGAATGTCAC |
| Fr 1_196_fw_Xho I | CCG CTCGAG CTCACACTAGTGCACACTTG |

The underlined sequences correspond to the enzymatic cleavage sites.

**Table 2.7 Oligonucleotides for X. laevis/X. tropicalis hybrid assay**

| Name | Sequence 5' – 3' |
|---|---|
| *X. laevis*_cpeb1_S_fw | TCCAGCAGCCCTTCTGACTC |
| *X. laevis*_cpeb1_S_rev | GCCATCCCTTTGTTATGCCA |
| *X. tropicalis*_cpeb1_S_fw | CTAAAGACGTCGGCCCTTGGAG |
| *X. tropicalis*_cpeb1_S_rev_1 | CATTGCTTACTTTCAGCAACG |
| *X. tropicalis*_cpeb1_S_rev_2 | TAAACCTTAAGAAAACGAGGC |
| ODC_fw | GCCATTGTGAAGACTCTCTCCATTC |
| ODC_rev | TTCGGGTGATTCCTTGCCAC |

The underlined sequences correspond to the enzymatic cleavage sites.

### 2.6 MORPHOLINO AND 2'O-METHYL OLIGONUCLEOTIDES

Antisense translational blocking and target protector morpholino (MO) oligonucleotides, were purchased from Gene Tools, LLC (Philomath, USA) and 2' O-Methyl oligonucleotides (2'OMe) from Sigma-Aldrich Chemie. Morpholinos were dissolved in RNase-free water to a 1 µM concentration and stored in aliquots at -20 °C.

**Table 2.8 Translational blocking and target protector morpholino oligonucleotides**

| Name | Sequence 5' – 3' |
|---|---|
| tMO_CPEB1_S and CPEB1_L (NM_001090603) | AATCATCTTTCAGTGGGAAGGCCAT |
| CoMo (scrambled) | CCTCTTACCTCAGTTACAATTTATA |
| TPMO_1 | CTAGTGCTTCCAGTGCTAGAGGGAG |
| TPMO_2 | CACTGATTGCTGATCTATCCCTGGA |

The underlined nucleotide corresponds to a mismatch between cpeb1_S and cpeb1_L.

**Table 2.9 miRNA blocking 2'OMe oligonucleotides**

| Name | Sequence 5' – 3' |
|---|---|
| 2'OMe-anti-xtr-miR-302 | UAAGUGCUCCAAUGUUUUAGUGG |
| 2'OMe-anti-xtr-miR-17-5p | CAAAGUGCUUACAGUGCAGGUAGU |
| 2'OMeO-anti-43-66nt | CCAGGGAUAGAUCAGCAAUCAGUG |
| 2'OMeO-ctrl (scrambled) | UGGGCGUAUAGACGUGUUACAC |

## 2.7 CONSTRUCTS

**Table 2.10 Expression constructs**

| Insert | Vector | Kindly provided by |
|---|---|---|
| Ptbp1 | pCS2+Flag | M. Claußen |
| CPEB1_S | pCS2+Flag | M. Claußen |
| CPEB1_S | pGEMT-easy | M. Claußen |
| CPEB1_S | pCS2+Myc | M. Claußen |
| CPEB1 RRM12ZZ wt | pBlueScript+HA | E. Belloc |
| CPEB1 RRM12ZZ 365 | pBlueScript+HA | E. Belloc |
| CPEB1 RRM12ZZ 395 | pBlueScript+HA | E. Belloc |

**Table 2.11 Constructs for *in vitro* transcription of *cpeb1_S* 3'UTR fragments**

| Insert | Vector | Kindly provided by |
|---|---|---|
| mGFP dnd1-LE F2 | pGEMT-easy | M. Claußen |
| mGFP ß-globin 3'UTR | pGEMT-easy | M. Claußen |
| mGFP cpeb1_S 3'UTR full | pSP64 | |
| mGFP cpeb1_S 3'UTR 1 | pSP64 | |
| mGFP cpeb1_S 3'UTR 2 | pSP64 | |
| mGFP cpeb1_S 3'UTR 3 | pSP64 | |
| mGFP cpeb1_S 3'UTR 4 | pSP64 | |
| mGFP cpeb1_S 3'UTR 5 | pSP64 | |
| mGFP cpeb1_S 3'UTR 6 | pSP64 | |
| mGFP cpeb1_S 3'UTR 7 | pSP64 | |
| mGFP cpeb1_S 3'UTR 1a | pSP64 | |
| mGFP cpeb1_S 3'UTR 1b | pSP64 | |
| mGFP cpeb1_S 3'UTR 1c | pSP64 | |
| mGFP cpeb1_S 3'UTR 1d | pSP64 | |
| mGFP cpeb1_S 3'UTR 1e | pSP64 | |
| mGFP cpeb1_S 3'UTR 1f | pSP64 | |
| mGFP cpeb1_S 3'UTR 1g | pSP64 | |

**Table 2.12 Control constructs for PCR**

| Insert | Vector | Kindly provided by |
|---|---|---|
| odc | pGEMT-easy | T. Klisch |

**Table 2.13 Constructs for the preparation of *in situ* probes**

| Insert | Vector | Kindly provided by |
|---|---|---|

| | | |
|---|---|---|
| mgfp5 (Koebernick, 2010) | pGEMT-easy | T. Klisch |
| Pgat (Hudson and Woodland 1998b) | pBluescriptSK | J. Loeber |
| cpeb1_S | pGEMT-easy | |

**Table 2.14 Primary antibodies**

| Name | Company | Source | Dilution |
|---|---|---|---|
| Flag | Sigma | Rabbit | 1.500 |
| CPEB1 | Trenzyme | Rabbit | 1:500 |
| CPEB1 | Weil, 2005 | Mouse | 1:500 |
| Dazl | Mita, 2000 | Mouse | 1:10 000 |

**Table 2.15 Secondary antibodies**

| Name | Company | Source | Dilution |
|---|---|---|---|
| IRDye 800CW Goat anti-Mouse | Li-COR | Goat | 1:20 000 |
| IRDye 800CW Goat anti-Rabbit | Li-COR | Goat | 1:20 000 |
| IRDye 680CW Goat anti-Mouse | Li-COR | Goat | 1:20 000 |
| IRDye 680CW Goat anti-Rabbit | Li-COR | Goat | 1:20 000 |

**Table 2.16 Commercially available kits for nucleic acid analysis**

| Method | Kit | Manufacturer |
|---|---|---|
| DNA isolation, DNA gel extraction | Invisorb DNA CleanUp Mini Kit | Stratec biomedical |
| RNA clean-up (Digoxigenin, Fluorescein labelled) | RNeasy Mini Kit | Qiagen |
| Cap mRNA clean-up | Illustra RNA spin Mini Kit | GE Healthcare |
| Plasmid isolation mini | GeneJET Plasmid Miniprep Kit | Thermo Scientific |
| Plasmid isolation midi | NucleoBond Xtra Midi/Maxi Kit | Macherey-Nagel |

### 2.8 EQUIPMENT LIST

All commodities and appliances were purchased from the following companies: Eppendorf (Hamburg), Falcon (Heidelberg), Schütt (Göttingen), Greiner (Frickenhausen), Qiagen (Hilden), Sarstedt (Nürnbrecht), Thermo Fisher Scientific (Karlsruhe), Perkin Elmer (Rodgau), Boehringer Ingelheim (Ingelheim am Rhein), Life Technologies (Darmstadt).

NanoDrop-2000c Spectrophotometer (Thermo Fisher Scientific)

UV-trans-illuminator (Bio-Rad)

GDS documentation system (INTAS)

Thermomixer comfort (Eppendorf)

SteREO Lumar.V12 (Zeiss)

LSM780 (Zeiss)

Typhoon 9400 (GE Healthcare Life Sciences)

Fastblot B34/B44 (Biometra)

Needle puller PN-30 (Narishige)

## 2.9 PLASMIDS

**pCS2+Flag**

The pCS2+ vector is optimal for protein expression in *X. laevis* embryos. The Flag epitope facilitates detection of proteins for which there are no available antibodies. The backbone comprises the simian cytomegalovirus IE94 enhancer/promoter sequence, a viral SP6 promoter, the sequence encoding the Flag-epitope 'DYKDDDK' at the 5' of the polylinker sequence, a T7 promoter in reverse orientation and SV40 viral polyadenylation signal. The SP6 promoter allows the *in vitro* transcription of sense mRNA for microinjection. The SV40 facilitates polyadenylation and the T7 promoter allows antisense probe synthesis (Rupp et al. 1994).

**MT-pCS2+**

Contains the pCS2+ vector backbone and the sequence encoding for the hexameric repeat of the Myc epitope tag (Rupp et al. 1994), allowing for Myc-tagged protein expression.

**pGEM-T easy**

This vector is a commercially available and convenient system for cloning of PCR products. The backbone contains a T7 and a Sp6 polymerase promoter, single 3´-T overhangs within the multiple cloning site that enhance ligation efficiency, and an amp$^r$. The multiple cloning site is located within the region coding the enzyme beta-galactosidase, enabling blue/white selection on IPTG/Xgal plates due to the disruption of the gene upon successful cloning (Promega).

**pMAL$^{TM}$-c2**

This commercially available vector provides a means for expressing and purifying an MBP-tagged protein. The cloned gene is inserted downstream from the *malE* gene of *E.coli*, encoding for maltose binding protein (MPB). The backbone contains a *tac* promoter, amp$^r$ malE gene upstream from the beta-galactosidase coding region, allowing for blue/white selection on ITPG/Xgal plates (New England Biolabs).

**pSP64**

The vector pSP64, a standard cloning vector, can be used for *in vitro* transcription from the SP6 promoter (Promega). The modified pSP64-mGFP5 expression vector, kindly provided by E. Raz (Institute of Cell Biology, Münster, Germany), was employed for chimeric reporter construct expression.

## 2.10 METHODS

All molecular biology standard techniques, such as polymerase chain reaction, analysis of DNA and RNA, and enzymatic reactions, bacterial protein synthesis and plasmid propagation were performed according to Sambrook (Sambrook 2001).

### 2.10.1 Construct generation

**Flag-tagged protein expression constructs**

For protein expression in embryos/oocytes and *in vitro* translations, Myc-tagged CPEB1, Flag-tagged CPEB1, Flag-tagged Ptbp1 (Ptbp1) in the pCS2+Flag vector were kindly provided by Maike Claußen. For generating the Flag-tagged GFP construct, the *gfp_orf* was enzymatically excised (EcoRI and XhoI) from the pSP64mGFP-XDE-LE construct and ligated into the pCS2+Flag vector, generating a construct encoding for Flag-GFP with a predicted molecular weight of 28.23kDa. The ORF of CPEB1 was cloned into the pCS2+ vector by excising the coding sequence from pGEXGp1_CPEB1 construct (kindly provided by Maike Claussen) with BamHI and XhoI and ligating into the pCS2+ vector via sticky end ligation. The Myc-tagged CPEB1 construct was generated by excising the CPEB1 coding sequence from the pCS2+Flag-CPEB1 construct with EcoRI and XhoI and ligating into the pCS2+Myc.

**MPB-tagged protein expression constructs**

For bacterial expression of MPB-tagged CPEB1_S protein regions, the pGEMT_CPEB1-ORF-3'UTR was used as template. Segments corresponding to the 71-892nt and 755-1777nt *cpeb1_S_orf* were amplified with primers containing flanking sequences for enzyme restriction (XbaI and EcoRI). After PCR amplification, the products were digested with the corresponding enzymes to generate sticky ends, which enhance the ensuing ligation into the multiple cloning site of pMAL-c2 vector downstream of MBP. Two chimeric proteins were generated with the MBP-N-terminus-CPEB1 at a predicted molecular weight of 72.56kDa and the MPB-C-terminus-CPEB1 at a predicted molecular weight of 80 kDa.

**Constructs for *in vitro* transcription of capped sense mRNAs for microinjection**

The High Fidelity Amplification Kit (Fermentas) was used according to the protocol provided by the manufacturer for the amplification of 3'UTR segments. The pGEMT_CPEB1-ORF-3'UTR generated by 5'RACE from oocyte stage III cDNA (kindly provided by Maike Claußen was used as a template for 3'UTR fragmentation Sequences were amplified and purified with the Invisorb DNA CleanUp Mini Kit. Direct ligation into the pGEMTeasy vector served as an intermediary step. Then, fragments were amplified with enzyme restriction sites (XhoI and NotI) used for the generation of sticky ends for enhanced ligation into the pSP64mGFP vector. Vector preparation involved restriction digestion with the XhoI and NotI enzymes of the

pSP64mGFP-XDE-LE template, followed by size separation on a 1 % agarose gel, excision, extraction and purification from the gel and dephosphorylation with SAP to prevent self-ligation. The pSP64_mGFP_dnd1-LE was kindly provided by E. Raz and ß-globin-3'UTR in pGEMTeasy was kindly provided by Maike Claußen.

### 2.10.2 Plasmid DNA isolation and purification

Analytical amounts of plasmid DNA (miniprep) were isolated with the GeneJET Plasmid Miniprep Kit and plasmid DNA in preparative amounts (midiprep) with the NucleoBond Xtra Midi/ Maxi Kit according to the protocol provided by the manufacturer. The plasmid DNA was eluted in 50 µl RNase free H2O. DNA concentrations were measured using the NanoDrop-2000c spectrophotometer (blank measurement for HPLC water).

### 2.10.3 Plasmid DNA restriction digestion

For analytical digests, 200-500 ng DNA were incubated for 30 min-2 h at 37°C with 2-10 U of an appropriate enzyme in the corresponding enzyme buffer in a total reaction volume of 20 µl. For preparative digests, 1-5 µg DNA were digested in a total reaction volume calculated according to the DNA amount – 1 µg per 10 µL volume – for a time interval varying between 4h at RT and 16h at 16°C. The enzyme volume was less than 10% of total volume to prevent star activity (Fermentas).

### 2.10.4 Agarose-gel electrophoresis

DNA/RNA fragments were separated using standard agarose gel electrophoresis (Fisher and Dingman 1971; Helling et al., 1974). 6x loading buffer (Fermentas) and Gel Loading buffer II (Ambion) were added to the DNA and RNA samples respectively. Samples were run 1 % (w/v) agarose gels prepared with 1x TAE buffer and 0.5 µg/ml EtBr (Sharp P. A. 1973). Gel run parameters: 80 -100 V in 1x TAE for 20-30 min. Standard DNA ladders were used to determine the sizes of DNA/RNA fragments (High, Middle or Low Range, Fermentas). A UV-transilluminator was used for visualization of DNA/RNA and the INTAS GDS documentation system for documentation.

### 2.10.5 DNA fragment isolation from agarose gels or restriction digest

PCR amplification products were purified from agarose gels or restriction digestion mixtures with the Invisorb DNA CleanUp Kit according to the provided protocol. DNA was eluted with 20-50 µL HPLC-water.

### 2.10.6 Polymerase chain reaction

DNA fragments were amplified by standard PCR (Bartlett and Stirling, 2003) using the High Fidelity Amplification Kit (Fermentas) and the DreamTaq polymerase (Thermo Scientific) or GoTaq polymerase (Promega) for analytical amplifications. The reaction mix contained the following in a total volume of 20 µL:

| Component | Volume (µL) | PCR program | |
|---|---|---|---|
| Buffer (10x) | 2 | 95°C | 3 min |
| dNTPs (10mM) | 0.4 | 95°C | 45 sec |
| Fw primer (10 µM) | 0.4 | 56°C | 45 sec |
| Rev primer (10 µM) | 0.4 | 72°C | 3 min |
| Template (10 ng) | 2 | Repeat 30x | Steps 2-4 |
| Polymerase (5U/µL) | 0.5 | 72°C | 5 min |
| dd$H_2O$ | 14.3 | 12°C | pause |

### 2.10.7 DNA Sequencing and Sequence Analysis

Sequencing was performed using the 3130 XI Genetic analyzer (Applied Biosystems, HITACHI) with the Big Dye Terminator Cycle Sequencing Kit based on the following protocol (Sanger et al., 1977):

| Component | Volume (µL) / Quantity (ng) | PCR program | |
|---|---|---|---|
| Plasmid/PCR fragment | 200 – 400 ng | 95°C | 3 min |
| Primer (10 mM) | 0.8 | 94°C | 45 sec |
| Sequencing Buffer (5x) | 1.5 | 56°C* | 45 sec |
| dd$H_2O$ | 5.7 | 60°C | 3 min |
| Seq Mix | 1.5 | Repeat 24x | Steps 2-4 |
| Total volume | 10 | 12°C | pause |

* annealing temperatures were adjusted for each oligonucleotide

Product purification involved the following steps: addition of 1 µl EDTA (125 mM), 1 µl NaAc (3 M, pH 5) and 50 µl 100 % ethanol; incubation for 5 min at RT; 20 min centrifugation at 13000 rpm; washing pellet with 70 % ethanol; 5 min centrifugation at 13000 rpm. The air-dried pellet was resuspended in 15 µl HiDi. The analysis of the retrieved sequences was performed using the DNA Star programs (Inc. Madison, USA).

### 2.10.8 Ligation of DNA Fragments

DNA fragments were ligated in the appropriate vector with 5 U T4 DNA ligase (Fermentas, Germany) in a total volume of 10 µl, with an insert to vector ratio of 3:1 (w/w). The ligation mixture was incubated at 16°C overnight (Sambrook, 2001).

### 2.10.9 Chemical transformation

Ligation products were transformed into the chemical competent E.coli XL1-Blue as follows: 200 µl competent cells were thawed on ice for 20 min, 5 µl ligation mix were added, cells were incubated on ice for 30 min and heat-shocked at 42°C for 90 sec. The tubes were placed on ice for 2 min, 800 µL room-temperature LB-medium was added and cells were incubated at 37°C for 30-40 min at 150 rpm. Subsequently, the cells were pelleted by centrifugation at 4 000 rpm for 1 min and the supernatant was

removed such that only approximately 100 µL would remain for resuspension of the bacterial pellet. Cells were plated on LB plates containing the appropriate antibiotic and/or IPTG/XGal; IPTG (100 mM stock, 100 µl/plate), X-gal (100 mM stock, 100 µl/plate)). Colonies were grown overnight at 37°C (Sambrook 2001). Single colonies were innoculated into LB-medium containing 100 µg/ml ampicillin and incubated overnight on a rotary shaker (220rpm) at 37°C. The bacterial cells were pelleted and used for plasmid isolation or stored at -20°C until further use.

### 2.10.10 *In vitro* synthesis of capped sense mRNA

*In vitro* capped sense mRNA for microinjection procedures was synthesized using the "SP6/T3/T7 mMESSAGE mMACHINE" Kit (Ambion Inc.) following the protocol provided by the manufacturer. For a 10 µl reaction, 200-500ng linear template DNA was used. Reactions were incubated for 2-3h at 37°C. The synthesized mRNA was purified with the IllustraTM RNA Spin MiniRNA Isolation Kit (GE Healthcare). The mRNA was eluted in 15 µL RNase-free water at room temperature, aliquoted and stored at -80 °C.

### 2.10.11 *In vitro* synthesis of Digoxigenin and Fluorescein-labeled antisense RNA

Synthesis of labeled antisense RNA for whole mount in situ hybridization (WMISH) was performed as follows:

| Component | Volume (µL) / Quantity (ng) |
|---|---|
| Linearized template DNA | 9 µL (approx. 1 µg) |
| Transcription buffer (5x) | 5 µL |
| Dig mix (10 mM; DIG/Flu-rUTP – 0.36 µL and 0.64 µL rUTP) | 1 µL |
| rATP (10 mM) | 1 µL |
| rCTP (10 mM) | 1 µL |
| rGTP (10 mM) | 1 µL |
| DTT (750 mM) | 1 µL |
| RNA polymerase (Sp6/T7) | 1 µL |
| Pyrophosphatase | 0.5 µL |
| RNase Out (Ribolock) | 0.5 µL |
| RNase-free $H_2O$ | 3 µL |
| Total Volume | 25 µL |

The reaction was incubated for 2 h 30 min at 37 °C and then the DNA template was digested with TURBO DNase (2 U/µl, Ambion) for 15 min at 37 °C. The *in vitro* transcribed RNA was purified with the RNeasy Mini Kit (Qiagen) and was eluted in 50 µL RNAase free dd$H_2O$. The quality RNA was analyzed on a 1 % agarose gel. ,

### 2.10.12 Extraction of total RNA from *X. laevis* Oocytes and Embryos

Snap frozen embryos or oocytes were lysed in 500 µL peqGOLD TriFast (peQlab) with a Omnican 40 syringe (Braun) and vortexed for 30 sec. Then 80 µL chloroform were added, the sample was vortexed for 30 sec

followed by centrifugation for 10 min at 4 °C and 13000 rpm. The upper phase containing the total RNA (approximately 200 µL), was transferred to a new eppendorf tube, 200 µL chloroform were added. The sample was vortexed for 30 sec and centrifuged for 10 min at 4 °C and 13000 rpm. The upper phase was transferred into a new eppendorf tube and one volume of isopropanol was added. Samples were vortexed and incubated at -20 °C overnight for RNA precipitation. After 30 min of centrifugation at 4 °C and 13000 rpm, the pellet was washed with 500 µl of 70 % ethanol and centrifuged for 5 min at 4 °C. The ethanol was removed, the pellet was air-dried and dissolved in 12.5 µL RNase-free water. Genomic DNA digestion was performed for 1h at 37°C with DNase I (1U/ µL) (Thermo Scientific). Inactivation of DNase I by incubation for 10 min at 80°C ensued.

### 2.10.13 Generation of cDNA by reverse transcription

Total RNA was reverse transcribed following the protocol:

| Component | Volume (µL) | PCR program | |
|---|---|---|---|
| Random hexamer mix | 200 – 400 ng | 22°C | 10 min |
| MuLV RTase | 0.8 | 42°C | 1 hour |
| RNase Out | 1.5 | 99°C | 5 min |
| Template (100 ng) | 5.7 | 4°C | pause |
| RNase free dd$H_2O$ | 1.5 | | |
| Total volume | 10 | | |

Random hexamer mix composition for a total volume of 750 µL: dNTP mix (10 µM each) 100 µL, $MgCl_2$ (25 mM) 200 µL, 5x PCR-buffer 200 µL, RNase free water 200 µL, Random hexamers 50 µL.

### 2.10.14 Semiquantitative real-time PCR

Total mRNA obtained from oocyte and embryos at the stages of interest was reverse transcribed and amplified with specific primers for CPEB1 (28/30 cycles) and ornithine decarboxylase (ODC, 25 cycles). A standard reaction with a 12.5 µL total reaction volume contained 2 µL cDNA, 1x Green Go Taq Flexi buffer, 0.2 µM RT primers forward and reverse, 1.5 mM MgCl2 and 0.5 U Go Taq polymerase (Mullis, 1986). ODC served as a control for equal starting material. DNA contamination was tested for by amplifications without cDNA.

### 2.10.15 Whole mount *in situ* hybridization (WMISH)

Whole mount *in situ* hybridization on whole embryos allows the detection of RNAs in a spatially resolved fashion and was performed as previously described (Harland 1991, Hollemann and Pieler 1999). Embryos were fixed at the desired stage in 1x MEMFA for 1h at RT, followed by 3 wash steps with 100% ethanol. The fixed embryos were rehydrated step-wise (100% ethanol, 75 % ethanol – 25 % PTw, 50 % ethanol – 50 % PTw, 25 % ethanol – 75 % PTw), washed 3x 5min in PTw and permeabilized with 10 µg/ml proteinase K in

PTw for the appropriate length of time according to embryonic stage (16 min stage 28-32). Subsequently, proteinase K was inactivated by 2x washes in 0.1 M triethanolamine, pH 7.5. Then the embryos were acetylated by adding 25 µl acetic anhydride to fresh triethanolamine twice. Each of the previous steps lasted 5 min. Embryos were washed 2x 5 min in PTw and refixed in PTw containing 4 % formaldehyde for 20 min, washed five times in PTw, transferred to Hyb Mix and incubated for 5 h at 65°C. Following this pre-hybridization step, the samples were incubated with the digoxigenin/fluorescein asRNA probes for 14 - 16 h at 65°C. The following day, the asRNA probes were collected, embryos were washed in Hyb Mix, and washed 3x for 20 min in 2x SSC at 65°C. Non-hybridized asRNA probe was digested with 20 µg/ml RNase A and 10 U/ml RNase T1 in 2x SSC for 1 h at 37°C. Samples were washed 2x 10 min in 2x SSC at RT, 2x 30 min in 0.2x SSC at 65°C for 30 min each, and 2x 15 min in MAB. Then blocking was performed by the addition of MAB/BMB for 20 min and MAB/BMB/Horse serum for 40 min to minimize unspecific binding of the antibody. The antibody (1:5000 in MAB/BMB/HS) incubation followed for 4 h at RT. Thereafter, embryos were washed 3x 10 min followed by overnight incubation in MAB. After 3x 5min washing with MAB, the caps were exchanged and alkaline phosphatase buffer (APB) was used in the following steps. After 3x 5min washes in APB, the embryos were incubated in the color reaction solution (APB+NBT/BCIP). When the signal was clearly detected, the color reaction was stopped and background staining removed by washing the embryos with 100 % methanol. Then the embryos were washed with 50% methanol and $ddH_2O$, and then fixed in MEMFA for 20 min and stored at 4°C.

Double in situ hybridization was the same as the normal procedure with the following modifications: both Dig and Flu-labeled asRNA probes were added to the samples overnight. The first color reaction performed was for the Fluorescein as the signal is reduced in intensity as compared to the Digoxigenin probe. A FastRed tablette (Roche) was dissolved in 2mL 100mM TrisHCl (pH 8.2) and added to the samples for an overnight incubation at 4°C. The following day, the reaction was stopped by incubation in 1xMAB 100mM EDTA at 65°C for 10 min. Then the samples were washed two times more in 1xMAB and the procedure was repeated from the second day was for developing the color reaction for the second dye.

### 2.10.16 Embryo bleaching and clearing

To remove pigmentation, the samples were washed 2x 5min in 0.5x SSC, followed by an incubation in bleaching solution for 2h at RT. Bleached embryos were washed 2x with 0.5x SSC and fixed in MEMFA for an hour at RT. To clear the embryos, the MEMFA solution was replaced by 100% methanol for at least 1 hour and then the embryos were cleared with BB:BA (1:1 ratio) for counting PGCs located in a deeper layer in the endoderm. After counting, the embryos were washed 3x 2min in 100% methanol and were transferred back to the vial in 100% methanol.

### 2.10.17 Protein isolation from *X. laevis* embryos and oocytes

For total protein extraction, 5 or 6 flash-frozen embryos or oocytes were lysed with 50 µL 1x IPP145 CoIP buffer using a Micropestle (Eppendorf). For CoIP experiments, 5 µL/oocyte and 10 µL/embryo 1x IPP145 buffer was used for homogeniztion. Lysates were centrifuged at 4°C and 13000 rpm for 15 min, the upper

clear phase was transferred into a new eppendorf tube and another centrifugation at 4°C and 13000 rpm for 15 min ensued for the removal of yolk proteins. The clear phase was transferred to a new eppendorf tube an appropriate volume of 2x SDS Loading buffer was added. The samples were used either for immunoprecipitation or western blotting. Samples were stored at -20°C until further use.

### 2.10.18 Immunoprecipitation using oocyte and embryo lysates

Immunoprecipitation (IP) of *in vivo* expressed proteins, either in oocytes or embryos was performed as follows. Stage VI oocytes and two-cell stage embryos were injected with 1.2ng and 2.5 ng transcripts encoding for FLAG-epitope-tagged proteins. The embryos were injected in the vegetal hemisphere, close to the cleavage furrow, to target the germ plasm. Embryos were cultured until stage 13 and oocytes were incubated for 24h. 100 embryos per sample and 200 oocytes per sample were collected and flash-frozen in liquid nitrogen and stored at -80°C. Total protein extraction proceeded as described above and a 60 µl input aliquot was taken from each sample and 80 µl 2x SDS Loading buffer were added. The remaining of the protein lysate was incubated for 3-4h at 4°C, end-over-end rotation, with 30 µL FLAG antibody coupled beads (Sigma), which were previously equilibrated to the buffer by 4-5x washing steps with 1mL 1x IPP145 buffer. After incubation, the samples were centrifuged for 1min at 800 rpm to prevent the alteration of the beads. A 60 µL sample of the supernatant was taken, the rest was discarded and the pelleted beads were washed 4-5 times with 1mL 1x IPP145 buffer. Beads were resuspended in 100 µL 2x SDS buffer, boiled at 70°C for 10 min, centrifuged once more, then the supernatant was transferred to a new eppi as the IP fraction and the an additional volume of 50 µL was added to the beads, which will serve as a control for protein dissociation from the beads. For each fraction, 40 µL were used in the following experiments.

### 2.10.19 *In vitro* transcription coupled translation (TNT)

The *in vitro* transcription coupled translation-assay was performed using the TNT Coupled Reticulocyte Lysate System (Promega) according to the protocol provided by the manufacturers. TNT reactions were carried out in volumes of 12.5 µl using 1 µg of plasmid DNA. Incubation times ranged from 2 h to 2 h 30 min at 30°C.

Translational MO efficiency was verified by the addition of the tMO (concentrations 0.1mM to 8mM) in the TNT reaction mix and monitoring protein levels by western blot.

### 2.10.20 SDS-PAGE electrophoresis

SDS polyacrylamide gels (12%) were prepared for protein analysis (Laemmli 1970). Samples were loaded onto the gel along with PageRuler Prestained Protein Ladder (Fermentas) for Western Blot analysis and for Coomassie Blue staining. The gel run was performed in 1x Laemmli running buffer at 80 V for an hour for the stacking gel and 180 V for 2-3 hours for the resolving gel.

### 2.10.21 Western Blot Analysis

After SDS-PAGE, proteins blotted onto a Propan Nitrocellulose membrane (0.45 µm, Whatman) (Towbin et al. 1979) using a semi-dry blotting technique. Blotting was carried out in Protein Blotting buffer (semi dry) for 1 h applying 40 V. After blotting, the membrane was incubated for 1 h at RT in 5% non-fat milk TBST blocking solution. After blocking, the membranes were incubated with anti-CPEB1 (1:500 rabbit, polyclonal; mouse, monoclonal from D. Weil), anti-flag (1:1000, rabbit) overnight at 4 °C. The next day, the membrane was washed three times for 10 min each, with TBST at RT. Horseradish peroxidase (HRP) coupled or fluorescent IRDyes coupled (LI-COR) secondary antibodies in blocking buffer were added and incubated at RT for 1 h. The membrane was washed three times for 10 min each, with TBST at RT. HRP-activity was detected using the ECL Kit SuperSignal West Dura (Pierce) on X-ray detection films (Amersham). Fluorescent signals were detected using the LI-COR Odyssey Infrared Imaging system.

### 2.10.22 Coomassie Blue Staining

The procedure was performed according to an online available protocol from Roger Rowlett, Colgate University for rapid ethanol-based Coomassie Blue staining of SDS-polyacrylamide gels. After the gel run, the SDS-PAGE was rinsed for 1 h in ddH2O. In between the water was changed for three times. After rinsing, Coomassie staining solution was added. Gel was incubated in the Coomassie staining solution for 15-60 minutes until the bands were detectable. The staining solution was removed and the gel was rinsed with water to remove excess of staining solution. Coomassie destaining solution was added. The gel was destained until the background was removed. Destained gels were rinsed thoroughly with and stored in distilled water.

### 2.10.23 Bacterial protein expression of MBP-CPEB1-N-terminus

MBP-CPEB1-N-terminus was expressed in the E. coli strain BL21 (DE3). Cells were disrupted using a fluidizer and proteins were resuspended in 2x SDS buffer. Samples were stored at -20 °C.

### 2.10.24 Nitrocellulose membrane based antibody purification

The MPB-CPEB1-N-terminus protein fusion was run on an SDS-PAGE gel (12%) and was blotted on a nitrocellulose membrane. The band corresponding to the fusion protein was cut out, poorly bound protein was removed by soaking in acidic glycine buffer for 5 min and the membrane was blocked with 5% non-fat milk in TBS for 1h at RT with gentle rocking. After 2x 5min washes in TBS, a dilution of serum (1:1 serum:TBS) was incubated with the membrane strip overnight at 4$^{o}$C with end-over-end rotation. The supernatant was recovered and the antibodies were eluted with 1mL acidic glycine buffer, then transferred to 1mL 1M tris pH 8.0, which should bring the final pH of the solution to pH 7. The membrane stripes were

stored in PBS supplemented with 5mM Sodium azide. The antibody eluate is stabilized by the addition of Bovine Serum Albumin to 1 mg/mL and 5mM sodium azide.

### 2.10.25 Whole mount immunofluorescence

Immunostaining of embryos was tested with the protocols of Dubaissi et al., 2012 and of Gagnon and Mowry 2011a. Embryos were fixed in MEMFA, Dent's fix or glyoxal solution (kindly provided by Dr. N. Revelo). In case they were fixed with Dent's fix, the embryos were rehydrated in a step-wise manner and then they were subjected to the procedure. The protocol from Gagnon and Mowry proved most successful and was used for several experiments to verify the localization of CPEB1 in parallel to that of Dazl/GFP-XDE-LE. Primary antibodies used: anti-CPEB1 (mouse polyclonal, Trenzyme), anti-Dazl (kindly provided by Mita, 2000) and anti-GFP (mouse, Roche). Secondary antibodies were anti-mouse-Alexa633 (A21052, Invitrogen), and anti-rabbit-Oregon-Green488 (O-11038, Invitrogen). All antibodies were diluted 1:500 in PBT + 2 % horse serum + 2 % BSA, except for anti-CPEB1 which was diluted 1:50. Negative controls: $2^{ry}$ antibodies only.

### 2.10.26 Mass spectrometry analysis of Flag-CPEB1 candidate protein interaction partners

The proteins obtained as described (see 2.10.18) were separated on precast TG PRIME Tris/glycine 8-16% gradient gels (Serva) and visualized by colloidal Coomassie staining. Entire gel lanes were cut into 24 equally-sized pieces with the help of a self-made punching tool and were subjected to automated in-gel tryptic digestion (Schmidt et al., 2013). The obtained tryptic peptides were dried in a vacuum centrifuge, re-dissolved in 0.1% trifluoro acetic acid. For quantification purposes, the samples were spiked with 2.5fmol/ µL yeast enolase 1 tryptic digest standard (Waters Corporation, Silva et al., 2006).

In the following step, tryptic peptides were reverse-phase separated over one hour at a flow rate of 300 nL/min with a linear gradient of 1-45% mobile phase B (acetonitrile containing 0.1% formic acid) and mobile phase A (water containing 0.1 % formic acid) on a nanoAcquity UPLC system equipped with a Symmetry C18 5 µm 180 µm x 20 mm trap column and a BEH C18 1.7 µm, 75 µm x 100 mm analytical column (Waters Corporation).

Tryptic peptides were run on a Synapt G2-S quadrupole time-of-flight mass spectrometer equipped with ion mobility option (Waters Corporation). Positive ions in the mass range m/z 50 to 2000 were acquired in the ion mobility-enhanced data-independent acquisition (DIA) mode with a typical resolution of at least 20000 FWHM (full width at half maximum, Silva et al., 2005, Geromanos et al., 2012) with drift time-specific collision energies (Distler et al., 2014). To identify the proteins, the Waters ProteinLynx Global Server version 3.0.2 (Li et al., 2009) was used for searching and processing of continuum LC-MS data (including lock mass correction). The Swiss-Prot/TrEMBL *Xenopus laevis* proteome (UniProtKB release 2016_05; 16,398 entries; 3402 reviewed; 12996 unreviewed) together with the sequence information for porcine trypsin, yeast 1 enolase, flag-tagged CPEB, GFP and Ptbp1 and the reversed sequence of each entry were compiled into a custom database used for protein identification and false discovery rate (FDR) determination.

Precursor and fragment ion mass tolerances were automatically determined by PLGS 3.0.2 (typically below 5ppm (root mean square) for precursor ions and below 10 ppm for fragment ions). Carbamidomethylation of cysteine was specified as fixed and oxidation of methionine as variable modification. One missed trypsin cleavage was allowed and the FDR for protein identification was set to a threshold of 1%.

For post-identification analysis, the 24 LC-MS datasets per gel lane were merged and the absolute in-sample amounts for each detected protein were calculated according to the TOP3 quantification approach with the freely available software ISOQuant (http://www.isoquant.net; Distler et al., 2014; Kuharev at al., 2015). The stringency for reporting a protein was further increased by considering only peptides with a minimum length of six amino acids, with scores above or equal to 5.5 FDR. Only Proteins reported by two or more peptides were quantified.

More than 675 proteins were identified for each sample. For selecting the top candidates and removing false positives, stringent thresholds were used. Several parameters were considered, namely pulled down amounts (> 5 ng), protein coverage (>30%), reported peptide number (> 8), QC score (< 0.02), fold changes respective to the negative controls (> 6), FDR (1%).

### 2.10.27 *X. laevis* embryo culture and microinjections

In female *X. laevis* female frogs ovulation was induced by injection of 1000 units human chorionic gonadotropin (hCG, Sigma Aldrich) into the dorsal lymph sac, approximately 16 hours before supposed egg-laying. Eggs were *in vitro* fertilized with 0.1 x MBS minced testis. Fertilized eggs were dejellied with 2 % cysteine hydrochloride, pH 7.8 - 8.0 for 5 min, dead embryos were removed and the remaining embryos were cultured in 0.1 x MBS at 12.5 – 18 °C. Injections were performed in injection buffer on a cooling plate (12.5 - 16 °C). For microinjections, the solutions were loaded into the glass needles (Science Products, GB 100F-8P) prepared on a needle puller. Two cell stage embryos were injected vegetally with 4.2 nl of the injection solution were injected per blastomere. Then, embryos were kept for at least 30 min in injection buffer to allow healing and were thereafter were transferred into 0.1x MBS. At the appropriate stage the embryos were flash-frozen in liquid N2 for protein and RNA isolation or in 1x MEMFA for whole mount *in situ* hybridization. For WMISH the embryos were dehydrated in EtOH and stored in 100 % EtOH. For *X. laevis/tropicalis* hybrid embryo generation the *X. laevis* females were prepared as before, and an *X. tropicalis* male was injected with 20 units human chorionic gonadotropin (hCG, Sigma Aldrich) into the dorsal lymph sac approximately 16 hours before testes preparation. The next day, the male sacrificed and the testes was isolated as described above. The embryos were cultured at 12 °C until the desired stages was achieved. They were fixed in liquid nitrogen and used for RNA extraction.

### 2.10.28 Preparation of *X. laevis* testis

The *X. laevis* male frog was narcotized for 20 - 30 min at RT in 0.25% 3-aminobenzoic methanesulfonate solution. The frog was decapitated and testes were retrieved. The adipose tissue and the surrounding blood

vessels were removed, the testes was washed 3x with 1x MBS and were stored in 1x MBS buffer at 4 °C for ~ 1 week.

### 2.10.29 Oocyte culture and microinjection

Oocytes were isolated from adult, female *X. laevis.* The frogs were anesthetized for 20 min in 0.25% 3-aminobenzoic methanesulfonate solution and the operation per se was performed on ice. An incision measuring maximum 1cm was made in the skin and muscle layers on the lateral side of the abdomen. Oocyte sacks were gently pulled out and when the amount of oocytes was sufficient for the following experiments, the incision was sewed sequentially, first the muscle layer with at least three sutures and then the skin with 4 sutures. Oocytes were treated with 1 mg/ml liberase blendzyme (Roche) in collagenase-buffer to facilitate their release from the ovary. The oocytes were incubated in liberase blendzyme collagenase buffer for 1 hour 20 min with end over end rotation. Then, they were washed using 1x MBS until the buffer was clear and incubated at 18$^{o}$C. The staging was performed according to Dumont (Dumont 1972). Oocytes were injected in 1x MBS using the appropriate injection solution in 2.1 nl for stage I-III and 4.2 nl for IV-VI oocytes. The same materials were used like for embryo injection. The mRNA was diluted to a concentration of 450 ng/µl, before injection. Injected oocytes were cultivated at 18$^{o}$C for 24h in 1x MBS and in oocyte culture medium if longer, rinsed in 1x MBS before they were transferred to 1x PBS for immunofluorescence staining.

# 3. RESULTS

## 3.1 CPEB1 TRANSCRIPT LEVEL

### 3.1.1 CPEB1 TRANSCRIPTS ARE PRESENT IN PRIMORDIAL GERM CELLS

The establishment of spatially restricted protein production through mRNA localization is an important regulatory mechanism governing development. In *Xenopus laevis*, germline development depends on inheriting specific mRNAs and proteins. The germ plasm arises during early oogenesis through the localization of maternal determinants at the vegetal (Zhou and King 2004; Koebernick et al., 2010; Kloc et al., 2014). During embryogenesis, those cells that inherit the germ plasm will become primordial germ cells (PGCs). Therefore an important step in characterizing PGCs is identifying and characterizing transcripts specific only to these cells. Previously, we have shown that c*peb1* is a PGC-enriched transcript in a comparative RNA sequencing analysis where the overlap between the transcript pool specific to primordial germ cells and neighboring somatic endodermal cells was examined at late neurula and tailbud stages (Dzementsei, 2013).

Previous WMISH experiments showed similarity in *Cpeb1* transcript distribution to that of *pgat*, an established germline marker (Hudson and Woodland 1998; **Figure 3.1.B**). In order to confirm the germline identity of the cells where *cpeb1* transcripts were observed, double whole mount *in situ* hybridization with *pgat* was performed.

There are two versions of *cpeb1* in the genome of *X. laevis*. Recent Xenbase annotations assign the homologues according to which chromosome the gene is present on – either the short or long subgenome (XB-GENEPAGE-946166). *Cpeb1_S* and *cpeb1_L* transcripts (formerly *cpeb1_a* and *cpeb1_b*) share 94% identity nucleotide similarity score with 0 gaps (blastn, U.S. National Library of Medicine), hence the four antisense RNA probes covering most of the *cpeb1* open reading frame (ORF) are not expected to discriminate between the two homologues. For these transcripts a digoxigenin-labeled antisense RNA probe was used, which marks the presence of the RNA duplex in purple (**Figure 3.1. A**).

Primordial germ cell-associated transcript protein (*pgat/xpat*) mRNA is present in the mitochondrial cloud (MC) since early oogenesis stages and remains in the germ plasm during embryogenesis, rendering it a suitable, high-confidence germline marker (Hudson and Woodland 1998). Therefore, an antisense RNA probe against *pgat* was employed to mark PGCs. Due to its

higher abundance, the probe was labeled with fluorescein, which is detected in red after the color reaction (**Figure 3.1.A**).

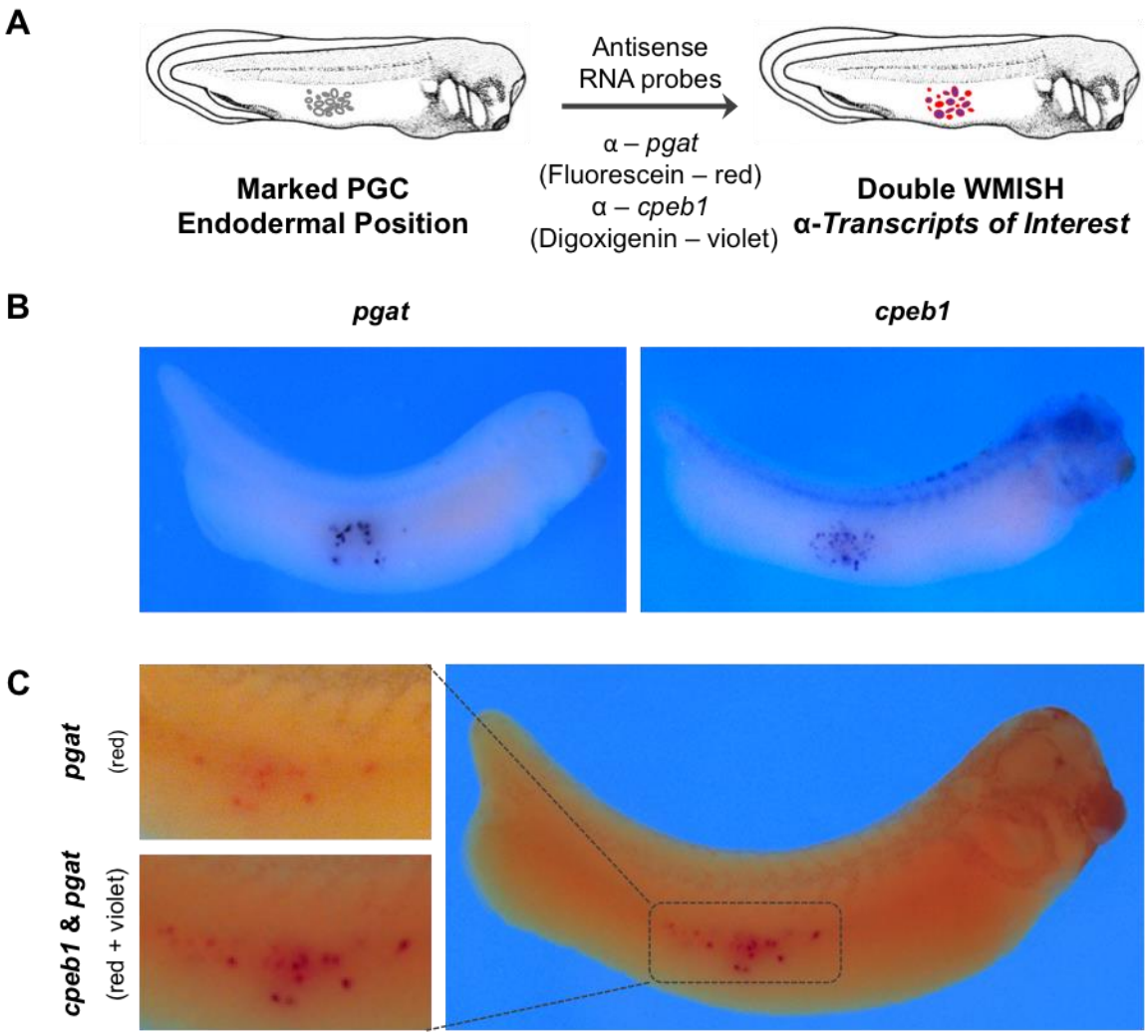


**Figure 3.1. *Pgat* and *cpeb1* transcripts colocalize in the germline in tailbud embryos.** A. WMISH asRNA probes hybridize with transcripts of interest, revealing their location. When the mRNAs are PGC specific, a punctate pattern is observed on the lateral side of the endoderm. dWMISH enables the detection of two transcript species, which may colocalize in the germline. B. Typical mRNA expression for endogenous *pgat* and *cpeb1* in tailbud embryos. C. *Cpeb1* and *pgat* colocalize in PGCs as shown in the right panel. The two In the left upper panel, *pgat* is detected after the fluorescein color reaction. Depicted in the left lower panel is the same area as above with both pgat and *cpeb1* transcripts marked by fluorescein and digoxigenin. N=2 biological replicates.

*Pgat* transcripts are present in the germline and *cpeb1* mRNAs recapitulate the pattern in tailbud embryos. In addition, *cpeb1* transcripts are also detected in the spinal chord, head and eyes (**Figure 3.1.B**). The colocalization of *cpeb1* and *pgat* in the double *in situ* hybridization experiment validates the germline identity of the cells where *cpeb1* transcripts are detected (**Figure 3.1.C**).

In the introduction the mRNA profile of *cpeb1* during early embryogenesis was illustrated as a classic maternally provided transcript, highly abundant until the MZT transition phase when degraded (Hake and Richter., 1994; Smarandache, 2013). Importantly, later during tailbud stages a resurgence in transcription resulting in low levels of *cpeb1* was detected by quantitative RT-PCR (Smarandache, 2013). By correlating this observation with the germline specific detection of *cpeb1* two questions arise. The first question addresses how post-transcriptional regulation of the *cpeb1* transcript at MZT takes place. The answer could have important implications for other germ plasm maternally derived mRNAs which could be regulated in a similar manner. Secondly, it would be interesting to see if the detectable mRNA is a result of zygotic transcription. Answering this question would bring insight into how germline specificity of *cpeb1* transcripts is achieved. Moreover, it would show the interplay between events occurring sequentially at different developmental time-points and their effect on development as a temporally and spatially regulated process.

### 3.1.2 Zygotic Transcription Begins at Stage 26

An elegant method employed for distinguishing the maternal from the zygotic pools of mRNA employs hybrid embryos obtained by crossing two closely related species (Yamaguchi et al., 2014). For this purpose *X. laevis* and *X. tropicalis* frogs were used for generating hybrid embryos. The transcript sequence similarity for the *cpeb1* ORF and three prime untranslated region (3'UTR) between the two species is 92%. This is a distinction that is sufficient for designing species specific primers.

The embryos from the two crossings will be referred to as *X.l * X.l* for the wild type *X. laevis* and as *X.l *X.t* for the hybrid embryos. The maternal mRNA pool is amplified with *X. laevis* primers and the zygotic pool with a combination of primers, *X. laevis* forward and *X. tropicalis* reverse. The resulting amplified segments were expected to run at approximately two hundred nucleotides for both maternal and zygotic transcripts (**Figure 3.2.**).

The embryonic stages obtained from the *X.l * X.l* crossing served as an archetype for the *cpeb1* maternally provided transcript profile. In the upper panel it is shown that the maternal mRNA is abundant before and degraded during gastrulation (St. 10-12.5). At tailbud stages, it is detected anew at low levels, all of which agrees with previously reported findings (Smarandache, 2013). The species specificity of the *X. tropicalis* primers is validated by the lack of amplification products from cDNA extracted from wild type embryos (**Figure 3.2.A**, middle panel).

The *X.l * X.t* hybrid embryos were used to identify the beginning of zygotic transcription for *cpeb1*. The upper panel depicts the maternal contribution and should recapitulate the profile for the *X.l * X.l* embryos for early stages, before degradation of the maternal pool. The zygotic *cpeb1* transcripts were detected with the *X.l* and *X.t* primer combination, shown in the lower panel (**Figure 3.2.B**). Zygotic transcription is first detected in tailbud stage 26 and continues throughout the analyzed developmental time-span.

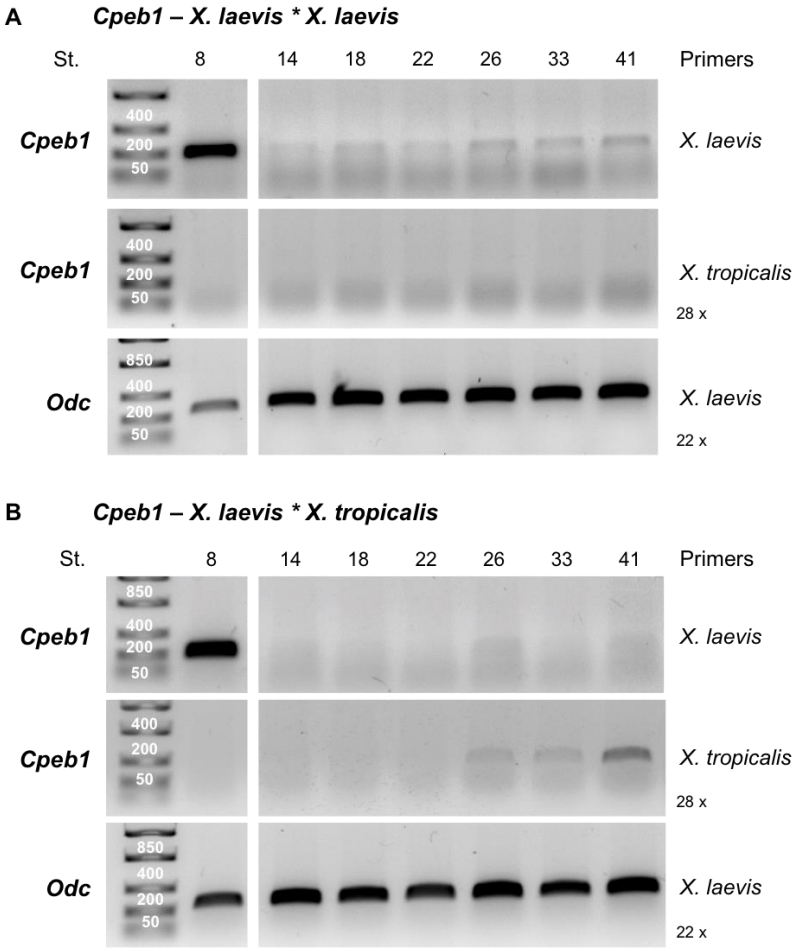


**Figure 3.2. Zygotic transcription starts at stage 26 and the number of transcripts is lower than during early embryogenesis.** *X. laevis* oocytes were fertilized either with *X. laevis* (A) or *X. tropicalis* (B) spermatozoa and embryos were collected at the indicated stages. Total mRNA was extracted, reverse transcribed and the cDNA was amplified with gene and species-specific primers, to distinguish between maternal and zygotic pools of transcripts, which are expected to run at 200 nucleotides (A). The upper panel of the *X.l * X.l* embryos shows the maternally provided *cpeb1*. The lower panel shows the negative control where the *X. laevis* with *X. tropicalis* primers were used for *X.l * X.l* cDNA amplification. B. Transcripts from hybrid embryos, *X.l * X.t* were also amplified with both sets of primers, as indicated in the upper and lower panels. Ornithine decarboxilase (*Odc*) served as a house keeping gene control. The blurred band running lowest on the gel corresponds to the primers. N=2 technical replicates.

### 3.1.3 REGULATION COORDINATED BY THE *CPEB1* 3'UTR

Transcript stability is dependent on three regions of the mature mRNA: the 5'UTR, the open reading frame and the 3'UTR. The 3'UTR harbors multiple regulatory elements, which can be recognized either by proteins which lead to mRNA processing or by miRNAs, which frequently lead to mRNA destabilization and depletion (Wormington, 1994; Yartseva and Giraldez, 2015).

Two remarkable findings brought the *cpeb1* transcript into the focus of my work. Firstly, *cpeb1* is present in the germline at tailbud stages, despite no obvious germ plasm enrichment in late oocytes (Dzementsei, 2013; Smarandache, 2013). Secondly, in an experiment to identify transcripts affected by miRNA-mediated decay, *cpeb1* levels were elevated more than seven fold as compared to control, uninjected embryos at stage 11 (Lund et al., 2009, 2011, Pfennig, 2014). This result supports the role of miRNAs in the regulation of *cpeb1*. Additionally, the 3'UTR was previously shown to be sufficient for the presence of reporter constructs in the germline (Smarandache, 2013). This was true for both *X. laevis* versions *cpeb1_S* and *cpeb1_L* (Smarandache, 2013). Therefore, to the best of my knowledge, *cpeb1* may be the first example of a transcript restricted to the germline primarily by somatic clearance via miRNA mediated decay.

Henceforth, the analysis is directed towards identifying regions of the 3'UTR responsible for *cpeb1* clearance during maternal-to-zygotic transition. The sequences of *cpeb1_S* and *cpeb1_L* are very similar throughout the transcript, with a calculated 3'UTR sequence similarity of 90% between the two versions (blastn, U.S. National Library of Medicine). Version *cpeb1_S* was selected for ensuing experiments, which involved a blind-folded approach towards separating the 3'UTR into fragments for analysis. To ensure that all sequences involved in regulation are found, the division of the 3'UTR was unbiased towards any specific region predicted *in silico* to contain miRNA target sites.

Reporter experiments were employed, where the fragments of interest were fused to the green fluorescence protein (GFP) coding open reading frame (ORF; similar to Yamaguchi et al., 2014). As GFP is an exogenous protein, it does not have any characteristic localization or function in the cell. When an mRNA coding only for the GFP ORF is injected vegetally, the transcript can be detected in the entire endoderm, similarly to the protein. However, at no stage were there any developmental defects observed. Therefore, the sequences fused to its ORF coding sequence dictate the fate of the *gfp* transcripts and the GFP protein. For comparison, *Dead end 1* localization element (*dnd1*-LE, 173 nucleotides), a somatically depleted germline specific sequence served as a PGC specific positive control (Horvay et al., 2006; Koebernick et al., 2010). Additionally, the full length 3'UTR reporter was included as a positive control in all fragmentation

experiments. The reporter constructs were microinjected vegetally in both blastomeres of two-cell stage embryos. The area located laterally to the cell cleavage furrow was aimed for in order to enrich the reporter amounts in the germ plasm (**Figure 3.3 A**). The distribution of the reporter was visually analyzed at tailbud stages (between stage 28 and 34), when germline cells are in their migratory phase. At this time PGCs translocate laterally and then dorsally in the endoderm allowing for easier detection close to the endodermal wall (Whitington and Dixon, 1975; Terayama et al., 2013).

The 3'UTR was fragmented in five consecutive fragments with overlapping regions (**Figure 3.3 A**). The first and third fragments were depleted in the soma most efficiently and restricted to the germline. The other three fragments were moderately depleted in the soma and also present in the germline (**Figure 3.3 B**). An *in sillico* prediction with the program miRanda identified a potential miR-18 target site in the first fragment. As this miRNA was previously shown to be involved in somatic depletion of mis-localized germline transcripts (Koebernick et al., 2010) I decided to focus on verifying whether the minimal region involved in somatic depletion of fragment 1 encompasses the miR-18 putative target site. Therefore, the following experiment was generating 3' and 5' sequential deletions of the fragment 1 sequence. Their regulatory effect on the behavior of the injected reporter was analyzed as described for the previous experiment.

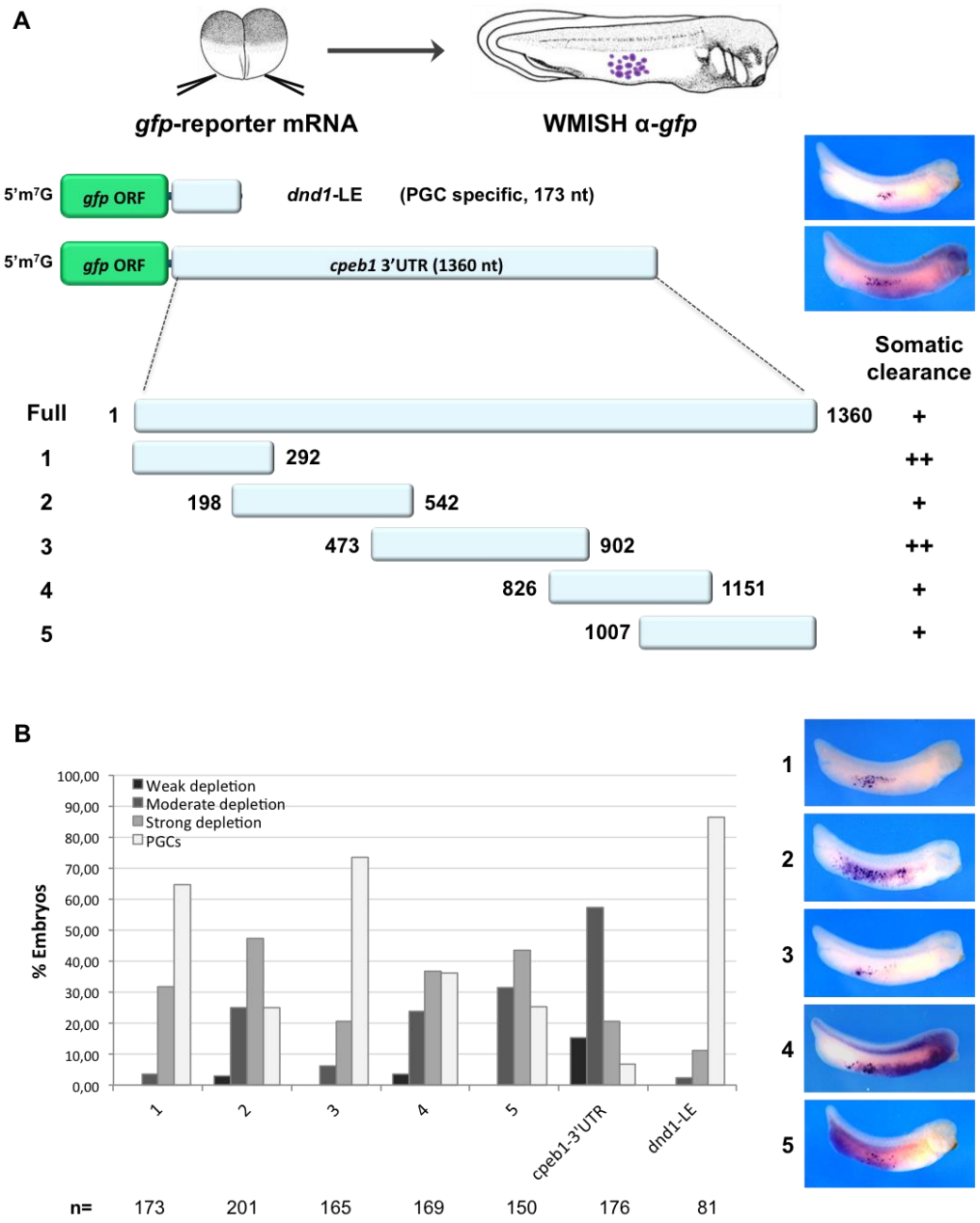


**Figure 3.3 Two segments of the *cpeb1* 3'UTR are involved in post-transcriptional regulation.** A. Reporter constructs were built by fusing the regions of interest to the *gfp*_ORF. The defined localization element of *dnd1* (*dnd1*-LE) served as a germ cell specific positive control. An additional positive control included in all experiments was the full-length 3'UTR reporter. Constructs (450pg) were microinjected in the vegetal side of two-cell stage embryos, which were cultured up to late tailbud stages (stage 28-34). The distribution of the reporter was observed by asRNA probing for *gfp* in WMISH. Images representative of the distribution of the reporter for *dnd1*-LE and *cpeb1*-3'UTR are shown on the right. The 3'UTR was separated into five fragments, the first and last, highlighted. On the right side somatic clearance is indicated as very efficient (++) or moderate (+). B. Embryos were quantified according to the efficiency with which the reporter was somatically depleted. On the right side embryos representative of the major effect on somatic depletion of the reporter are shown. N = 2 independent biological replicate experiments. n= number embryos/construct.

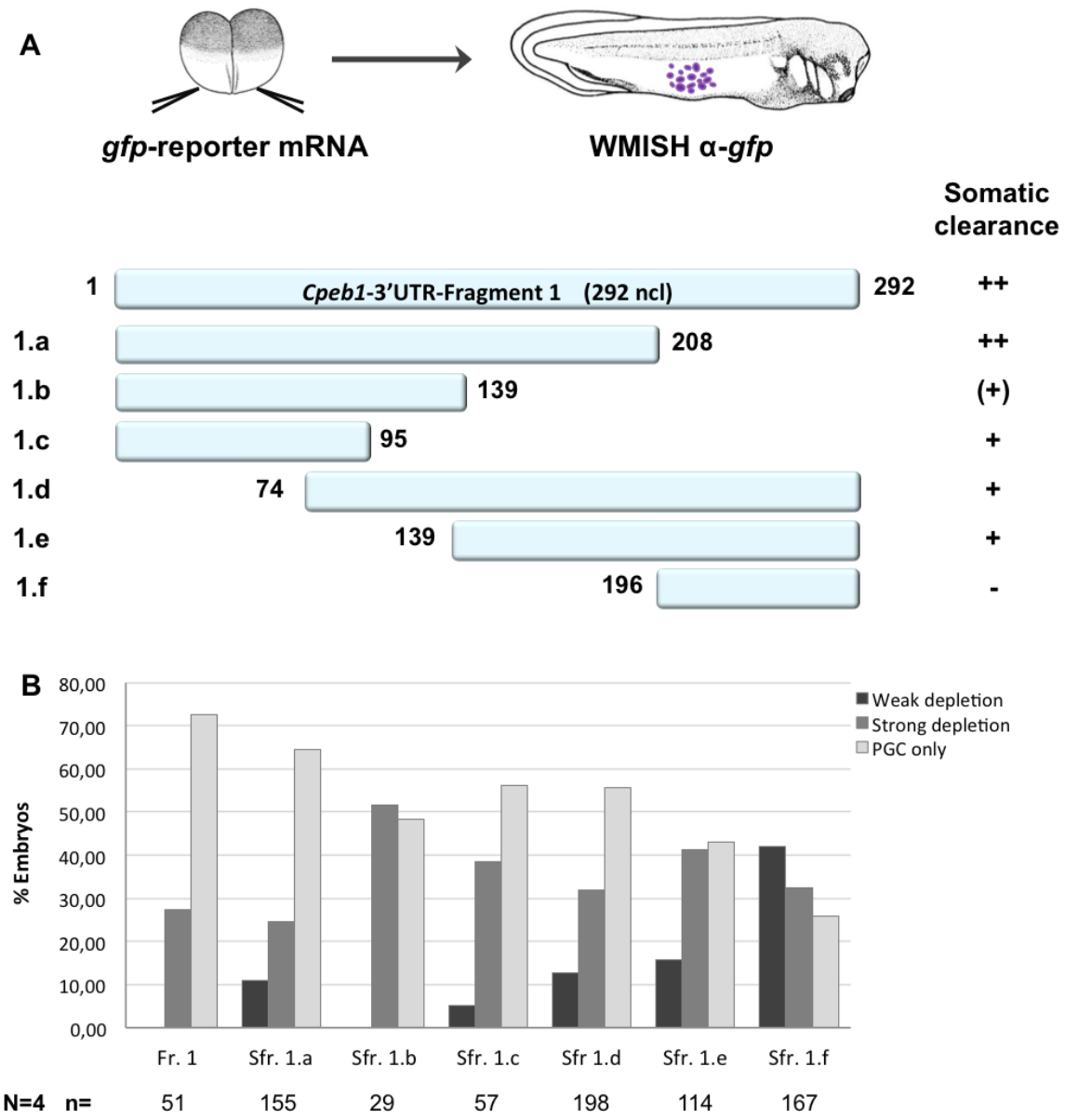


**Figure 3.4. The sequence between nucleotides 74-139 might be sufficient for somatic depletion and germline restriction.** A. Fragment one was systematically mapped from the 3' and 5' sites as shown in the scheme. Reporter constructs were built by fusing the regions of interest to the *gfp_ORF*. Once more, *gfp_dnd1_LE* and fragment 1 served as positive controls. Constructs (450pg) were microinjected in the vegetal side of two-cell stage embryos, which were cultured up to late tailbud stages (stage 28-34). The distribution of the reporter was determined by WMISH probing for *gfp*. B. Quantification of embryos based on the somatic depletion activity of the investigated regions on the reporter mRNA. N = 4 independent experiments, n = number embryos/sample.

The 3' deletions (1.a, 1.b, 1.c) are efficiently depleted in the soma, whereas the 5'deletions (1d, 1.e, 1.f) reporter distribution showed a less efficient depletion, which is especially observed for fragment 1.f (**Figure 3.4.B**). In the light of these experimental results I asked whether the region spanning nucleotides 74-139 (Fr_74-139) may contain a potential regulatory site. To address this

question, the focus of the ensuing procedures is identifying miRNA target sites in this short fragment.

### 3.1.4 Fragment 74-139 Harbours a Potential Regulatory Region

miRNAs are small RNAs with regulatory function, measure 20 to 25 nucleotides in length. The seed sequence of miRNAs, where perfect complementarity is required, is composed of only six nucleotides. Therefore, delineating miRNA target sequences in Fr_74-139 requires additional steps.

One possibility is preventing miRNA binding by employing target protector morpholinos (TPMOs). These antisense oligonucleotides are perfectly complementary to the presumptive miRNA target sites and form stable interactions, hence preventing miRNA binding (Choi et al., 2007; Koebernick et al., 2010; Staton and Giraldez, 2011; Bonev and Papalopulu 2012). If the sequence is relevant for miRNA mediated decay, then the reporter will not be degraded (**Figure 3.5.A**). These modified oligonucleotides are stable during early development for five days, which is the period necessary for the embryos to develop to the analyzed tailbud stage (Koebernick et al., 2010). The reporter construct and the TPMO were co-injected in both vegetal blastomeres and the embryos were analyzed at tailbud stage for *gfp* reporter distribution (**Figure 3.5. B,C**). The short length of the identified minimal fragment meant that only two TPMOs with the optimal length of 25 nucleotides needed to be designed. The polythymidine stretch in the center of the sequence could not be used as a TPMO template due to problematic design on repetitive stretches and high probability of off-target effects.

Fr_74-139 alone is restricted to the germline and is rarely and weakly detected in the endoderm. When analyzing the effect of the protector oligonucleotides it was found TPMO_1 has a slight effect on clearance. However, the results clearly show that TPMO_2 exerts the highest protective effect, as somatic depletion is weak for 99% of the embryos. Hence, the sequence that potentially harbours regulatory sites was identified in the latter part of Fr_74-139.

Typically miRNA binding requires perfect complementarity in the seed sequence which spans six nucleotides, whereas mismatches are allowed for the rest of the miRNA:mRNA pairing region. Therefore in the length of a twenty five nucleotide region multiple seed regions could be found. In order to discover miRNAs involved in somatic degradation of *cpeb1*, an alternative approach, complementary to protecting putative target sites, was employed as a next step.

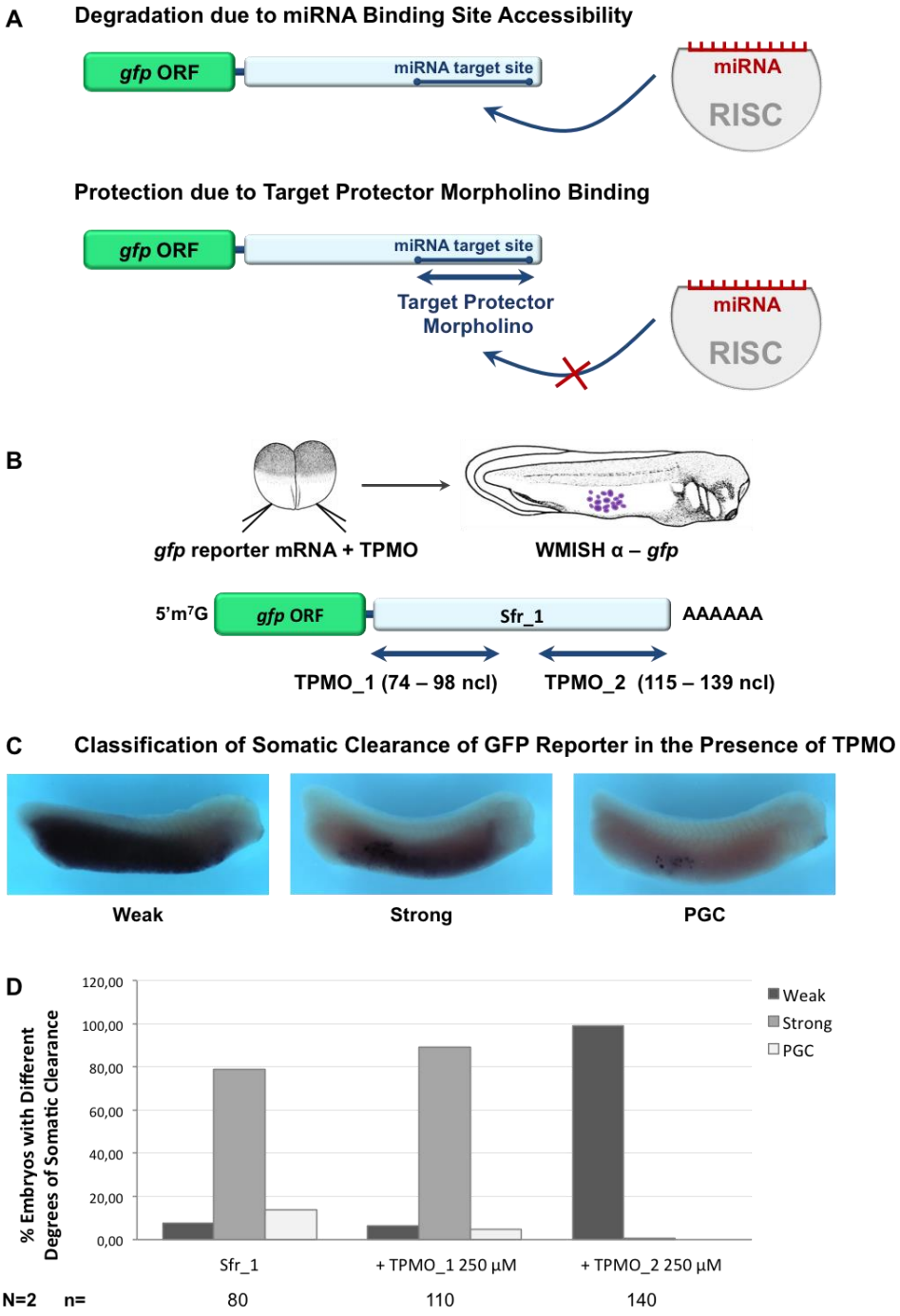


**Figure 3.5. TPMO_2 efficiently protects the reporter from somatic clearance.** A. TPMOs protect transcripts from miRNA mediated degradation by impeding RISC complex binding to the miRNA target site. B. Fr_74-139 reporter transcripts (450 ng) were injected vegetally in both blastomeres of two-cell stage embryos with TPMOs (250 µM) or alone serving as a positive control. Tailbud embryos were analyzed for endodermal distribution of the reporter by probing against *gfp* in WMISH. C. Representative embryos are shown for each of the categories: weak, moderate and strong depletion. D. Quantification of somatic depletion of Sfr_1 alone or in the presence of TPMOs. N=2 biological replicates.

### 3.1.5 BLOCKING *IN SILICO* PREDICTED MIRNAS HAD LITTLE EFFECT ON SOMATIC DEPLETION

In order to identify individual miRNAs involved in somatic degradation, the system was saturated with antisense oligonucleotides complementary to *in silico* predicted potential miRNA. The oligonucleotides used in this case are methylated on the 2' oxygen molecule of the ribose, conferring them a higher stability and lower susceptibility to base hydrolysis and nucleases (Stein et al., 1997). Similarly to blocking miRNA maturation, target transcripts will be stabilized. In contrast, in this setup only one individual miRNA is blocked at one time. In case the respective miRNA was responsible for the degradation of the construct, blocking it with 2'O-Methyl oligoribonucleotides (2'OMe oligos) would result in reporter detection in the entire endoderm.

Putative miRNAs that bind the minimal region were predicted *in silico* with the miRanda program (Betel et al., 2010) and antisense 2'O-methyl oligoribonucleotides (2'OMeOs) were designed according to the prediction or the available sequence if no potential target site was identified in the analyzed fragment. An advantage for this latter 2'OMe could be that it may cover multiple potential seed sequences. The only moderate effect was observed for 2'OMeO-α-xtr-miR-17-5p and it was comparable to that of the scrambled control (**Figure 3.6. A**). Microinjections and analysis were performed as for the TPMO experiment. In short, Fr_74-139 (500pg) was injected either alone as a reference, or together with 2'OMe oligos (25 µM) targetting miR-17-5p, miR-302, bases 43-66, or a scrambled control (ctrl; **Figure 3.6. B**).

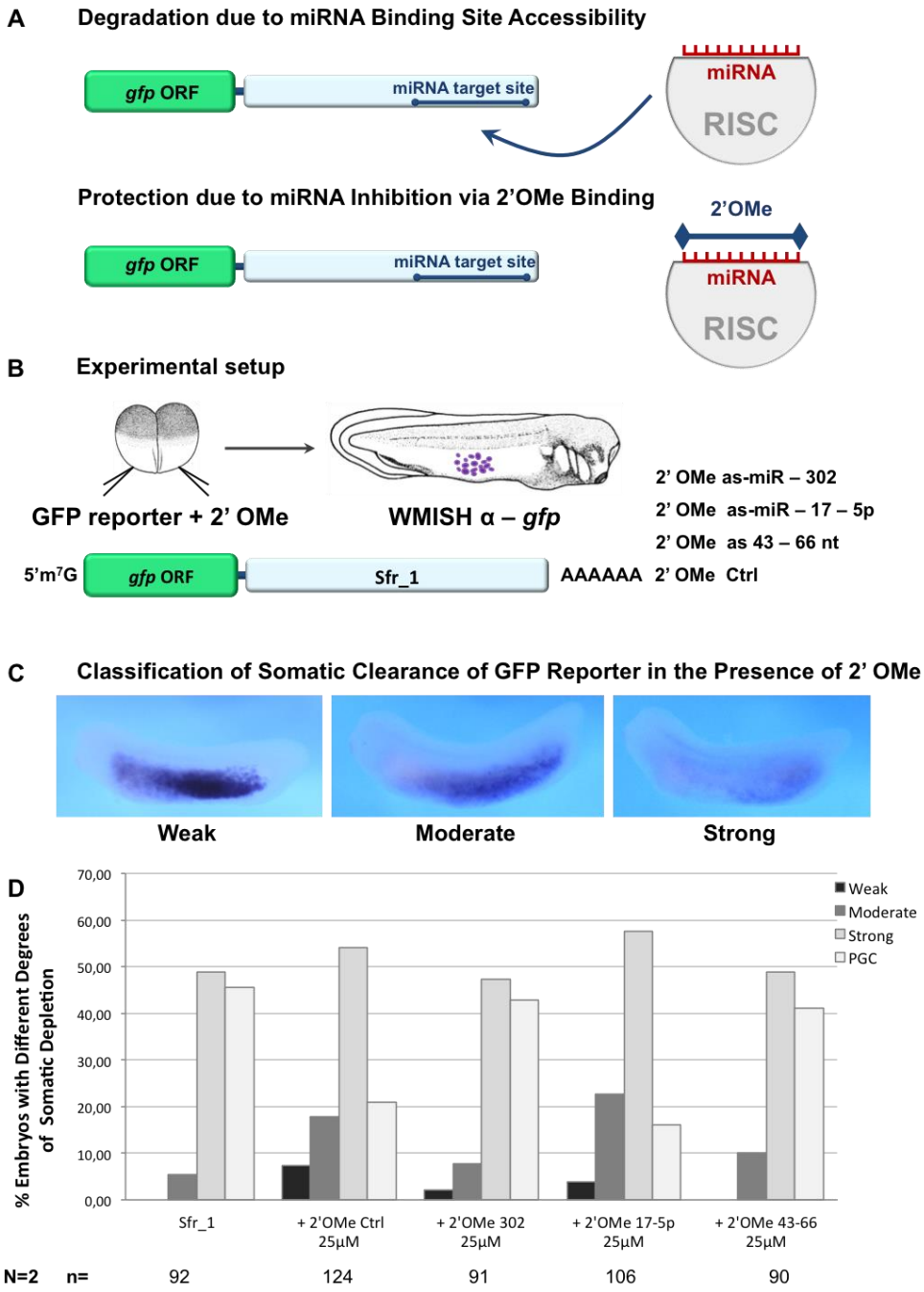


**Figure 3.6. Somatic depletion of the reporter construct was not affected by blocking the selected miRNAs.** A. 2'OMe oligonucleotides bind complementary miRNAs, hence preventing their action through the activity of the RISC complex. B. Sfr_1 reporter constructs were vegetally injected either with 2'OMe oligos (25 µM) or alone (500 pg) as a positive control, in both blastomeres of two cell stage embryos. This was followed by analysis of endodermal distribution at tailbud stages. C. Examples of the efficiency of somatic depletion are categorized as weak, moderate and strong, while the reporter was present only in the germline in the remaining embryos. D. Quantification of embryo numbers showing somatic clearance according to the mentioned categories. N=2 biological repeats, n= number of embryos analyzed per sample.

2'OMe oligos saturate the pool of the targeted miRNA species in the embryo alleviating somatic clearance of the reporter. None of the coinjected 2'OMe oligos prevented somatic depletion of

Sfr_1 to an extent comparable to the TPMOs. Nonetheless, a slight increase in endodermal distribution was observed for 2'OMe 17-5p, just above 20% of the embryos showing moderate depletion. However, this effect is comparable to that obtained by co-injecting the control oligonucleotide. The 2'OMe targeting miR-302 did not have an effect on the Sfr_1 reporter distribution and most surprisingly, 2'OMe 43-66 did not block somatic clearance either. This was unexpected as the TPMO_2 results clearly show a protective effect.

To summarize, a minimal sequence spanning nucleotides 74-139 of the *cpeb1*-3'UTR was found to be sufficient for somatic depletion and germline maintenance. It seems to be mainly regulated by the last 25 nucleotides in its sequence. However, further experiments are required for the identification of the miRNA responsible for its clearance during the maternal to zygotic transition.

### 3.2 CPEB1 Expression during Embryogenesis and Function in PGC development

#### 3.2.1 CPEB1 Protein Expression during Early Embryogenesis

Previous results demonstrated that *cpeb1* post-transcriptional regulation results in *cpeb1* germline specificity later during embryogenesis. Next I wanted to verify if transcript and protein expression correlate.

CPEB1 protein expression has been described upon discovery in the *Xenopus laevis* system twenty years ago. Its expression profile in a time course starting from ovulated egg to tailbud stage shows a steady decrease until gastrulation and then the protein is no longer detected (Hake and Richter, 1994). The protein amount varies considerably between stage VI oocytes and ovulated egg, as approximately 75% of the protein is degraded during progesterone induced oocyte maturation (Hake and Richter, 1994). To confirm and expand on the already present knowledge, the first step was to analyze CPEB1 protein expression throughout early embryogenesis. For this purpose polyclonal antibodies recognizing the full CPEB1 protein were produced in rabbit (Trenzyme). In the context of oocyte and embryonic extracts the protein runs at 58kDa, correlating with to the mobility of *in vitro* transcribed CPEB1 protein (Fig. S5B). An additional unexpected signal running at 38kDa was detected (**Figure 3.8. A**). Similar to the overview at the transcript level, a time course of protein expression was outlined by blotting against CPEB1 on total protein extracts at consecutive stages of embryogenesis (**Figure 3.7.**). The serum was used in this experiment. Protein expression analysis during early *X. laevis* development shows that CPEB1 was expressed in higher amounts in stage VI oocytes as compared to the rest of the analyzed time span. Despite lower levels of expression, the protein seemed to be stable throughout early embryogenesis, from egg until late tailbud stage (**Figure 3.7.**).

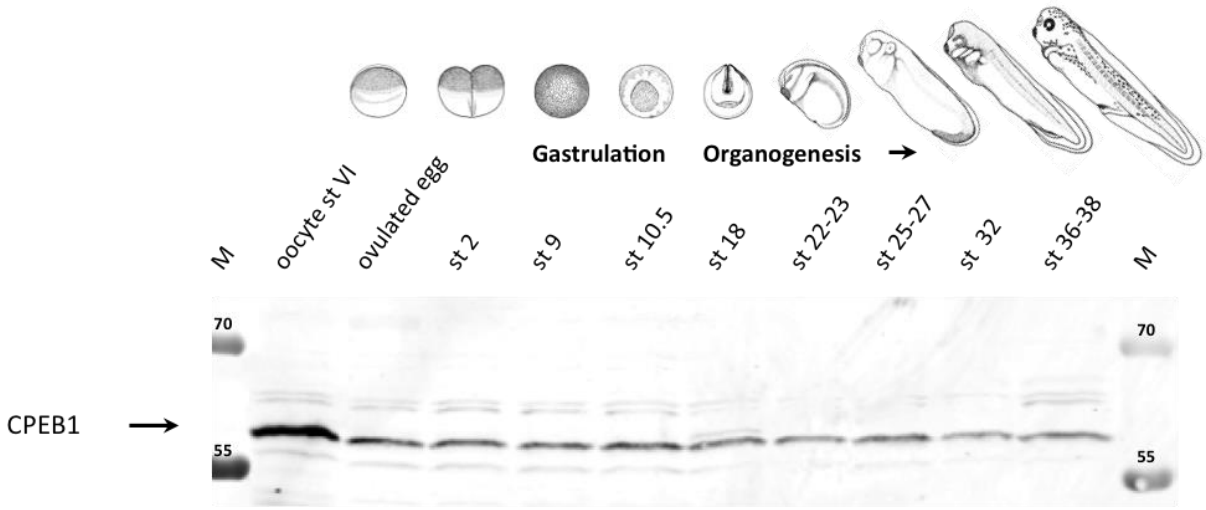


**Figure 3.7. CPEB1 protein is stable and steady levels are maintained throughout early embryogenesis.** Protein expression was analyzed over a time-course encompassing the first 5 days of development, starting with st VI oocytes and continuing with successive embryo stages encompassing early cleavage stages, gastrulation and organogenesis. Total protein extracts were probed for CPEB1 protein by Western blot (rabbit polyclonal; α-CPEB1;1:500). Two embryo equivalents were loaded for each stage. N=3 biological replicates.

To determine whether transcript presence is mirrored by protein translation, whole mount immunostaining was employed for late tailbud stage embryos (**Figure 3.9.**). It is crucial that the antibody pool used to accurately determine the localization of CPEB1 protein in whole embryos is specific. This prompted attempts aimed at purifying the fraction of the antibody pool (**Figure 3.8. C**) which recognizes only the CPEB1 protein running at the predicted molecular weight, while excluding all antibodies that recognize other unspecific protein(s) (**Figure 3.8. D**). The purified antibody was used in the following immuno-fluorescence experiments.

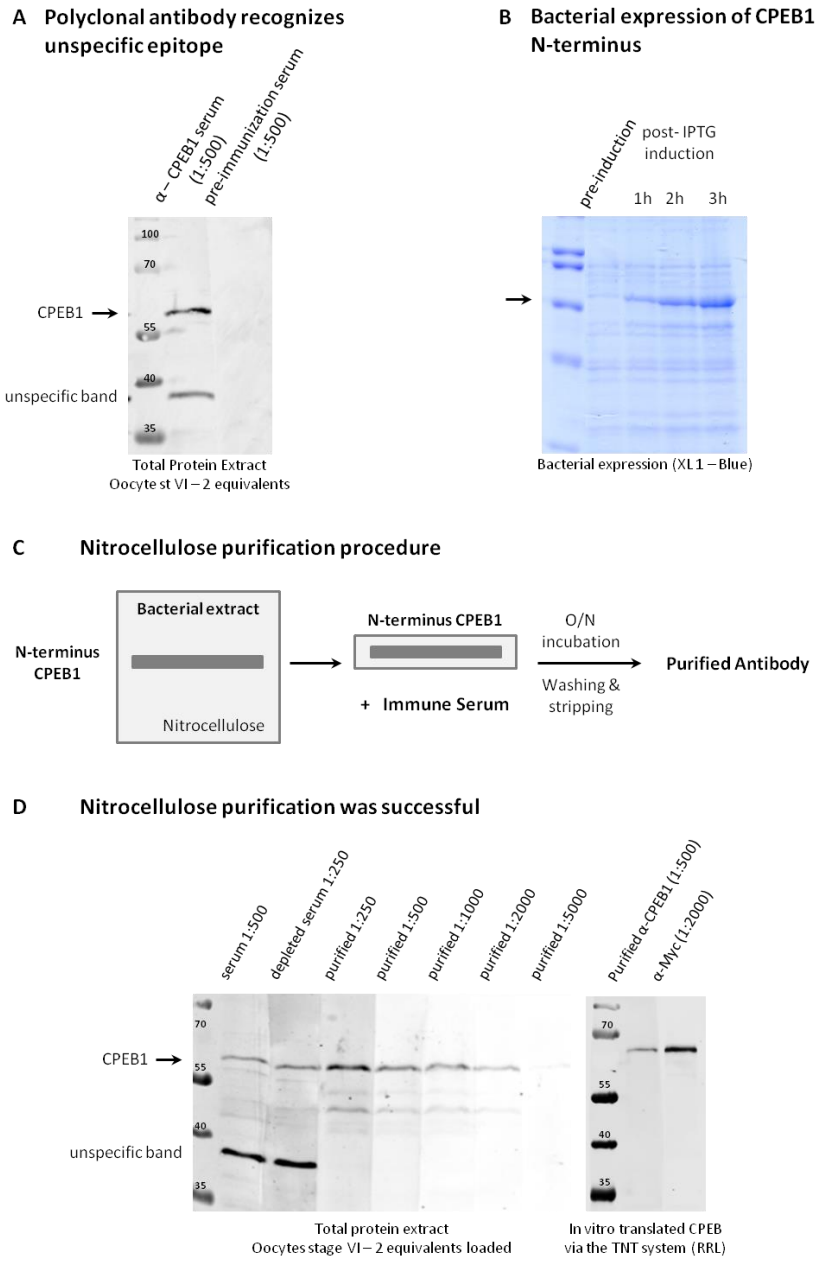


**Figure 3.8. Antibody purification was successful.** A. The polyclonal antibody recognizes an unspecific epitope, a protein running at approximately 38 kDa. B. The N-terminus of CPEB1 was bacterially expressed. C. The purification procedure involved running the bacterially expressed N-terminus CPEB1 on a 12% polyacrylamide gel, transferring it to a nitrocellulose membrane, cutting out the band corresponding to the correct size and incubating it with the serum. After an overnight incubation the membrane was washed to eliminate weakly bound antibody and stripped to elute the specific antibody. D. The purified antibody recognizes the CPEB1 protein from oocyte extracts and the Myc-CPEB1 from an *in vitro* transcription and translation reaction. The unspecific band is not observed. N=2.

To mark germline cells, two antibodies were used as positive controls, an antibody against DAZL (deleted in azoospermia like), a protein known to be germline specific (**Figure 3.9.**) and an anti-GFP antibody on GFP-XDE-LE injected embryos (**Figure S4.**). In this latter case, the GFP protein is translated mainly in PGCs as a virtue of the LE sequence conferring localization and specificity to

the germline (**Figure 3.1. C** shows germline specificity of transcript, **Figure S4.** shows GFP protein in putative PGCs). To control for background staining, the negative control embryos were treated only with secondary antibodies (**Figure S3.**).

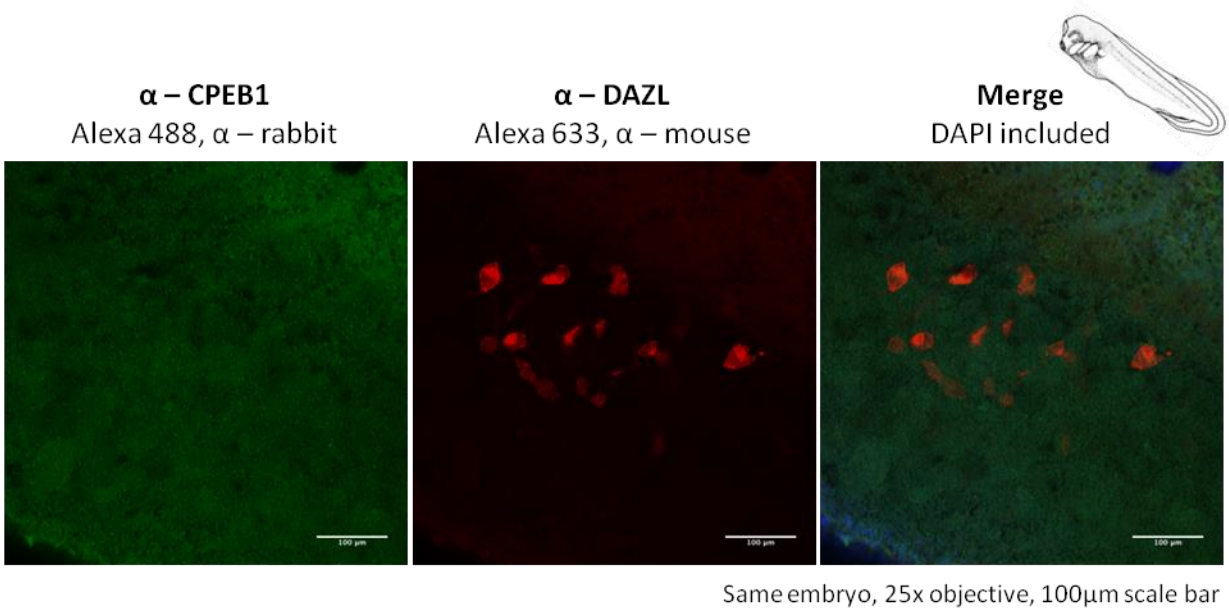


**Figure 3.9. In contrast to DAZL, CPEB1 protein is not detected by whole mount immunostaining.** Whole mount immunostaining was carried out on tailbud embryos against CPEB1 and DAZL, serving as a germline specific positive control. Antibodies: mouse α-DAZL detected with Alexa 633 α-mouse; rabbit α-CPEB1 detected with Alexa 488 α-rabbit. Pictures were taken with a 25x objective. Scale bar = 100 µM. N=3 biological replicates.

DAZL protein was detected in the germline, while no signal was observed for CPEB1, neither in PGCs nor in any other tissue. This was the case despite employing two different protocols, three fixation methods and two antibodies against CPEB1 (one kindly provided by Prof. D. Weil). Hence the distribution of the protein of interest remained elusive. Nevertheless this protocol worked best, proof being that two different antibodies employed to recognize proteins in the germline were successfully detected.

### 3.2.2 Functional Analysis of CPEB1 in the Germline

A classical way to define the function of a protein of interest is by removing it from the system and observing phenotypic effects. In *X. laevis* absolute clearance is difficult to achieve mainly for two reasons: the *X. laevis* genome is allotetraploid and the protein is maternally supplied. For many proteins, a fraction of the maternal protein supply is stable until late tailbud stages. Despite these limitations, an indication of a potential protein function can be obtained from knock-down experiments.

The first choice for a knock-down was to employ translational blocking MOs (tMOs) which inhibit translation of bound transcripts by preventing ribosomal assembly at the translation start site (TSS). These antisense oligonucleotides have several structural particularities: the riboside moiety in RNA is replaced by a morpholino moiety and the intersubunit linkage is a non-ionic phosphorodiamidate type conferring excellent base stacking, high water solubility and resistance to a wide range of nucleases, making them stable in the cellular environment (Summerton and Weller, 1997). Nutt and co-workers (2001) assessed the efficiency of translational morpholinos in *X. laevis* and *X. tropicalis* at different doses until late tadpole stages. Their work has shown tMOs are stable and active until at least stage 43 at doses between 4 and 10ng, without inducing any developmental defects. A dose of 20ng resulted in malformations for 20% of embryos (Nutt et al., 2001). Hence, as CPEB1 protein is maternally provided, a dose of 16ng was selected (250 µM). A successful knock-down implies blocking translation for all transcribed alleles of the protein of interest. There are two versions of *cpeb1* found in the *X. laevis* genome, both of which are predicted to be efficiently silenced by the designed tMO, targeting the first twenty five nucleotides of the open reading frame (including the start codon). There is only one mismatch relative to the *cpeb1_L* version, at the seventeenth position in the morpholino, where a cytosine (in *cpeb1_S*) is substituted for a thymine (*cpeb1_L*). However, the efficiency of the tMO should not be affected, as this one base mismatch is compensated by the positive energy interaction between guanine and thymine, qualifying as no mismatch in the end (Gene tools customer service).

First the functionality of the morpholino was tested in a rabbit reticulocyte lysate *in vitro* transcription and translation system. Considering that the tMO translational repression can be hampered by replacing the 5'UTR with a tag, a plasmid containing a myc-tag fused to the *cpeb1* open reading frame was selected as a suitable negative control. Hence, decreasing concentrations of tMO (5 µg, 1 µg and 0.1 µg) were added to reactions containing either a template plasmid encoding for the *cpeb1* sequence including the 5'UTR or one encoding for *myc_cpeb1*. The efficiency of the tMO was determined by analyzing the levels of translated protein.

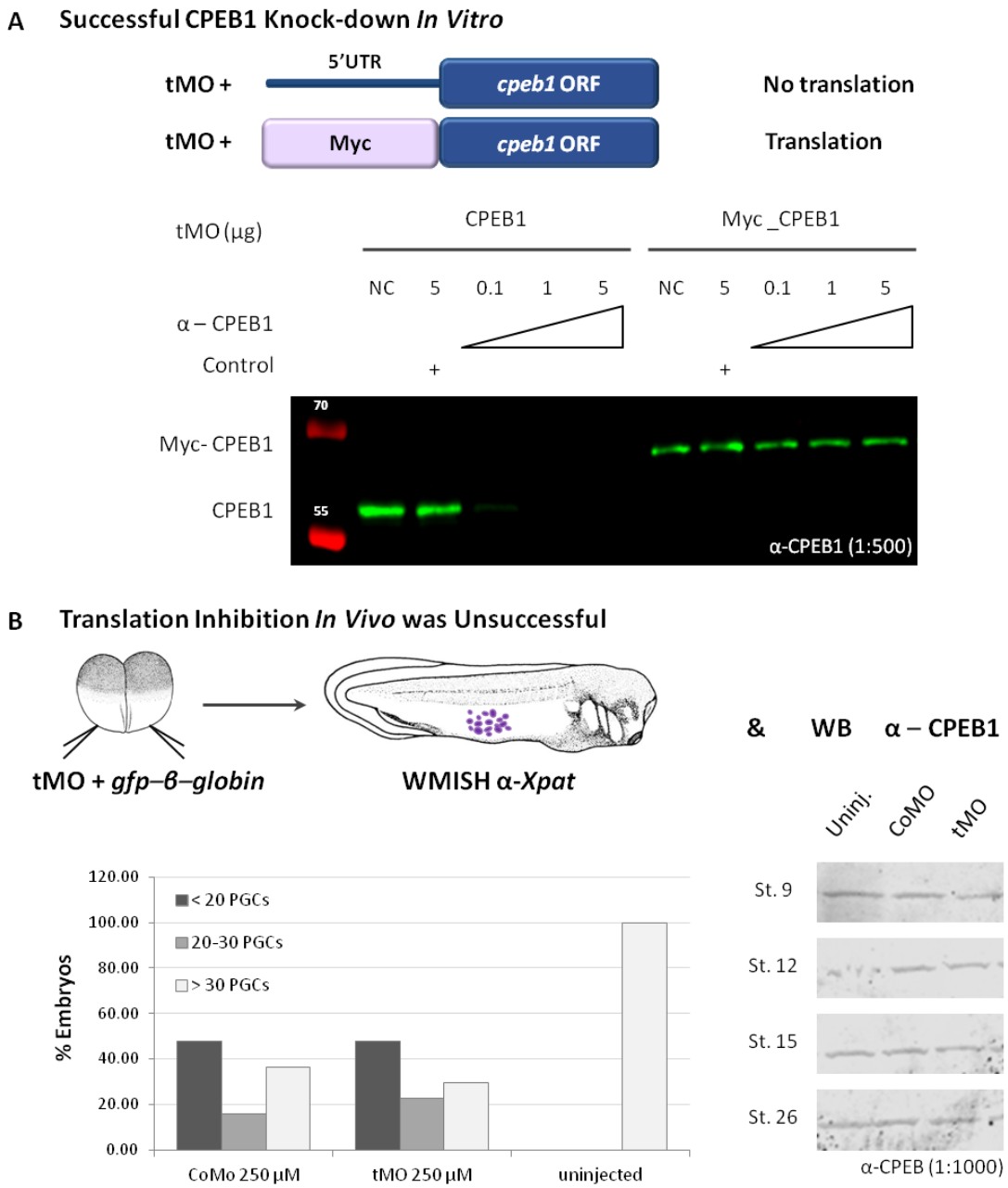


**Figure 3.10. CPEB1 knock-down is successfully achieved *in vitro* but not *in vivo*.** A. Different concentrations of tMOs were added to an *in vitro* transcription and translation system. The negative control had a myc tag instead of the wild type 5'UTR. Protein fractions were loaded onto SDS-PAGE gels, transferred to nitrocellulose membranes and blotted against CPEB1 with the purified antibody. B. To test for tMO functionality *in vivo*, embryos were injected vegetally at one cell stage, forty minutes after fertilization. Six embryos per sequential developmental stage were flash-frozen for protein extract preparations and the remaining embryos were fixed for WMISH against *Pgat*. Total extracts were analyzed for CPEB1 protein levels. Fifty embryos per sample were quantified according to the numbers of *pgat* positive PGCs. Co-injection of a reporter construct (*gfp_β_globin*) with tMOs was used to distinguish injected from non-injected embryos. N=2.

As the tMO successfully knocked down translation of the mRNA containing the 5'UTR but not that of the myc-taged transcript *in vitro* (**Figure 3.10. A**), it was further employed in *in vivo* experiments.

Due to the fact that there is no way to distinguish injected from uninjected embryos if the tMO is injected alone, a reporter construct coding for GFP was added to the injection mixture to enable selection of embryos for further analysis based on their fluorescence. This transcript consists of the GFP ORF fused to the *β-globin* 3'UTR. Its translation does not affect embryonic development and the protein is expected to be detected mainly in the endoderm, due to diffusion from the location of the injection site, at the vegetal pole. Embryos were injected vegetally at the one cell stage with a total amount of 16 ng (250 µM) tMO and 450 pg mRNA in 8.4 nL. To look at translational inhibition, embryos were flash-frozen at various stages, and total protein extracts were prepared. There was no obvious difference between the uninjected, control injected and translational morpholino injected in the amount of translated CPEB1 protein (**Figure 3.10. B**).

Minute protein level changes induced by the tMOs could have an effect at the germline level, therefore the embryos were further analyzed. As seen in the 3'UTR mapping experiments, during the developmental interval tailbud stages 28-34, germline cells are distributed closer to the surface on the lateral endodermal sides of the embryo and they are actively migrating towards the future gonads/genital ridges (Terayama et al., 2013). Therefore, potential effects on germline development are observable by eye, including identifying any anomaly in the number, distribution and migratory behavior of PGCs. The uninjected embryos have above 30 germline cells. The germline cell number decreases for both the *cpeb1* tMO and the CoMO, above 40% of embryos having less than 20 PGCs and approx. 20% between 20 and 30 PGCs. However, there is no discernible difference between the CoMo and tMO (**Figure 3.10. B**). The PGC distribution in the endoderm is similar to that of the uninjected embryos. These results show that despite the proven *in vitro* functionality of the tMO, *in vivo* no significant effects on germline development were observed. In consequence an alternative procedure to limit the function of the endogenous protein was used.

Dominant negative (DN) versions of the protein of interest lack functionality either due to (best case point-) mutations or to lacking important parts required for its role. When the system is saturated with DN, the endogenous protein is outcompeted, resulting in a partial knock-down. CPEB1 protein has two main parts, an intrinsically disordered N-terminal domain, responsible for recruiting proteins important for RNA processing or scaffolding and the C-terminal domain comprising of two RNA recognition motifs and a zinc finger motif which has the role of binding mRNAs. CPEB1 RBP recognizes the 3'UTR U-rich cytoplasmic polyadenylation element (CPE), with the consensus sequence of $U_5A_{1\text{-}3}U$ (see introduction, McGrew et al., 1989, Gebauer et al., 1994).

Recently, Afroz and colleagues (2014) have published the three dimensional structure of the CPEB1 C-terminal region, comprising two RRMs and one Zn-finger domain, alone and in complex with its target CPE sequence. Moreover, they have described the effects of certain point-mutations on the RNA-binding capacity of the C-terminal region to determine which residues are essential for mRNA binding. For this purpose, the polyadenylation of known target transcripts was compared between wild type and binding mutants in stage VI oocytes (Afroz et al., 2014). With this information and several constructs kindly provided by E. Belloc at hand, the pursuit for revealing the function of CPEB1 in germline development was resumed. In this context, the C-terminal region in its wild type form acts as a dominant negative, as it retains the capacity of binding mRNAs but is not capable of recruiting additional factors required for transcript processing, for example polyadenylation as mentioned previously. Therefore, when the system is saturated with the C-terminal region of CPEB1, the endogenous protein is superseded by the DN on a major proportion of newly transcribed transcripts, resulting in alterations of their post-transcriptional regulation. Bound targets would have a lower extent of polyadenylation, potentially leading to their degradation or repression (**Figure 3.11. A**; modified from Afroz et al., 2014). Additionally, two mutants with impaired RNA binding capacity were included to verify whether the interaction of CPEB1 with its target transcripts may be involved in germline development.

Embryos were injected with dominant negative constructs (500 pg) and the number of primordial germ cells was analyzed at tailbud stages. PGCs were identified by the presence of the *pgat* transcript. The embryos were rendered transparent after clearing with a solution of benzyl-benzoate: benzyl-alcohol (BB:BA).

Uninjected embryos typically have above 20 germ cells (approx. 75% counting the grey and dark grey columns combined), while all the DN constructs show a high reduction in germ cell numbers. The three injected constructs lead to a fraction above 80% of embryos with less than 20 PGCs. Interestingly, even the DN versions that cannot bind RNA show a convincing impact (**Figure 3.11. C**).

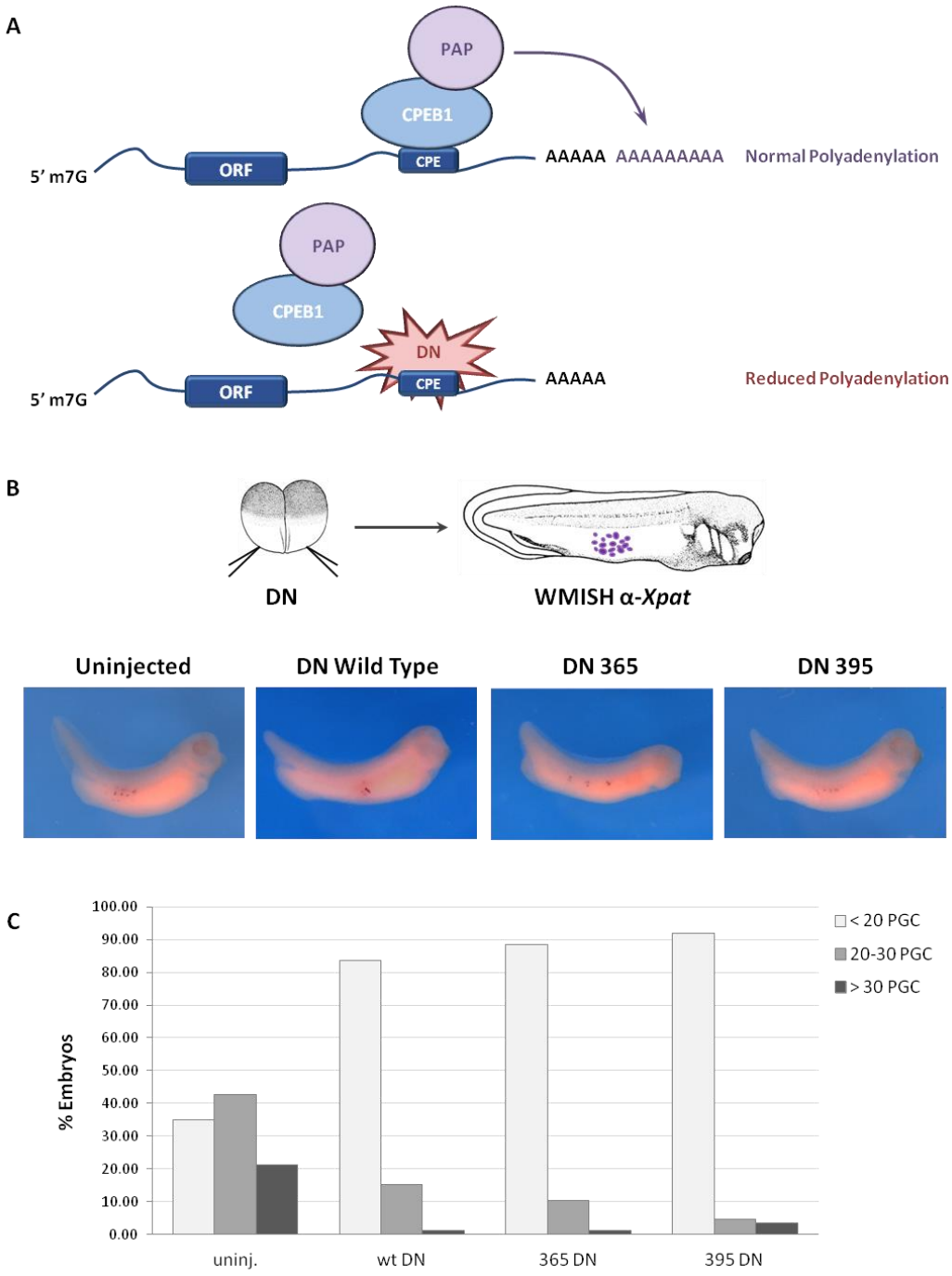


**Figure 3.11. DN overexpression leads to a reduction in PGC number, irrespective of RNA binding capacity.** A. Under normal conditions, the endogenous CPEB1 protein binds to its target mRNAs and recruits poly(A) polymerases (PAP), resulting in a longer poly(A) tail, facilitating translational activation. Overexpression of exogenous DN outcompetes the endogenous CPEB1, hindering the polyadenylation of its target transcripts (Modified from Afroz et al., 2014). B. Illustrative examples for all conditions. Embryos were injected with 500 pg of one of the following three DN constructs: wild type (wt DN), DN 365 and DN 395. C. Quantification according to PGC numbers visible per embryo after clearing with BB:BA solution. N = 2 biological replicates, n=85 embryos per condition.

Considering that the outcome of DN overexpression leads to a decline in the germ cell population, the next question asked was whether the PGC number would be positively influenced by over-expressing a flag-epitope tagged version of the full length wild type protein.

To this end, *in vitro* transcribed mRNAs (2.4 ng) encoding for flag-tagged versions of the full length CPEB1 (F-CPEB1), GFP (F-GFP) and Ptbp1 (F-Ptbp1) were injected in two-cell stage embryos. F-GFP served as a negative control along with uninjected embryos. Ptbp1 is also an RNA-binding protein and a known component of the transcript transport and localization during oogenesis. Therefore, Ptbp1 was injected in parallel as a positive control. PGCs were identified by antisenseRNA (asRNA) hybridization to *pgat* in WMISH and their number was analyzed in cleared embryos at tailbud stages.

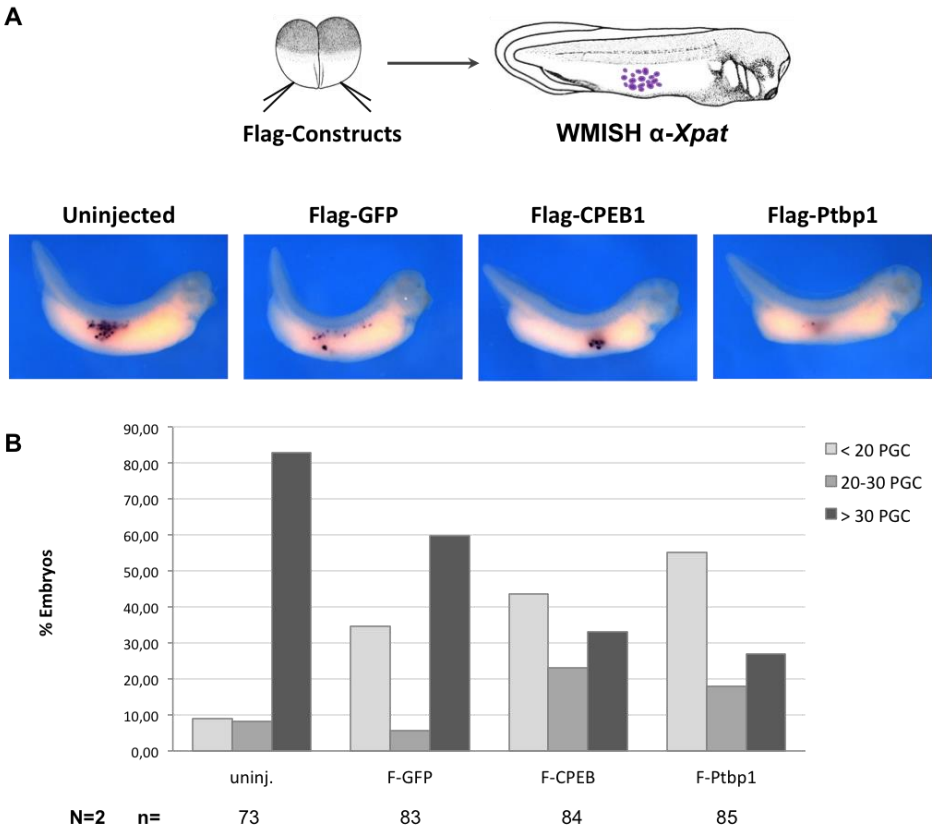


**Figure 3.12. Flag-CPEB1 overexpression has moderate effects on the germline population.** A. Overexpression of ectopic full-length protein may interfere with the normal regulation conferred by the endogenous pool of CPEB1. The effects are to be resolved, potentially involving modifications at the poly(A) tail level. B. *In vitro* transcribed mRNAs encoding for flag-tagged proteins, CPEB1 (F-CPEB1), GFP (F-GFP) and Ptbp1 (F-Ptbp1) were injected in two-cell stage embryos. They were cultured until tailbud stages when the number of PGCs was analyzed. Examples of embryos for each sample. C. Quantification of the number of germ cells for each sample. N=2; n= 28 per sample for one and n>40 for the other biological replicate.

Uninjected embryos once more show a number of germ cells exceeding 30 at the analyzed stage (**Figure 3.12. B**). The injection of F-GFP appears to negatively influence the germline. F-CPEB1

overexpression reduces the population of PGCs and F-Ptbp1 shows the most pronounced effect, with more than 50% of the counted embryos having less than 20 germ cells (**Figure 3.12. B**).

To gain further knowledge about the mechanism driving these changes, I turned to identifying protein interaction partners.

### 3.2.3 IDENTIFYING PROTEIN-PROTEIN INTERACTIONS

CPEB1 is a RNA-binding protein (RBP) and nucleates complexes important for mRNA processing. Its influence on bound target transcripts is exerted via recruited proteins belonging to the same RNP complex. Therefore, investigation of the interaction network could bring new light on the function of CPEB1 in embryos. With the aim of identifying protein binding partners I opted for immunoprecipitation (IP) experiments against flag-tagged CPEB1 in embryos and oocytes followed by mass spectrometry analysis. Having in view that several CPEB1 interactions have already been described in the oocyte background, the IP performed in oocytes was used as archetype.

Ideally only the proteins found in a complex with the protein of interest would be detected. To control for unspecific interactions, three control samples were analyzed in parallel with the protein of interest, namely uninjected embryos, flag-GFP (F-GFP) and flag-Ptbp1 (F-Ptbp1). Each of these controls raised the specificity bar due to their contribution to eliminating false positive hits. The uninjected sample was tested for proteins interacting with the beads or coupled antibodies. F-GFP, an exogenous protein with no functionality in this model organism, was included for unspecific complex formation. F-Ptbp1 has in its structure four RRM domains involved in transcript localization to the vegetal pole during oogenesis (Cote et al., 1999). This RBP served to confirm the functionality of the applied method. Moreover, the experiments were performed in RNase free conditions, thus the mRNA scaffold is assumed to be intact. This means that protein complexes that are simultaneously bound along the transcript may also be pulled down. In consequence, it additionally serves as a positive control for what other proteins are potentially present in RNPs.

Embryos and oocytes were injected with the three constructs at a concentration of 300ng/µL, hence with approximately 2.4 ng/embryo in 8.4 nL respectively 1.2 ng/oocyte in 4.2 nL. Stage VI oocytes were injected mainly in the animal pole to ensure highest translation rate and 200 oocytes per sample were collected and flash frozen twenty-four hours later. Embryos were injected vegetally in both blastomeres at the two-cell stage, to target the germ plasm area. They were cultured until stage 13 when 100 embryos per sample were flash frozen and further used for the immunoprecipitation procedure. Several steps were optimized such as the concentration of

injected mRNA, duration of time after injection before embryo/oocyte collection, the incubation time for immunoprecipitation, the type of sample buffer used and the sample preparation method for gel loading. These were implemented in the course of at least fifteen experiments. The protein samples resulting from the IP procedure were divided such that one part would be used for a test western blot against the flag epitope to verify the levels of protein expression and the other for label-free mass spectrometry analysis (**Figure S5. A**). When the test blot showed optimal levels of expressed protein for all constructs (**Figure S5. B**), the twin samples were sent for mass spectrometry.

For the oocyte experiment only three samples were sent for analysis. The reasons are that the F-GFP construct was available only before the last few immunoprecipitation procedures and whereas the embryos survived and translated it well, the last three oocyte isolations and injections were not successful. In two cases, the oocytes died before injection and in the last case, they survived the injection and incubation time, but the injected constructs were not translated in sufficient amounts. Therefore, the best oocyte samples, without the F-GFP construct were sent in for analysis.

The injected transcripts were translated with different efficiencies, resulting in differential expression of the flag-tagged proteins. As a consequence, the protein amounts pulled down differed between samples. While Ptbp1 was highly expressed, F-CPEB1 was modestly expressed in both oocytes and embryos. F-GFP was also expressed in moderate amounts. Nevertheless, the immunoprecipitation procedure was successful for all three constructs as can be observed in the IP fractions ( **Figure S5. B**). In the portrayed experiments protein expression for the injected constructs was at its optimum, thus the samples were sent for mass spectrometry analysis.

Subsequent to the mass-spectrometry procedure the pool of pulled down proteins were identified. At least 675 proteins were identified for each sample for both oocytes and embryos. To verify whether the protein samples were pure, meaning that the flag-tagged proteins appeared only in their respective samples, the pulled down amounts for the exogenous proteins were analyzed first. The levels of pulled down endogenous proteins was also considered, to see whether dimerization and cross-interaction occur (**Table S1.**).

Each of the constructs appeared only in the corresponding injected sample, hence no cross-contaminations occurred at any step of the procedure. F-CPEB1 was pulled down in both embryos and oocytes in similar amounts. The two variants were present only in the F-CPEB1 oocyte fraction. F-Ptbp1 was translated and pulled down in much higher quantities. In both oocytes and

embryos, the edogenous HnRNP related transport protein Ptbp1 was also detected. F-Ptbp1 was specific only to the embryo fraction.

To continue the selection of the top candidates and removing false positives, stringent thresholds were used. Several parameters were considered such as: pulled down amounts (> 5 ng), protein coverage (> 30%), reported peptide number (> 8), QC score (< 0.02), fold changes respective to the negative controls (> 6), FDR (1%). The additional candidates selected according to lower yet still very strict stringency values (fold change enrichment >2; protein coverage > 20%; FDR 1%) also showed limited overlap between the embryo and oocyte series. It is important to mention that several of the top potential candidates were not detected in all samples.

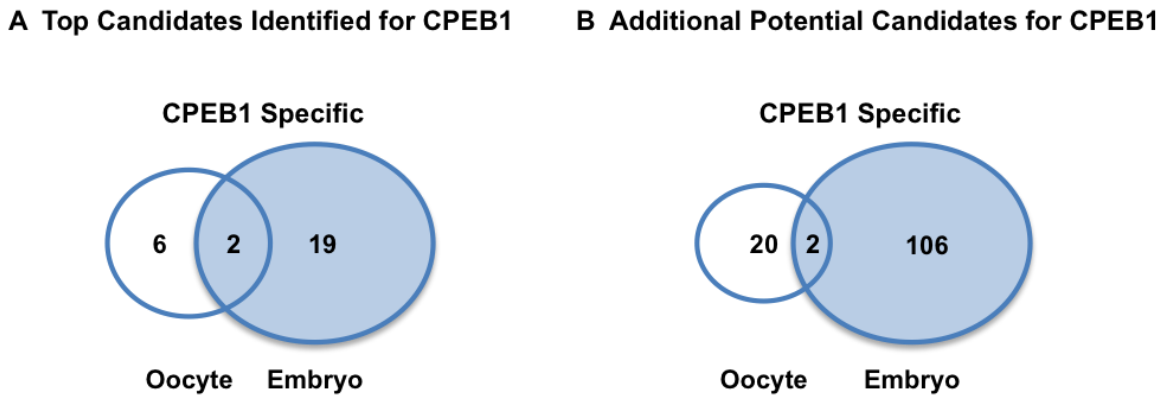


**Figure 3.13. Few CPEB1 potential protein partners are in both embryos and oocytes.** Venn diagrams show the number of oocyte and embryo specific top and additional for CPEB1 and the overlap between the oocyte nd embryo candidates.

Only two CPEB1 candidates are common for both the embryo and oocyte samples, namely Cpsf2 and Symplekin (**Table 3.1.**). These two proteins are established CPEB1 protein partners involved in translational regulation as Symplekin acts as a scaffold onto which CPSF2 and other proteins involved in polyadenylation can assemble (Mendez et al., 2000b; Barnard et al., 2004). In order to select potential CPEB1 interaction partners I examined the available information for the identified top candidates and chose the most promising candidates (**Table 3.1.**).

**Table 3.1. Selected top CPEB1 candidates.** Additional to the aforementioned selection criteria, the fold change compared to Ptbp1 is higher than five ($FC_{CPEB1/Ptbp1} > 5$).

| Candidate Name | Gene name | Structure/Complex | Process/Function |
|---|---|---|---|
| Symplekin | *sympk*°* | Cytoplasmic polyadenylation complex | mRNA polyadenylation |
| Mitochondrial ribosomal protein L11 | *mrpl11* | Ribosome component | mRNA polyadenylation |
| Vac 14 homolog | *vac14* | Component of PAS regulation complex | Phosphoinositide PI(3,5)P2 metabolism, protein trafficking |
| Cleavage and polyadenylation | *cpsf2** | Polyadenylation complex | mRNA 3'end processing |

| | | | |
|---|---|---|---|
| specificity factor 2 | | | |
| Cleavage and polyadenylation specificity factor 3 | *cpsf3* | Polyadenylation complex | mRNA 3'end processing |
| Splicing factor 3b subunit 1 | *sf3b1* | spliceosome | Spliceosome anchoring to mRNA |
| Eukaryotic translation initiation factor 6 | *eif6* | ribosome | Ribosome biogenesis and assembly |
| X-ray repair complementing defective repair in Chinese hamster cells | *xrcc6* | nucleus | Double strand break repair |
| NMD3 ribosome export adaptor | *nmd3* | Adaptor for XPO/CRM1 mediated export | 60S ribosomal subunit export |
| Glutaryl-CoA dehydrogenase | *Gcdh*[§] | Mitochondrial matrix | Acyl-CoA dehydrogenase |
| Glutaminyl-tRNA synthetase | *Qars*[§] | cytoplasmic | Glutaminyl-t-RNA synthetase |

*detected in CPEB1 oocyte and embryo samples; ° not detected in the F-GFP negative control. [§]oocyte specific

The candidates pulled down from the embryo samples are described as having functions related to various cellular processes. Sympk, Cpsf2 and Cpsf3 have established roles in mRNA polyadenylation (Mendez et al., 2000b; Barnard et al., 2004). Sf3b1 is important for correct splicing and somatic mutations lead to myeloid neoplasms (Cazzola et al., 2012). Eif6 was previously shown to be involved in mRNA translation regulation by regulating 80S ribosomal assembly (Ceci et al., 2003). Another important ribosome component is Mrpl11, which when deregulated may contribute to carcinoma development (Sugimoto et al., 2009). Nmd3 is important for coordinating ribosomal export (Trotta et al., 2003). Xrcc6 is involved in DNA repair and interfering with its function can lead to higher cancer risks (Jia et al., 2015). Interestingly, some of the candidates are involved in different aspects of general metabolism cell signaling. Vac14 plays a role in PI signaling regulation, protein trafficking and vacuole membrane recycling (Dove et al., 2002). Gcdh and Qars were detected in the CPEB1 oocyte sample. Mutations in *gcdh* lead to glutaric aciduria type neurometabolic disorder (Keyser et al., 2008) and mutations in *quars* cause microcephaly (Zhang et al., 2014). The direct interaction and the role of this interaction between CPEB1 and the above mentioned partners remain to be determined experimentally.

# 4. DISCUSSION

In this study, I identified a minimal fragment in the *cpeb1* 3'UTR instrumental in somatic depletion and sufficient for germline restriction. The onset of *cpeb1* zygotic transcription was demonstrated to occur at tailbud stages, a time that correlates with the initiation of autonomous germ cell migration. Reducing the levels of endogenous CPEB1 by morpholino translational inhibition does not have a significant effect on germ cell number. Modulating the levels of functional CPEB1 by overexpression of dominant negative variants leads to a substantial decrease in germ cell number when compared to the uninjected embryos. However, when a flag-tagged version was overexpressed, only a moderate reduction was observed. Furthermore, candidate CPEB1 interacting proteins were identified through immunoprecipitation coupled with mass spectrometry analysis. These interactions will provide insight into the cellular processes where CPEB1 may play a role.

## 4.1. CONFIRMING GERMLINE SPECIFICITY

Germline segregation in *X. laevis* depends on the formation and proper vegetal localization of the germ plasm during oogenesis (Tada et al., 2012; Cuykendall and Houston 2010). A comprehensive molecular picture of the germ plasm is beginning to emerge as the functions of the individual components are being elucidated (Mosquera et al 1993; Houston and King 2000a; Cuykendall and Houston 2010; Dzementsei, 2013). A significant contribution to the characterization of the germ cell lineage was the comparative analysis of distinct transcript populations inherent to isolated germ cells versus endodermal cells (Dzementsei, 2013). This RNA-sequencing screen identified *cpeb1* as a member of the germline mRNA pool (Dzementsei, 2013). Remarkably, *cpeb1* is ubiquitously distributed in late stage oocytes, according to both a comparative RNA-sequencing experiment and quantitative PCR performed on the isolated transcript population from dissected vegetal and animal hemispheres (Claussen et al., 2015; Smarandache, 2013). From this perspective, *cpeb1* is more similar to *nanos* and *hsp83,* which are ubiquitously distributed in the syncytial *Drosophila* embryo (Bashirullah et al., 1999). In contrast, classical *Xenopus* germ plasm mRNAs, such as *dnd1*, *pgat* or *ddx25* are restricted to the vegetal hemisphere of the oocyte and are mainly associated with the germ plasm in the embryo (Hudson and Woodland 1998; Claussen et al., 2015). To confirm that *cpeb1* is present in the germ cell lineage, a double *in situ* hybridization with antisense RNA probes complementary to *cpeb1* and *pgat*, an established germline marker (Hudson and Woodland 1998) was performed. *Cpeb1* transcripts colocalized with *pgat* in tailbud stage embryos demonstrating germline specificity (**Figure 3.1.**).

## 4.2 REGULATION OF *CPEB1* EXPRESSION

### 4.2.1 Zygotic transcription

In the previous experiment it was shown that *cpeb1* is detected in primordial germ cells. Two mechanisms by which the restriction of *cpeb1* to the germline may occur are (1) maternally provided mRNAs are somatically depleted, but maintained in the PGCs or (2) global degradation of the mRNA is succeeded by tissue specific zygotic transcription. A fundamental component of both mechanisms is partial or total depletion, respectively, of the maternal pool of *cpeb1*. To distinguish between the two options, the timing of zygotic *cpeb1* transcription was determined. An elegant experimental setup based on the generation of hybrid embryos between the closely related species *X. laevis* and *X. tropicalis* allowed me to differentiate between the paternal and maternal contributions (Yamaguchi et al., 2014). Zygotic genome activation in the germline is delayed as compared to somatic cells by the inhibition of polymerase II at the elongation step due to the lack of phosphorylation on the serine 2 of the CTD (Venkatarama et al., 2010; Lai and King 2013). The earliest time point of zygotic transcription initiation was reported to be at neurula stages for *pou5f3.1* (also known as *oct-91*; st. 14; Venkatarama et al., 2010). In agreement with the delayed zygotic gene expression observed in the PGCs, zygotic *cpeb1* transcripts were not detected until tailbud stages (**Figure 3.2. B**). A similar expression profile was also observed for *dazl*, whose zygotic initiation also occurs in a similar time frame. *Dazl* is a transcript encoding for a translational regulator important for germline development and DAZL and CPEB1 were recently shown to synergistically regulate common target transcripts (Collier et al., 2005; Pfennig, 2014; Martins et al., 2016). A potential sign of tissue specific expression was the low level of transcripts as compared to the maternally provided fraction. Lower transcript levels were also observed in similar experiments for *ddx25*, *dazl* and *dnd1*, transcripts that likewise become restricted to the germline (Yamaguchi et al., 2014; Pfennig, 2014).

### 4.2.2 Somatic clearance

Subsequently, the intrinsic transcript elements that regulate *cpeb1* degradation were investigated. Several germline specific transcripts have been described whose localization to the germ plasm is coordinated by a localization element in the 3'UTR such as *pgat*, *nanos1*, *dnd1* and *dazl* to name a few (Hudson and Woodland 1998; Horvay et al., 2006; Koebernick et al., 2010; Pfennig, 2014). Coincidentally, the somatic depletion of these transcripts is also coordinated by the same 3'UTR elements (Koebernick et al., 2010). Previous experiments have shown that the 3'UTR of *cpeb1* can mediate germline restriction of GFP fusion reporter construct (**Figure 3.3**; Smarandache, 2013). Furthermore, evidence for miRNA mediated depletion of *cpeb1* transcripts

stems from experiments entailing the block of miRNA maturation. This was achieved by saturating and inactivating maternal Argonaute proteins by siRNA injection. In this condition *cpeb1* levels increased, being at least 7-fold greater in the siRNA injected versus wild type embryos (from just over 1 200 transcripts to 12 000 in the siRNA injected; Pfennig, 2014; Lund et al., 2011). Transcript differential regulation is a conserved mechanism across many species. It entails selective somatic destabilization, typically coupled with ensuing translational silencing or degradation (Yartseva and Giraldez, 2015; Swartz and Wessel, 2015). Canonical examples of initially ubiquitously distributed transcripts in the early *Drosophila* syncytial embryo are *Hsp83* and *nanos1*. They subsequently become restricted to the germline by the collaborative action of the maternal and zygotic degradation machineries in the somatic lineage (Bashirullah et al., 1999). In the teleost *D. rerio*, *nanos1* is first deadenylated and translationally silenced and then degraded in the soma as a result of miR-430 action, a miRNA responsible for the decay of several hundred maternally provided mRNAs (Mishima et al., 2006; Giraldez et al., 2006). Several transcripts with differential regulation have also been identified in *X. laevis*. *Dnd1* (previously known as *Dead end* or *XDE*) is protected in the germline by ElrB1 and depleted in the soma due to miR-18 binding to the 3'UTR (Horvay et al., 2006). Germline restriction was also described for the *ddx25* mRNA (previously known as *DEADSouth*), and depletion relies on the targeting of several miR-427 target sites in its 3'UTR in the soma but not in the germline after MBT (Yamaguchi et al., 2014). Notably, in the mentioned study, the measured levels of miR-427 were low in germ cells. Coupled with zygotic transcription it may provide an explanation for the maintenance of the *ddx25* transcript in the germ cell lineage, a mechanism that may be characteristic of *cpeb1* as well (Yamaguchi et al., 2014).

From the above information I deduced that the *cpeb1* 3'UTR could harbor one or multiple minimal regulatory elements, targeted by the miRNA coordinated RISC degradation pathway. The blind-folded approach for fragmenting the 3'UTR determined two independent regulatory regions (**Figure 3.3**). This is consistent with evidence that the localization of *cpeb1 Drosophila* homologue *orb* is dependent on multiple *cis*-elements in the 3'UTR (Lantz and Schedl 1994). Furthermore, a 66 nucleotide sequence (73-139 - proper nomenclature) was established to be sufficient for efficient somatic depletion and germline restriction of the reporter (**Figure 3.4.**).

To identify potential miRNA target sites, two complementary approaches were employed. In order to interfere only with the interaction of the miRNA-mRNA pair of interest I employed target protector morpholinos (TPMOs). The minimal fragment was protected most efficiently by the second TPMO complementary to the last 25 nucleotides (**Figure 3.5. D**). This suggests that the last 25 nucleotides harbor a miRNA target site.

To more directly address the question of which miRNAs are involved in the somatic clearance of *cpeb1* a complementary approach entailing blocking individual miRNAs was employed (Koebernick et al., 2010). The only moderate effect was observed for 2'OMeO-α-xtr-miR-17-5p and it was comparable to that of the scrambled control (**Figure 3.6. D**). MiR-17-5p was found to be expressed in many adult *X. laevis* tissues, such as muscle, liver, skin, spleen, kidney, heart but not in the ovary (Tang and Maxwell 2008). Correlations with the situation in the embryo need to be established before any conclusion can be drawn. It is intriguing though that no effect was obtained with the antisense oligonucleotide sequence corresponding to the last 25 nucleotides. This opens the possibility that the respective region is important for RBP binding. Nonetheless, miRNAs relevant for somatic degradation are yet to be identified.

Notably, screening for potential miRNA binding sites in the entire length of the 3'UTR identified a miR-427 target sequence, located outside the identified minimal fragment. This is in agreement with previous findings where *cpeb1* is predicted to be a miR-427 target transcript, together with *dazl* and *ddx25* (Lund et al., 2009). The expression of miR-427 is first detected in its mature form at stage 9, it exhibits highest levels during the mid-blastula transition and remains stable up to neurula stage 26 (Watanabe et al., 2005; Lund et al., 2009). Together with the observed onset of zygotic transcription observed for *cpeb1* (**Figure 3.2.**), the miR-427:*cpeb1* pair would be a good candidate for testing if this anti-correlation profile in the context of somatic depletion is real.

Several of the predicted miRNAs show expression starting with the onset of gastrulation and are expressed until tailbud stages. Consequently, they are valuable candidates such as xtr-miR-145, members of the xtr-miR-18 family, xtr-miR-302, xtr-miR-19a and b, xtr-miR-130, xtr-miR-301, xtr-miR-216 to name a few (Smarandache, 2013). Interestingly, *cpeb1* paralogs belonging to the *cpeb2* family (*cpeb2-4*) were shown to be coordinately regulated by miRNAs recognizing conserved binding sites in paralog positions of their 3'UTR, miR-92 and miR-26. These target sites were present in the ancestral gene and maintained after gene duplications and divergence of the lineages (Morgan et al., 2010). Evidence to further support the notion that *cpeb1* is regulated by miRNAs emerged from human carcinoma cell lines. One example is the downregulation of *cpeb1* in endometrioid endometrial carcinoma, potentially due to an upregulation of hsa-miR-183-5p (Xiong et al., 2016).

Furthermore, validating the interaction of other predicted miRNA with *cpeb1* will be instrumental in characterizing the regulatory network for this germ cell specific transcript. One promising method is tagged RNA purification MS2-TRAP (Yoon et al., 2012). The transcript of interest is tagged with MS2 RNA hairpins which are recognized by the concomitantly expressed MS2-GST protein. After pulldown of the RNP complex comprising [MS2-GST/*transcript-of-interest-MS2*], the

RNA is isolated, reverse transcribed and real-time qPCR is employed to determine the presence of computationally predicted miRNAs (Yoon et al., 2012).

One essential question that remains is how transcripts are protected in the germline. Evidence from several studies support the speculation that miRNAs and the associated machinery are not inactive, but rather that additional *cis*-elements present in the 3'UTRs of the mRNAs recruit factors that enhance transcript stability and translation (Bashirullah et al., 1999; Mishima et al., 2006; Kedde et al., 2007; Takeda et al., 2009). A slight contradiction comes from the analysis of germline restriction of *ddx25* as in this study the levels of miR-427 detected in germ cells are very low, thus presumably not sufficient for transcript degradation in the germline. However, the activity or presence of the RISC complex was not investigated (Yamaguchi et al., 2014).

An additional layer of complexity to the posttranscriptional regulation of *cpeb1* would be conveyed by RNA-binding proteins. Notably, some members of the *cpeb2* subfamily, for example *cpeb4*, are regulated by CPEs present in their 3'UTR (Igea et al., 2010). The *cpeb1* transcript also contains a CPE located at least 200 nucleotides upstream the hex-element. Determining its functionality is important, as is to identify potential binding sites for known germline specific RNA binding proteins, for example Dazl, Elr proteins, Dnd1, and to verify their role in *cpeb1* regulation.

To conclude, I found that the zygotic transcription of *cpeb1* begins at tailbud stages and I identified a minimal sequence in the *cpeb1* 3'UTR to be sufficient for somatic depletion and germline restriction. Nevertheless, many open questions remain to be addressed in future experiments. An essential question is how the interplay between miRNA and protein mediated regulation models the transcriptional landscape of the germline. Potentially, an answer may lie within the mode of *cpeb1* regulation, as it potentially implicates multiple mechanisms including somatic depletion via 3'UTR *cis*-elements, zygotic transcription and possibly RBPs.

### 4.3. CPEB1 PROTEIN EXPRESSION DURING EARLY DEVELOPMENT

A second line of investigation aimed at characterizing CPEB1 during early embryogenesis specifically in the context of germline development. Prior to functional analysis it is important to determine whether the protein of interest is expressed at the investigated developmental time point. Endogenous CPEB1 protein is stably expressed until late tailbud stage, albeit at lower levels in comparison with late stage oocytes (**Figure 3.7.**). This protein expression profile spanning early development shows similarities and discrepancies with knowledge gathered from previous investigations of CPEB1. Similarly to several studies, the protein amount decreases considerably from oocyte to egg (Hake and Richter, 1994; Reverte et al., 2001). A detailed analysis of CPEB1

protein dynamics in *X. laevis* oocytes determined that during late maturation, 75% of the total protein is degraded shortly after germinal vesicle breakdown in a proteasome dependent manner (Reverte et al., 2001). In contrast, a separate study provided evidence for the complete degradation of CPEB1 between oocyte and egg, a finding that is contradictory to the results of the present work (Thom et al., 2003; Minshall et al., 2007). In the earliest analysis of CPEB1 expression during embryogenesis it was detected only until gastrula stage, whereas levels were stable throughout the analyzed developmental interval in the present study (Hake and Richter 1994). Evidence to support the maintenance of CPEB1 protein is provided by a recent investigation of the relationship between mRNA and protein expression during early embryogenesis using genome-wide RNA sequencing and MultiNotch MS3 analysis (Peshkin et al., 2015). The provided quantitative time-resolved inventory of RNA and protein also includes CPEB1, which based on these measurements shows an increase in protein levels from egg (34 nM) to late tailbud (56 nM; Peshkin et al., 2015).

Protein phosphorylation is a preponderant posttranslational regulatory mechanism involved in modulating cellular processes (Fischer, 2013). Oocyte maturation proceeds as a hormone induced cascade leads to the phosphorylation of several downstream targets, including CPEB1 (Mendez et al., 2000a; Castro et al., 2001; Sato, 2014). This posttranslational change was observed in maturing oocytes where CPEB1 has a slower electrophoretic mobility as compared to immature oocytes (Paris et al., 1991; Hake and Richter 1994; de Moor and Richter, 1999; Reverte et al., 2001; Sarkissian et al., 2004; Kim and Richter, 2006; Nechama et al., 2013). The phosphorylated CPEB1 was reported to persist in the egg, yet at later developmental stages only the dephosphorylated species was observed (Hake and Richter 1994). Nevertheless, phosphorylated CPEB1 is transiently expressed and its detection requires careful timing (Thom et al., 2003). In the current analysis no CPEB1 phosphorylation could be recognized in the egg, potentially reflecting the transient nature of this posttranslational modification. Together with the steady expression observed in the developmental time series analyzed, this fact may dispute the specificity of the employed antibody. To confirm that the anti-CPEB1 antibody used in this study is specific, it was tested on and it recognized CPEB1 tagged with various epitopes, flag-tag, myc-tag and BMP-fusion, produced in oocyte, embryo, bacteria and *in vitro* in rabbit reticulocyte lysate (**Figure 3.8.**, **Figure 3.10.**, **Figure S5.**).

Generally, transcript abundance correlates poorly with protein expression in the embryo (Smits et al., 2014; Peshkin et al., 2015). Whereas the *cpeb1* mRNA is depleted during MZT (**Figure 3.2.**), CPEB1 amounts stay constant (**Figure 3.7.**), suggesting that the observed protein is maternally provided. This is in agreement with genome wide proteome and transcriptome findings, showing

that CPEB1 is present in the embryo subsequent to *cpeb1* degradation (Smits et al., 2014; Peshkin et al., 2015). Moreover, zygotic transcription may account for a newly translated fraction of CPEB1 protein. In the present study, mass spectrometry analysis on oocytes (stage VI) and neurula embryos (stage 13) revealed an increase in the pulled down CPEB1 protein (**Table S1.**), reflecting an increase in the levels of endogenous protein. This result correlates with the increase detected in a separate study (Peshkin et al., 2015).

Genome-wide analyses are invaluable for generating an overview of the mRNA and protein economy in the entirety of an embryo (Smits et al., 2014). Nevertheless, it is relevant to study changes specific to distinct cell populations in an embryo. It was shown previously that *cpeb1* transcripts are restricted to the germline at late tailbud stages (**Figure 3.1.**, Dzementsei, 2013). Consequently my aim was to determine whether transcript presence and protein translation correlate in the germline in tailbud stages. Whole mount immunostaining performed with the antibody described above and a second antibody used in a separate study did not reveal the endogenous localization of CPEB1 in the spatial context of the embryo (**Figure 3.9.**). The monoclonal antibody used by Wilczynska and colleagues was produced in mouse against the N-terminally GST-tagged human CPEB1-Δ5 and it was successfully used in immunofluorescence staining on human HeLa cell lines. In this study, CPEB1 was detected in P bodies (referred to as 'dcp1 bodies' in the paper) and stress granules in association with the DEAD box helicase rck/p54 (Wilczynska et al., 2005). Interestingly, stress granules share components with germ cell granules such as proteins belonging to the Argonaute family (Miwi, Mili, Ago2 in mouse) and Dicer (in mouse) involved in small RNA processing and Sm proteins involved in splicing in *X. laevis* (Voronina et al., 2011). Despite the wealth of studies on CPEB1 function, only one focuses on the expression of CPEB1 in the *X. laevis* embryo and only until gastrula stages. This analysis provided insight on the localization of CPEB1 at the mitotic apparatus together with Maskin and *cyclin B1* in a microtubule dependent manner (Groisman et al., 2000).

### 4.4 Alteration of CPEB1 levels reduces primordial germ cell number

Extensive studies on the implication of CPEB1 in the *X. laevis* oocyte revealed the molecular mechanism set in place for flexible and timely translational regulation of CPEB1 target transcripts according to the time point in the cellular transition from an immature to a mature oocyte (Paris et al., 1991; Hake and Richter, 1994; Stebbins-Boaz et al., 1996; Stebbins-Boaz et al., 1999; Mendez et al., 2000a; Mendez et al., 2000b; Mendez et al., 2002; Cao and Richter, 2002; Groisman et al 2002; Reverte et al., 2001; Thom et al., 2003; Sarkissian et al., 2004; Kim and Richter, 2006; Kim and Richter, 2007; Minshall et al., 2007; Piqué et al., 2008). Nevertheless, there

are no investigations that interrogate the potential function of CPEB1 in the segregation of the *X. laevis* germ cell lineage. As *X. laevis* is an allotretraploid organism, genetic manipulations are not straightforward (Khokha and Loots 2005; Uno et al., 2013; Matsuda et al., 2015). Generally, functional investigations begin with altering the levels of the protein of interest. Traditionally, antisense methods for altering gene expression have been described already 30 years ago (Harland and Weintraub, 1985; Izant and Weintraub, 1985). A relatively recent and widely used methodology for knock-down effects is the use of translational blocking morpholinos (tMO; Summerton and Weller, 1997; Summerton et al., 1997; Summerton, 2007; Heasman et al., 2000; Nutt et al., 2001; Heasman, 2002; Eisen and Smith, 2008). Using this tool I wanted to verify whether CPEB1 knock-down would have any effect on germline development. Despite the successful use of the tMO *in vitro*, this approach was not efficient in the embryo (**Figure 3.10.**). Consequently I applied an alternative approach, which employs dominant negative variants of the protein of interest. Because the binding of CPEB1 to its preferred sequence element has been minutely described, the functional analysis employed previously characterized dominant negative mutants of CPEB1 (DN; Afroz et al., 2014). The effect of the overexpression of the DN in the oocyte was monitored before and after progesterone induced maturation. The polyadenylation of known target transcripts was reduced in the case of a RNA binding DN comprising the wild-type RRM1 and RRM2 and Zn-finger domains (RRM12ZZ) and not affected in DN with mutations in amino acids essential for RNA binding (Afroz et al., 2014). In the current study the output measurement is the number of primordial germ cells in the endoderm, similarly to other functional studies of proteins with potential roles in germline development (Horvay et al., 2006; Koebernick et al., 2010). The overexpression of DN CPEB1 led to a substantial increase in the percentage of embryos with less than 20 PGCs per individual. Interestingly, all mutants, irrespective of their RNA-binding capacity, had an influence on the number of primordial germ cells (**Figure 3.11.**). This outcome suggests that saturating the system with the RRM12ZZ variant may affect the endogenous protein-protein interactions. An argument supporting this interpretation is that the RRM interface of CPEB1 is capable of dimerization in the oocyte (Lin et al., 2012). Consequently, this knowledge may be conveyed to the embryo system. It can be speculated that CPEB1 proteins belonging to the endogenous pool are sequestered and maintained in an inactive form, precluded from RNA-binding. Furthermore, it is possible that spare polyadenylation factors are also recruited, hence preventing them from inducing polyadenylation on transcripts with low affinity CPE sites (Mendez et al., 2002; Reverte et al., 2001; Lin et al., 2012). In the oocyte background, maturation induced phosphorylation of CPEB1, including the dimer pool, triggering their destruction and releasing associated factors. Therefore it

was postulated that CPEB1 dimers serve as a molecular hub for polyadenylation factors required for translational activation (Lin et al., 2012).

In addition to its essential role in the meiotic cell cycle, CPEB1 together with CPEB2 and CPEB4 have distinct roles and are essential for in the mitotic cell cycle (Novoa et al., 2010; Giangarrà et al., 2015). Consequently, a possible explanation for the reduced PGC number in the DN injected embryos may reflect complications occurring during primordial germ cell mitosis which happens between gastrula and tailbud stages (Whitington and Dixon, 1975). Interestingly, CPEB1 was reported to be involved in mRNA localization at the mitotic spindle in the *X. laevis* embryo, together with Maskin and *cyclin B1* (Groisman et al., 2000). Furthermore, CPEB1 is known to form RNA-dependent interactions with a germ cell specific factor, such as Ybx2 (previously known as FRGY-2; Standart and Minshall 2008). Consequently, it can be deduced that the localization and equal distribution of essential germ plasm factors at the two mitotic spindle poles was affected (Whitington and Dixon, 1975; Taguchi et al., 2012). An attractive potential interpretation may be that due to faulty distribution at the spindle, only one of the daughter cells may inherit germ plasm, hence the number of PGCs is reduced. To support this supposition, the reorganization of germ plasm during embryogenesis was shown to be blocked by tubulin inhibitors (Taguchi et al., 2012).

Considering that the DN experiment led to a reduction in primordial gem cell number it could be inferred that the overexpression of a full-length epitope-tagged CPEB1 variant could lead to a similar result. In partial agreement with this deduction, the number of PGCs observed per embryo was reduced for a higher proportion of the total examined embryos than for uninjected or F-GFP injected negative controls. Nonetheless, the observed phenotypes were milder in this experiment (**Figure 3.12.**). It must be considered that one major difference to the RRM12ZZ DN mutant experiment is the presence of the N-terminal domain in the F-CPEB1 variant. This region of CPEB1 lacks obvious functional motifs as it is an intrinsically disordered domain and is the core of posttranslational regulation (Hake et al., 1998; Mendez et al., 2000a; Mendez et al., 2000b; Reverte et al., 2001; Mendez et al., 2002; Setoyama et al., 2007). It contains sites that are phosphorylated during oocyte maturation, the Pin1 interaction site and the PEST domain recognized by the ß-transducin repeat containing protein (Btrc, formerly known as ß-TrCP), all being essential for 26S proteasome mediated degradation (Reverte et al., 2001; Mendez et al., 2002; Setoyama et al., 2007; Nechama et al., 2013). Moreover, the LDSR motif and PEST domain were demonstrated to be essential for microtubule binding (Groisman et al., 2000). Injection of a mutant lacking the PEST domain and flanking regions led to retarded rates of cell division despite no effect on polyadenylation induced translation. Similarly, a mutant with an N-terminal deletion

lacking the Aurora A phosphorylation site induces slower division rates, nonetheless, an effect on CPE-dependent translation is additionally observed (Mendez et al., 2000; Groisman et al., 2000). Moreover, when embryos were injected with anti-CPEB1 antibodies, effects on cell division were observed once more in that the mitotic apparatus was abnormal and the localization of the *cyclin B1* and *bub3* localization was abrogated (Groisman et al., 2000). In contrast, the injection of the wild-type full length CPEB1 did not have any deleterious effect on cell division (Groisman et al., 2000). Overall, the DN experiment may have had a more pronounced outcome as compared to F–CPEB1 overexpression, as the regulatory regions are intact and protein-protein interactions required for microtubule binding and degradation of CPEB1 are permitted. Hence, the F-CPEB1 variant could be regulated similarly to the endogenous protein at the posttranslational level, in contrast to the DN lacking the N-terminus. In support of this notion, injection of non-degradable CPEB1 mutants in oocytes prohibits progression to meiosis II, probably through the prevention of *cyclin B1* synthesis, demonstrating the importance of posttranslational regulation (Mendez et al., 2002). Nevertheless, a decrease in the germline cell population was observed. A potential explanation could be that exogenous CPEB1 molecules may overpopulate the target transcripts by binding additional low affinity CPEs, thereby having an inhibitory effect on translation.

An additional control in this experiment was the injection of a RNA-binding protein, Ptbp1 (previously known as Ptbp1/hnRNP I; Xie et al., 2003). Early investigations on Ptbp1 determined its role in cytoplasmic RNA localization, for example the localization of *Vg1* to the vegetal cortex (Cote et al., 1999; Lewis et al., 2008; Kroll et al., 2009; Claussen et al., 2011). Several other studies revealed its involvement in RNA processing, more specifically in splicing (Noiret et al., 2016). Interestingly, in the present experiment the overexpression of Ptbp1 had a slightly more pronounced effect on germ cell number as compared to F-CPEB1 injection. This may be a reflection of its importance in RNA processing and localization events.

Functional studies are essential in determining whether a protein of interest potentially plays a role in a specific process, in this case germline development. Nevertheless, a molecular approach is required in order to identify a specific function of the protein. As both CPEB1 and Ptbp1 are known to form various interactions with other proteins, and in the case of CPEB1 to nucleate complexes vital for CPE-mediated translation, it is important to determine the identity of interacting protein partners. With the debut of genome-wide approaches, a comprehensive overview of protein-protein interactions can be resolved. For this purpose I performed a mass spectrometry based analysis in the late stage oocyte and the early neurula embryo.

### 4.5 CANDIDATE INTERACTION PARTNERS MAY REVEAL CPEB1 ROLE IN GERMLINE DEVELOPMENT

An exhaustive examination of the molecular interactions that CPEB1 and Ptbp1 have in the oocyte and embryo revealed candidates with diverse functions involved in cellular processes ranging from mRNA processing to ribosome biogenesis (**Table 3.1.**).

To begin with, the relative amounts for the injected transcript products and the corresponding endogenous proteins were analyzed. In both oocytes and embryos F-Ptbp1 was translated in higher amounts than F-CPEB1, despite the injection of the same amount of transcript. The endogenous amounts for CPEB1_S and CPEB1_L are relatively similar to each other in the oocyte. In the embryo, no distinction between the homeologs could be determined. However, the detected amount for CPEB1 in the oocyte, when summing up the amounts for CPEB1_S and CPEB1_L, is still lower than that detected in the embryo, presumably showing an increase in CPEB1 translation in the embryo (**Table S1.**). Interestingly, in the oocyte Ptbp1 fraction both CPEB1_S and CPEB1_L were detected but the opposite was not true. Conversely, no CPEB1 protein was detected in the embryo Ptbp1 fraction despite the high Ptbp1 protein levels. Intriguingly, Ptbp1 was precipitated in the corresponding embryonic CPEB1 sample.

Remarkably, the identified protein populations from the oocyte and embryo have a small or no overlap for both CPEB1 and Ptbp1 indicating high dynamics of protein-protein interactions in the two situations. This suggests a strict regulatory mechanism regarding establishing certain interactions in the oocyte which are then replaced by others in the embryo. Furthermore, it can be deduced that the interactome for both investigated proteins is highly dynamic during the oocyte to zygote transition.

The two top candidates that comprise the overlap between the embryo and oocyte series for CPEB1, namely Cpsf2 and Symplekin, were precipitated in considerable amounts and were detected in negligible amounts in the other samples, proving the reliability of the procedure. Coincidentally, they are established CPEB1 protein partners and are involved in the well-described cytoplasmic polyadenylation dependent translation (Mendez et al., 2000b; Barnard et al., 2004). Notably, other proteins reported to interact with CPEB1, Parn, Gld2 and Maskin, were not detected in neither the oocyte or the embryo samples (Stebbins-Boaz et al., 1999; Cao and Richter 2002; Kim and Richter 2006). In agreement with this observation, another investigation of CPEB1 interaction partners did not observe Maskin neither in early or late oocyte samples (Minshall et al., 2007).

Some of the top candidates are related to RNA processing for both CPEB1 and Ptbp1. However, many candidates are involved in processes as various as protein biosynthesis, protein transport,

signaling and metabolic pathways. This overview suggests that RNA processing is an integral part of cellular metabolism. For example, it was shown that Ptbp1 can prevent non-sense mediated decay on bound target transcripts (Ge et al., 2016). Furthermore, it was also reported to be involved in the posttranscriptional regulation of endothelial nitric oxide synthase, creating a link between RNA processing and metabolism (Yi et al., 2015). Therefore it would be interesting to determine how these candidates function in the context of germ cell development and to create correlations between cellular processes initially thought to be independent of one another. Moreover, discovering new RNA-binding properties of proteins not thought to be involved in RNA metabolism would contribute to the emerging atlas of enigmRBPs, RNA-binding proteins with non-canonical of unknown RNA binding function (Castello et al., 2013; Beckmann et al., 2015).

**BIBLIOGRAPHY**

Afroz T, Skrisovska L, Belloc E, Guillén-Boixet J, Méndez R & Allain FHT (2014) A fly trap mechanism provides sequence-specific RNA recognition by CPEB proteins. *Genes Dev.* 28, 1498–1514.

Arumugam, K., MacNicol, M.C., Wang, Y., Cragle, C.E., Tackett, A.J., Hardy, L.L., MacNicol, A.M., (2012). Ringo/Cyclin-dependent Kinase and Mitogen-activated Protein Kinase Signaling Pathways Regulate the Activity of the Cell Fate Determinant Musashi to Promote Cell Cycle Re-entry in *Xenopus* Oocytes. J. Biol. Chem. 287, 10639–10649. doi:10.1074/jbc.M111.300681

Bauermeister D, Claußen M & Pieler T (2014) Biochemical Aspects of Subcellular RNA Transport and Localization. In *Chemical Biology of Nucleic Acids, RNA Technologies*. pp.293–308.

Barnard, D.C., Ryan, K., Manley, J.L., Richter, J.D., (2004). Symplekin and xGLD-2 are required for CPEB-mediated cytoplasmic polyadenylation. Cell 119, 641–651. doi:10.1016/j.cell.2004.10.029

Bashirullah A, Halsell, S.R., Cooperstock, R.L., Kloc, M., Karaiskakis, A., Fisher, W.W., Weili, F., Hamilton, J.K., Etkin, L.D., Lipshitz, H.D., (1999). Joint action of two RNA degradation pathways controls the timing of maternal transcript elimination at the midblastula transition in Drosophila melanogaster. EMBO J. 18, 2610–2620. doi:10.1093/emboj/18.9.2610

Bava F-A, Eliscovich C, Ferreira PG, Miñana B, Ben-Dov C, Guigó R, Valcárcel J & Méndez R (2013) CPEB1 coordinates alternative 3'-UTR formation with translational regulation. *Nature* 495, 121–125.

Beckmann BM, Horos R, Fischer B, Castello A, Eichelbaum K, Alleaume A-M, Schwarzl T, Curk T, Foehr S, Huber W, Krijgsveld J & Hentze MW (2015) The RNA-binding proteomes from yeast to man harbour conserved enigmRBPs. *Nat. Commun.* 6, 10127.

Belloc E & Méndez R (2008) A deadenylation negative feedback mechanism governs meiotic metaphase arrest. *Nature* 452, 1017–1021.

Betel D, Koppal A, Agius P, Sander C & Leslie C (2010) Comprehensive modeling of microRNA targets predicts functional non-conserved and non-canonical sites. *Genome Biol.* 11, R90.

Billett FS & Adam E (1976) The structure of the mitochondrial cloud of Xenopus laevis oocytes. *J. Embryol. Exp. Morphol.* 36, 697–710.

Bohnsack M.T. (2004). Exportin 5 is a RanGTP-dependent dsRNA-binding protein that mediates nuclear export of pre-miRNAs. RNA 10, 185–191. doi:10.1261/rna.5167604

Bonev B &Papalopulu N (2012). Methods to analyze microRNA expression and function during Xenopus development. Methods Mol. Biol. 917, 445–459. doi:10.1007/978-1-61779-992-1_25

Brook M, Smith JWS & Gray NK (2009) The DAZL and PABP families: RNA-binding proteins with

interrelated roles in translational control in oocytes. *Reproduction* 137, 595–617.

Buehr M & Blacker A (1970) Sterility and partial sterility in the South African clawed toad following the pricking of the egg. *Journ. Emb. Exp. Morph.* 23, 375–384.

Burns DM, D'Ambrogio A, Nottrott S & Richter JD (2011) CPEB and two poly(A) polymerases control miR-122 stability and p53 mRNA translation. *Nature* 473, 105–108.

Cao, Q., Richter, J.D., (2002). Dissolution of the maskin-eIF4E complex by cytoplasmic polyadenylation and poly(A)-binding protein controls cyclin B1 mRNA translation and oocyte maturation. EMBO J. 21, 3852–62. doi:10.1093/emboj/cdf353

Castello, A., Fischer, B., Hentze, M.W., Preiss, T., (2013). RNA-binding proteins in Mendelian disease. Trends Genet. 29, 318–327. doi:10.1016/j.tig.2013.01.004

Castro A, Peter M, Lorca T & Mandart E (2001) c-Mos and cyclin B/cdc2 connections during Xenopus oocyte maturation. *Biol. Cell* 93, 15–25.

Cazzola M, Rossi M & Malcovati L (2013) Biologic and clinical significance of somatic mutations of SF3B1 in myeloid and lymphoid neoplasms. *Blood;* 121; 260-9.

Ceci M, Gaviraghi C, Gorrini C, Sala LA, Offenhäuser N, Marchisio PC, Biffo S (2003) Release of eIF6 (p27BBP) from the 60S subunit allows 80S ribosome assembly. *Nature;* 426; 578-84.

Charlesworth A, Wilczynska A, Thampi P, Cox LL & MacNicol AM (2006) Musashi regulates the temporal order of mRNA translation during Xenopus oocyte maturation. *EMBO J.* 25, 2792–2801.

Choi, W.-Y., Giraldez, A.J., Schier, A.F., (2007). Target Protectors Reveal Dampening and Balancing of Nodal Agonist and Antagonist by miR-430. Science (80-. ). 318, 271 LP-274.

Choo S, Heinrich B, Betley JN, Chen Z & Deshler JO (2005) Evidence for common machinery utilized by the early and late RNA localization pathways in Xenopus oocytes. *Dev. Biol.* 278, 103–117.

Cinalli RM, Rangan P & Lehmann R (2008) Germ Cells Are Forever. *Cell* 132, 559–562.

Claussen M, Horvay K & Pieler T (2004) Evidence for overlapping, but not identical, protein machineries operating in vegetal RNA localization along early and late pathways in Xenopus oocytes. *Development* 131, 4263–4273.

Claussen M & Pieler T (2010) Identification of vegetal RNA-localization elements in Xenopus oocytes. *Methods* 51, 146–151.

Claussen M, Tarbashevich K & Pieler T (2011) Functional dissection of the RNA signal sequence responsible for vegetal localization of XGrip2.1 mRNA in Xenopus oocytes. *RNA Biol* 8, 873–882.

Claussen, M., Lingner, T., Pommerenke, C., Opitz, L., Salinas, G., Pieler, T., (2015). Global analysis of asymmetric RNA enrichment in oocytes reveals low conservation between closely related Xenopus species. Mol. Biol. Cell 26, 3777–3787. doi:10.1091/mbc.E15-02-0115

Collier, B., Gorgoni, B., Loveridge, C., Cooke, H.J., Gray, N.K., (2005). The DAZL family proteins are PABP-binding proteins that regulate translation in germ cells. EMBO J. 24, 2656–2666. doi:10.1038/sj.emboj.7600738

Cote CA, Gautreau D, Denegre JM, Kress TL, Terry NA & Mowry KL (1999) A Xenopus protein related to hnRNP I has a role in cytoplasmic RNA localization. *Mol. Cell* 4, 431–437.

Cuykendall TN & Houston DW (2010) Identification of germ plasm-associated transcripts by microarray analysis of xenopus vegetal cortex RNA. *Dev. Dyn.* 239, 1838–1848.

Dawid IB & Sargent TD (1988) Xenopus laevis in developmental and molecular biology. *Science* 240, 1443–1448.

De Moor, C.H., Richter, J.D., (1997). The Mos pathway regulates cytoplasmic polyadenylation in Xenopus oocytes. Mol. Cell. Biol. 17, 6419–6426.

De Moor CH & Richter JD (1999) Cytoplasmic polyadenylation elements mediate masking and unmasking of cyclin B1 mRNA. *EMBO J.* 18, 2294–2303.

Dickson, K.S., Bilger, a, Ballantyne, S., Wickens, M.P., (1999). The cleavage and polyadenylation specificity factor in Xenopus laevis oocytes is a cytoplasmic factor involved in regulated polyadenylation. Mol. Cell. Biol. 19, 5707–17.

Distler, U., Kuharev, J., Navarro, P., Levin, Y., Schild, H., Tenzer, S., (2013). Drift time-specific collision energies enable deep-coverage data-independent acquisition proteomics. Nat. Methods 11, 167–170. doi:10.1038/nmeth.2767

Dubaissi, E., Panagiotaki, N., Papalopulu, N., Vize, P.D., (2012). Antibody Development and Use in Chromogenic and Fluorescent Immunostaining BT - Xenopus Protocols: Post-Genomic Approaches, in: HOPPLER, S., Vize, P.D. (Eds.), . Humana Press, Totowa, NJ, pp. 411–429. doi:10.1007/978-1-61779-992-1_23

Dove SK, McEwen RK, Mayes A, Hughes DC, Beggs JD & Michell RH (2002) Vac14 controls PtdIns(3,5)P(2) synthesis and Fab1-dependent proteni trafficking to the multivesicular body. *Curr. Biol*. 12;885-93.

Dumont JN (1972) Oogenesis in Xenopus laevis (Daudin). I. Stages of oocyte development in laboratory maintained animals. *J. Morphol.* 136, 153–179.

Dzementsei A, Schneider D, Janshoff A & Pieler T (2013) Migratory and adhesive properties of Xenopus laevis primordial germ cells in vitro. *Biol. Open* 2, 1279–1287.

Dzementsei A (2013) Role of cellular dynamics adheion and polarity in the context of primordial germ cell migration in Xenopus laevis embryos. GGNB program Genes and Development, Georg-August University Göttingen

Eisen JS & Smith JC (2008) Controlling morpholino experiments: don't stop making antisense. *Development* 135, 1735–1743.

Extavour CG & Akam M (2003) Mechanisms of germ cell specification across the metazoans: epigenesis and preformation. *Development* 130, 5869–5884.

Ferrell, J.E., (1999). Xenopus oocyte maturation: new lessons from a good egg. BioEssays 21, 833–842. doi:10.1002/(SICI)1521-1878(199910)21:10<833::AID-BIES5>3.0.CO;2-P

Fischer EH (2013) Cellular regulation by protein phosphorylation. *Biochem. Biophys. Res. Commun.* 430, 865–867.

Fisher, M. P., and C. W. Dingman. (1971). Role of molecular conformation in determining the electrophoretic properties of polynucleotides in agarose-acrylamide composite gels. Biochemistry 10: 1895-1899.

Fox, C.A., Sheets, M.D., Wickens, M.P., (1989). Poly(A) addition during maturation of frog oocytes: Distinct nuclear and cytoplasmic activities and regulation by the sequence UUUUUAU. Genes Dev. 3, 2151–2162. doi:10.1101/gad.3.12b.2151

Gagnon James, M.K., (2011). Visualization of mRNA localization in Xenopus oocytes. Methods Mol. Biol. 714, 1–10. doi:10.1007/978-1-61779-005-8

Galardi S, Petretich M, Pinna G, D'Amico S, Loreni F, Michienzi A, Groisman I & Ciafrè SA (2016) CPEB1 restrains proliferation of Glioblastoma cells through the regulation of p27Kip1 mRNA translation. *Sci. Rep.* 6, 25219.

Ge Z, Quek BL, Beemon KL & Hogg JR (2016) Polypyrimidine tract binding protein 1 protects mRNAs from recognition by the nonsense-mediated mRNA decay pathway. *Elife* 5, e11155.

Gebauer, F., Richter, J.D., (1996). Mouse cytoplasmic polyadenylylation element binding protein: an evolutionarily conserved protein that interacts with the cytoplasmic polyadenylylation elements of c-mos mRNA. Proc. Natl. Acad. Sci. U. S. A. 93, 14602–7.

Geromanos, S.J., Hughes, C., Ciavarini, S., Vissers, J.P.C., Langridge, J.I., (2012) Using ion purity scores for enhancing quantitative accuracy and precision in complex proteomics samples. Anal. Bioanal. Chem. 404, 1127–1139. doi:10.1007/s00216-012-6197-y

Giangarrà V, Igea A, Castellazzi CL, Bava FA & Mendez R (2015) Global analysis of CPEBs reveals sequential and non-redundant functions in mitotic cell cycle. *PLoS One* 10, e0138794.

Giraldez AJ (2006) Zebrafish MiR-430 Promotes Deadenylation and Clearance of Maternal mRNAs. *Science* 312, 75–79.

Graindorge, A., Le Tonquèze, O., Thuret, R., Pollet, N., Osborne, H.B., Audic, Y., (2008). Identification of CUG-BP1/EDEN-BP target mRNAs in Xenopus tropicalis. Nucleic Acids Res. 36, 1861–1870. doi:10.1093/nar/gkn031

Groisman I, Huang YS, Mendez R, Cao Q, Theurkauf W & Richter JD (2000) CPEB, maskin, and cyclin B1 mRNA at the mitotic apparatus: implications for local translational control of cell division. *Cell* 103, 435–447.

Groisman I, Jung MY, Sarkissian M, Cao QP & Richter JD (2002) Translational control of the embryonic cell cycle. *Cell* 109, 473–483.

Hake, L.E., Mendez, R., Richter, J.D., (1998). Specificity of RNA binding by CPEB: requirement for RNA recognition motifs and a novel zinc finger. Mol. Cell. Biol. 18, 685–693.

Hake, L.E., Richter, J.D., (1994). CPEB is a specificity factor that mediates cytoplasmic polyadenylation during Xenopus oocyte maturation. Cell 79, 617–627. doi:10.1016/0092-

8674(94)90547-9

Harland R & Weintraub H (1985) Translation of mRNA injected into Xenopus oocytes is specifically inhibited by antisense RNA. *J. Cell Biol.* 101, 1094–1099.

Harland, R. M. (1991). In situ hybridization: an improved whole-mount method for Xenopus embryos. Methods in cell biology 36: 685-695.

Heasman J (2002) Morpholino oligos: making sense of antisense? *Dev. Biol.* 243, 209–214.

Heasman J, Kofron M & Wylie C (2000) βCatenin Signaling Activity Dissected in the Early Xenopus Embryo: A Novel Antisense Approach. *Dev. Biol.* 222, 124–134.

Heasman J, Quarmby J & Wylie CC (1984) The mitochondrial cloud of Xenopus oocytes: The source of germinal granule material. *Dev. Biol.* 105, 458–469.

Helling, R.B., Goodman, H.M., Boyer, H.W., (1974). Analysis of endonuclease R· EcoRI fragments of DNA from lambdoid bacteriophages and other viruses by agarose-gel electrophoresis. Journal of virology 14(5), 1235-1244

Hollemann, T., and T. Pieler (1999) Xpitx-1: a homeobox gene expressed during pituitary and cement gland formation of Xenopus embryos. Mechanisms of development 88: 249-252.

Hörmanseder E, Tischer T & Mayer TU (2013) Modulation of cell cycle control during oocyte-to-embryo transitions. *EMBO J.* 32, 2191–2203.

Horvay K, Claußen M, Katzer M, Landgrebe J & Pieler T (2006) Xenopus Dead end mRNA is a localized maternal determinant that serves a conserved function in germ cell development. *Dev. Biol.* 291, 1–11.

Houston, D.W., King, M.L. (2000) Germ plasm and molecular determinants of germ cell fate. Curr. Top. Dev. Biol. 50, 155–181.

Houston DW & King ML (2000) A critical role for Xdazl, a germ plasm-localized RNA, in the differentiation of primordial germ cells in Xenopus. *Development* 127, 447–456.

Huang YS & Richter JD (2004) Regulation of local mRNA translation. *Curr. Opin. Cell Biol.* 16, 308–313.

Hudson C & Woodland HR (1998) Pgat, a gene expressed specifically in germ plasm and primordial germ cells of Xenopus laevis. *Mech. Dev.* 73, 159–168.

Igea, A., Méndez, R., (2010) Meiosis requires a translational positive loop where CPEB1 ensues its replacement by CPEB4. EMBO J. 29, 2182–2193. doi:10.1038/emboj.2010.111

Ivshina, M., Lasko, P., Richter, J.D., (2014) Cytoplasmic Polyadenylation Element Binding Proteins in Development, Health, and Disease. Annu. Rev. Cell Dev. Biol. 30, 393–415. doi:10.1146/annurev-cellbio-101011-155831

Izant JG & Weintraub H (1985) Constitutive and conditional suppression of exogenous and endogenous genes by anti-sense RNA. *Science* 229, 345–352.

Jia J, ren J, Yao D, Xiao L & Sun R (2015) Association between the XRCC6 polymorphism and cancer risks: a systematic review and meta-analysis. *Medicine*; 94; 1-15.

Johnson AD & Alberio R (2015) Primordial germ cells: the first cell lineage or the last cells standing? *Development* 142, 2730–2739.

Jong, H.K., Richter, J.D., (2007) RINGO/cdk1 and CPEB mediate poly(A) tail stabilization and translational regulation by ePAB. Genes Dev. 21, 2571–2579. doi:10.1101/gad.1593007

Karaiskou, A., Dupré, A., Haccard, O., Jessus, C., (2001) From progesterone to active Cdc2 in Xenopus oocytes: A puzzling signalling pathway. Biol. Cell 93, 35–46. doi:10.1016/S0248-4900(01)01126-1

Kedde M, Strasser MJ, Boldajipour B, Vrielink JAFO, Slanchev K, le Sage C, Nagel R, Voorhoeve PM, van Duijse J, Ørom UA, Lund AH, Perrakis A, Raz E & Agami R (2007) RNA-Binding Protein Dnd1 Inhibits MicroRNA Access to Target mRNA. *Cell* 131, 1273–1286.

Keyser B, Mühlhausen C, Dickmanns A, Christersen E, Muschol N, Ullrich K & Braulke T (2008) Disease causing missense mutations affect enzymatic activity, stability and oligomerization of glutaryl-CoA dehydrogenase (GCDH). *Hum Mol Genet.*17;3854-63.

Khokha MK & Loots GG (2005) Strategies for characterising cis-regulatory elements in Xenopus. *Briefings Funct. Genomics Proteomics* 4, 58–68.

Kim, J.H., Richter, J.D., (2006) Opposing polymerase-deadenylase activities regulate cytoplasmic polyadenylation. Mol. Cell 24, 173–83. doi:10.1016/j.molcel.2006.08.016

Kim, Y.-K., Kim, B., Kim, V.N., (2016) Re-evaluation of the roles of *DROSHA* , *Exportin 5* , and *DICER* in microRNA biogenesis. Proc. Natl. Acad. Sci. 113, E1881–E1889. doi:10.1073/pnas.1602532113

Kloc M & Etkin LD (1995) Two distinct pathways for the localization of RNAs at the vegetal cortex in Xenopus oocytes. *Development* 121, 287–297.

Kloc M, Jedrzejowska I, Tworzydlo W & Bilinski SM (2014) Balbiani body, nuage and sponge bodies - The germ plasm pathway players. *Arthropod Struct. Dev.* 43, 341–348.

Kloc M, Larabell C, Chan APY & Etkin LD (1998) Contribution of METRO pathway localized molecules to the organization of the germ cell lineage. *Mech. Dev.* 75, 81–93.

Kochanek DM & Wells DG (2013) CPEB1 regulates the expression of MTDH/AEG-1 and glioblastoma cell migration. *Mol. Cancer Res.* 11, 149–160.

Koebernick K, Loeber J, Arthur PK, Tarbashevich K & Pieler T (2010) Elr-type proteins protect Xenopus Dead end mRNA from miR-18-mediated clearance in the soma. *Proc. Natl. Acad. Sci. U. S. A.* 107, 16148–16153.

Kratassiouk G, Pritchard LL, Cuvellier S, Vislovukh A, Meng Q, Groisman R, Degerny C, Deforzh E, Harel-Bellan A & Groisman I (2016) The WEE1 regulators CPEB1 and miR-15b switch from inhibitor to activators at G2/M. *Cell Cycle* 15, 667–677.

Kress TL, Yoon YJ & Mowry KL (2004) Nuclear RNP complex assembly initiates cytoplasmic RNA

localization. *J. Cell Biol.* 165, 203–211.

Kroll TT, Swenson LB, Hartland EI, Snedden DD, Goodson H V. & Huber PW (2009) Interactions of 40LoVe within the ribonucleoprotein complex that forms on the localization element of Xenopus Vg1 mRNA. *Mech. Dev.* 126, 523–538.

Kuharev J, Navarro P, Distler U, Jahn O, Tenzer S (2015) In-depth evaluation of software tools for data- independent acquisition based label-free quantification. Proteomics 15:3140-51.

Laemmli, U. K. (1970) Cleavage of structural proteins during the assembly of the head of bacteriophage T4. Nature 227: 680-685.

Lai F & King M Lou (2013) Repressive translational control in germ cells. *Mol. Reprod. Dev.* 80, 665–676.

Langley AR, Smith JC, Stemple DL & Harvey S a (2014) New insights into the maternal to zygotic transition. *Development* 141, 3834–3841.

Lai, F., Singh, a., King, M.L., (2012) Xenopus Nanos1 is required to prevent endoderm gene expression and apoptosis in primordial germ cells. Development 139, 1476–1486. doi:10.1242/dev.079608

Lai, F., Zhou, Y., Luo, X., Fox, J., King, M. Lou, (2011) Nanos1 functions as a translational repressor in the Xenopus germline. Mech. Dev. 128, 153–163. doi:10.1016/j.mod.2010.12.001

Lantz, V., Chang, J.S., Horabin, J.I., Bopp, D., Schedl, P., (1994) The Drosophila orb RNA-binding protein is required for the formation of the egg chamber and establishment of polarity. Genes Dev. 8, 598–613. doi:10.1101/gad.8.5.598

Lee, Y., Ahn, C., Han, J., Choi, H., Kim, J., Yim, J., Lee, J., Provost, P., Rådmark, O., Kim, S., Kim, V.N., (2003) The nuclear RNase III Drosha initiates microRNA processing. Nature 425, 415.

Lee, Y., Kim, M., Han, J., Yeom, K.-H., Lee, S., Baek, S.H., Kim, V.N., (2004) MicroRNA genes are transcribed by RNA polymerase II. EMBO J. 23, 4051–4060. doi:10.1038/sj.emboj.7600385

Lewis R a, Gagnon J a & Mowry KL (2008) PTB/hnRNP I is required for RNP remodeling during RNA localization in Xenopus oocytes. *Mol. Cell. Biol.* 28, 678–686.

Li GZ, Vissers JP, Silva JC, Golick D, Gorenstein MV, Geromanos SJ. (2009) Database searching and accounting of multiplexed precursor and product ion spectra from the data independent analysis of simple and complex peptide mixtures. Proteomics 9:1696-719.

Lin, C.L., Evans, V., Shen, S., Xing, Y., Richter, J.D., (2010) The nuclear experience of CPEB: implications for RNA processing and translational control. Rna 16, 338–348. doi:10.1261/rna.1779810

Lin, C.L., Huang, Y.T., Richter, J.D., (2012) Transient CPEB dimerization and translational control. Rna 18, 1050–1061. doi:10.1261/rna.031682.111

Liu J, Grimison B, Lewellyn AL & Maller JL (2006) The anaphase-promoting complex/cyclosome inhibitor Emi2 Is essential for meiotic but not mitotic cell cycles. *J. Biol. Chem.* 281, 34736–34741.

Lund E, Sheets MD, Imboden SB & Dahlberg JE (2011) Limiting ago protein restricts RNAi and microRNA biogenesis during early development in Xenopus laevis. *Genes Dev.* 25, 1121–1131.

Lund, E., Güttinger, S., Calado, A., Dahlberg, J.E., Kutay, U., (2004) Nuclear Export of MicroRNA Precursors. Science (80-. ). 303, 95–98.

Lund, E., Liu, M., Hartley, R.S., Sheets, M.D., Dahlberg, J.E., (2009) Deadenylation of maternal mRNAs mediated by miR-427 in Xenopus laevis embryos. RNA 15, 2351–63. doi:10.1261/rna.1882009

Machado, R.J., Moore, W., Hames, R., Houliston, E., Chang, P., King, M. Lou, Woodland, H.R., (2005) Xenopus Xpat protein is a major component of germ plasm and may function in its organisation and positioning. Dev. Biol. 287, 289–300. doi:10.1016/j.ydbio.2005.08.044

Madgwick S & Jones KT (2007) How eggs arrest at metaphase II: MPF stabilisation plus APC/C inhibition equals Cytostatic Factor. *Cell Div* 2, doi:10.1186/1747-1028-2-4 This.

Marlow F (2015) Primordial Germ Cell Specification and Migration. *F1000Research* 4, pii: F1000.

Martins JPS, Liu X, Oke A, Arora R, Franciosi F, Viville S, Laird DJ, Fung JC & Conti M (2016) DAZL and CPEB1 regulate mRNA translation synergistically during oocyte maturation. *J. Cell Sci.* 129, 1271–1282.

Matsuda Y, Uno Y, Kondo M, Gilchrist MJ, Zorn AM, Rokhsar DS, Schmid M & Taira M (2015) A New Nomenclature of Xenopus laevis Chromosomes Based on the Phylogenetic Relationship to Silurana/Xenopus tropicalis. *Cytogenet. Genome Res.* 145, 187–191.

McGrew, L.L., Dworkin-Rastl, E., Dworkin, M.B., Richter, J.D., (1989) Poly(A) elongation during Xenopus oocyte maturation is required for translational recruitment and is mediated by a short sequence element. Genes Dev. 3, 803–815. doi:10.1101/gad.3.6.803

Mcgrew, L.L., Richter, J.D., (1990) During Xenopus oocyte maturation : characterization of cis and trans elements and regulation by cyclin / MPF A ( McGrew. EMBO J. 9, 3743–3751.

Mendez, R., Barnard, D., Richter, J.D., (2002) Differential mRNA translation and meiotic progression require Cdc2-mediated CPEB destruction. EMBO J. 21, 1833–1844.

Mendez, R., Hake, L.E., Andresson, T., Littlepage, L.E., Ruderman, J. V, Richter, J.D., (2000a) Phosphorylation of CPE binding factor by Eg2 regulates translation of c-mos mRNA. Nature 404, 303–307.

Mendez, R., Murthy, K.G.K., Ryan, K., Manley, J.L., Richter, J.D., (2000b) Phosphorylation of CPEB by Eg2 Mediates the Recruitment of CPSF into an Active Cytoplasmic Polyadenylation Complex. Mol. Cell 6, 1253–1259.

Mendez, R., Richter, J.D (2001) Translational control by CPEB: a means to the end. Cell 2, 1–9.

Minshall N, Reiter MH, Weil D & Standart N (2007) CPEB interacts with an ovary-specific eIF4E and 4E-T in early Xenopus oocytes. *J. Biol. Chem.* 282, 37389–37401.

Mishima, Y., Giraldez, A.J., Takeda, Y., Fujiwara, T., Sakamoto, H., Schier, A.F., Inoue, K., (2006) Differential Regulation of Germline mRNAs in Soma and Germ Cells by Zebrafish miR-430. Curr. Biol. 16, 2135–2142. doi:10.1016/j.cub.2006.08.086

Molyneaux K & Wylie C (2004) Primordial germ cell migration. *Int. J. Dev. Biol* 48, 537–544.

Morgan M, Iaconcig A & Muro AF (2010) CPEB2, CPEB3 and CPEB4 are coordinately regulated by miRNAs recognizing conserved binding sites in paralog positions of their 3'-UTRs. *Nucleic Acids Res.* 38, 7698–7710.

Mosquera, L., Forristall, C., Zhou, Y., King, M.L., (1993) A mRNA localized to the vegetal cortex of Xenopus oocytes encodes a protein with a nanos-like zinc finger domain. Development 117, 377–386. doi:10.1016/0168-9525(93)90157-D

Mowry KL & Cote C a (1999) RNA sorting in Xenopus oocytes and embryos. *FASEB J.* 13, 435–445.

Mullis, K., Faloona, F., Scharf, S., Saiki, R., Horn, G., Erlich, H., (1986) Specific enzymatic amplification of DNA in vitro: the polymerase chain reaction. Cold Spring Harb. Symp. Quant. Biol. 51 Pt 1, 263–273.

Nakamura A & Seydoux G (2008) Less is more: specification of the germline by transcriptional repression. *Development* 135, 3817–3827.

Nechama, M., Lin, C., Richter, J.D., (2013) An unusual two-step control of CPEB destruction by Pin1. Mol. Cell. Biol. 33, 48–58. doi:10.1128/MCB.00904-12

Newport, J., Kirschner, M., (1982a) A major developmental transition in early xenopus embryos: II. control of the onset of transcription. Cell 30, 687–696. doi:10.1016/0092-8674(82)90273-2

Newport, J., Kirschner, M., (1982b) A major developmental transition in early xenopus embryos: I. characterization and timing of cellular changes at the midblastula stage. Cell 30, 675–686. doi:10.1016/0092-8674(82)90272-0

Nishiumi F, Komiya T & Ikenishi K (2005) The mode and molecular mechanisms of the migration of presumptive PGC in the endoderm cell mass of Xenopus embryos. *Dev. Growth Differ.* 47, 37–48.

Noiret M, Méreau A, Angrand G, Bervas M, Gautier-Courteille C, Legagneux V, Deschamps S, Lerivray H, Viet J, Hardy S, Paillard L & Audic Y (2016) Robust identification of Ptbp1-dependent splicing events by a junction-centric approach in Xenopus laevis. *Dev. Biol.*, pii: S0012-1606(16)30197-X.

Novoa I, Gallego J, Ferreira PG & Mendez R (2010) Mitotic cell-cycle progression is regulated by CPEB1 and CPEB4-dependent translational control. *Nat. Cell Biol.* 12, 447–456.

Nutt SL, Bronchain OJ, Hartley KO & Amaya E (2001) Comparison of Morpholino based translational inhibition during the development of Xenopus laevis and Xenopus tropicalis. *Genesis* 30, 110–113.

Paris J & Richter J.D (1990). Maturation-specific polyadenylation and translational control: diversity of cytoplasmic polyadenylation elements, influence of poly(A) tail size, and formation of stable polyadenylation complexes. Mol. Cell. Biol. 10, 5634–45. doi:10.1128/MCB.10.11.5634.Updated

Paris J, Swenson K, Piwnica-Worms H & Richter JD (1991) Maturation-specific polyadenylation: In vitro activation by p34cdc2 and phosphorylation of a 58-kD CPE-binding protein. *Genes Dev.*

5, 1697–1708.

Pearl EJ, Grainger RM, Guille M & Horb ME (2012) Development of Xenopus Resource Centers: the National Xenopus Resource and the European Xenopus Resource Center. *Genesis* 50, 155–163.

Peshkin L, Wühr M, Pearl E, Haas W, Freeman RM, Gerhart JC, Klein AM, Horb M, Gygi SP & Kirschner MW (2015) On the Relationship of Protein and mRNA Dynamics in Vertebrate Embryonic Development. *Dev. Cell* 35, 383–394.

Pfennig J (2014) XDazl function in RNA metabolism in *Xenopus laevis*. GGNB program Genes and Development; Georg-August University Göttingen

Philpott A & Yew PR (2008) The Xenopus cell cycle: An overview. *Mol. Biotechnol.* 39, 9–19.

Piqué M, López JM, Foissac S, Guigó R & Méndez R (2008) A Combinatorial Code for CPE-Mediated Translational Control. *Cell* 132, 434–448.

Ressom RE & Dixon KE (1988) Relocation and reorganization of germ plasm in Xenopus embryos after fertilization. *Development* 103, 507–518.

Reverte CG, Ahearn MD & Hake LE (2001) CPEB Degradation during Xenopus Oocyte Maturation Requires a PEST Domain and the 26S Proteasome. *Dev. Biol.* 231, 447–458.

Richardson BE & Lehmann R (2010) Mechanisms guiring primordial germ cell migration: strategies from different organisms. *Nat. Rev. Mol. Cell Biol.* 11, 37–49.

Richter JD (2007) CPEB: a life in translation. *Trends Biochem. Sci.* 32, 279–285.

Richter JD & Smith LD (1983) Developmentally Regulated RNA Binding Proteins during Oogenesis in Xenopus laevis. *J. Biol. Chem.* 258, 4864–4869.

Rojas-Rìos, P., Chartier, A., Pierson, S., Séverac, D., Dantec, C., Busseau, I., Simonelig, M., (2015) Translational Control of Autophagy by Orb in the Drosophila Germline. Dev. Cell 35, 622–631. doi:10.1016/j.devcel.2015.11.003

Sagata, N., Oskarsson, M., Copeland, T., Brumbaugh, J., Woude, G.F. Vande, (1988) Function of c-mos proto-oncogene product in meiotic maturation in Xenopus oocytes. Nature 335, 519–525.

Sanger, F., Nicklen, S., Coulson, A.R., (1977) DNA sequencing with chain-terminating inhibitors. Proceedings of the National Academy of Sciences 74(12), 5463-5467.

Sambrook, J., and Russell, D. W (2001) "Molecular Cloning: a laboratory manual." Cold Spring Harbor Laboratory Press Cold Spring Harbor, New York.

Sarkissian, M., Mendez, R., Richter, J.D., (2004) Progesterone and insulin stimulation of CPEB-dependent polyadenylation is regulated by Aurora A and glycogen synthase kinase-3. Genes Dev. 18, 48–61. doi:10.1101/gad.1136004

Sato KI (2014) Transmembrane signal transduction in oocyte maturation and fertilization:

Focusing on Xenopus laevis as a model animal. *Int. J. Mol. Sci.* 16, 114–134.

Sharp P. A (1973) Detection of two restriction endonuclease activities in Haemophilus parainfluenzae using analytical agarose-ethidium bromide electrophoresis. Biochemistry 12:3055-63, 1973. [Cold Spring Harbor Laboratory, Cold Spring Harbor, NY.

Schier AF (2007) The maternal-zygotic transition: death and birth of RNAs. *Science* 316, 406–407.

Schmidt, C., Hesse, D., Raabe, M., Urlaub, H., Jahn, O., (2013) An automated in-gel digestion/iTRAQ-labeling workflow for robust quantification of gel-separated proteins. Proteomics 13, 1417–1422. doi:10.1002/pmic.201200366

Sengupta MS & Boag PR (2012) Germ granules and the control of mRNA translation. *IUBMB Life* 64, 586–594.

Setoyama, D., Yamashita, M., Sagata, N., (2007) Mechanism of degradation of CPEB during Xenopus oocyte maturation. PNAS 104, 18001–18006.

Seydoux G & Braun RE (2006) Pathway to Totipotency: Lessons from Germ Cells. *Cell* 127, 891–904.

Silva, J.C., Denny, R., Dorschel, C.A., Gorenstein, M., Kass, I.J., Li, G.Z., McKenna, T., Nold, M.J., Richardson, K., Young, P., Geromanos, S., (2005) Quantitative proteomic analysis by accurate mass retention time pairs. Anal Chem 77, 2187–2200. doi:10.1021/ac048455k

Silva JC, Gorenstein M V, Li GZ, Vissers JPC, Geromanos SJ (2006) Absolute quantification of proteins by LCMSE: a virtue of parallel MS acquisition. Mol Cell Proteomics 5:144-56.

Smarandache (2013) CPEB and Germ Cell Development in Xenopus laevis Embryos. Molecular Biology Graduate program, Georg-August University, Göttingen.

Smith LD (1966) The role of a “germinal plasm” in the formation of primordial germ cells in Rana pipiens. *Dev Biol* 14, 330–347.

Smits AH, Lindeboom RGH, Perino M, van Heeringen SJ, Veenstra GJ an C & Vermeulen M (2014) Global absolute quantification reveals tight regulation of protein expression in single Xenopus eggs. *Nucleic Acids Res.* 42, 9880–9891.

Standart N & Minshall N (2008) Translational control in early development: CPEB, P-bodies and germinal granules. *Biochem. Soc. Trans.* 36, 671–676.

Staton, A.A., Giraldez, A.J., (2011) Use of target protector morpholinos to analyze the physiological roles of specific miRNA-mRNA pairs in vivo. Nat. Protoc. 6, 2035–2049. doi:10.1038/nprot.2011.423

Stebbins-Boaz B, Cao Q, de Moor CH, Mendez R & Richter JD (1999) Maskin Is a CPEB-Associated Factor that Transiently Interacts with eIF-4E. *Mol. Cell* 4, 1017–1027.

Stebbins-Boaz B, Hake L.E, Richter, J.D (1996). CPEB controls the cytoplasmic polyadenylation of cyclin , Cdk2 and c-mos mRNAs and is necessary for oocyte maturation in Xenopus. EMBO J. 15, 2582–2592.

Stein, D., Foster, E., Huang, S.B., Weller, D., Summerton, J., (1997) A specificity comparison of four

antisense types: morpholino, 2'-O-methyl RNA, DNA, and phosphorothioate DNA. Antisense Nucleic Acid Drug Dev. 7, 151–157. doi:10.1089/oli.1.1997.7.151

Sugimoto T, Seki N, Shimizu S, Kikkawa N, Tsukada J, Shimada H, Sasaki, K, Hanazawa T, OkamotoY, Hata A (2009) The galanin signaling cascade is a candidate pathway regulating oncogenesis in human squamous cell carcinoma.*Genes Chromosomes Cancer*; 48; 132-42.

Summerton JE (2007) Morpholino, siRNA, and S-DNA compared: impact of structure and mechanism of action on off-target effects and sequence specificity. *Curr. Top. Med. Chem.* 7, 651–660.

Summerton JE & Weller D (1997b) Morpholino Antisense Oligomers: Design, Preparation, and Properties. *Antisense Nucleic Acid Drug Dev.* 7, 187–195.

Surani MA, Hayashi K & Hajkova P (2007) Genetic and Epigenetic Regulators of Pluripotency. *Cell* 128, 747–762.

Swartz, S.Z., Wessel, G.M., (2015) Germ Line Versus Soma in the Transition from Egg to Embryo, 1st ed, Current Topics in Developmental Biology. Elsevier Inc. doi:10.1016/bs.ctdb.2015.06.003

Tada, H., Mochii, M., Orii, H., Watanabe, K., (2012) Ectopic formation of primordial germ cells by transplantation of the germ plasm: Direct evidence for germ cell determinant in Xenopus. Dev. Biol. 371, 86–93. doi:10.1016/j.ydbio.2012.08.014

Tadros W & Lipshitz HD (2009) The maternal-to-zygotic transition: a play in two acts. *Development* 136, 3033–3042.

Taguchi A, Tak M, Motoishi M, Or H, Moch M & Watanabe K (2012) Analysis of localization and reorganization of germ plasm in Xenopus transgenic line with fluorescence-labeled mitochondria. *Dev. Growth Differ.* 54, 767–776.

Tang GQ & Maxwell ES (2008) Xenopus microRNA genes are predominantly located within introns and are differentially expressed in adult frog tissues via post-transcriptional regulation. *Genome Res.* 18, 104–112.

Tay, J., Richter, J.D., (2001) Germ Cell Differentiation and Synaptonemal Complex Formation Are Disrupted in CPEB Knockout Mice. Dev. Cell 1, 201–213.

Terayama K, Kataoka K, Morichika K, Orii H, Watanabe K & Mochii M (2013) Developmental regulation of locomotive activity in Xenopus primordial germ cells. *Dev. Growth Differ.* 55, 217–228.

Thom G, Minshall N, Git A, Argasinska J & Standart N (2003) Role of cdc2 kinase phosphorylation and conserved N-terminal proteolysis motifs in cytoplasmic polyadenylation-element-binding protein (CPEB) complex dissociation and degradation. *Biochem J* 370, 91–100.

Thompson, B.E., (2005) Dose-dependent control of proliferation and sperm specification by FOG-1/CPEB. Development 132, 3471–3481. doi:10.1242/dev.01921

Towbin, H., T. Staehelin, and J. Gordon. (1979). Electrophoretic transfer of proteins from polyacrylamide gels to nitrocellulose sheets: procedure and some applications. Proceedings of the National Academy of Sciences of the United States of America 76: 4350-4354.

Treiber T, Treiber N & Meister G (2012) Regulation of microRNA biogenesis and function. *Thromb. Haemost.* 107, 605–610.

Trotta CR, Lund E, Kahan L, Johnson AW, Dahlberg JE (2003) Coordinated nuclear export of 60S ribosomal subunits and NMD3 in vertebrates. *EMBO J*, 22; 2841-51.

Uno Y, Nishida C, Takagi C, Ueno N & Matsuda Y (2013) Homoeologous chromosomes of Xenopus laevis are highly conserved after whole-genome duplication. *Heredity (Edinb).* 111, 430–436.

Venkatarama T, Lai F, Luo X, Zhou Y, Newman K & King M Lou (2010) Repression of zygotic gene expression in the Xenopus germline. *Development* 137, 651–660.

Voronina E, Seydoux G, Sassone-Corsi P & Nagamori I (2011) RNA granules in germ cells. *Cold Spring Harb. Perspect. Biol.* 3, pii: a002774.

Watanabe, T., Takeda, A., Mise, K., Okuno, T., Suzuki, T., Minami, N., Imai, H., (2005) Stage-specific expression of microRNAs during Xenopus development. FEBS Lett. 579, 318–324. doi:10.1016/j.febslet.2004.11.067

Wakahara M (1978) Induction of supernumerary primordial germ cells by injecting vegetal pole cytoplasm into Xenopus eggs. *J. Exp. Zool.* 203, 159–164.

Wakahara M (1977) Partial characterization of “primordial germ cell-forming activity” localized in vegetal pole cytoplasm in anuran eggs. *J. Embryol. Exp. Morphol.* 39, 221–33.

Whitington, B.P.M., Dixon, K.E., (1975) Quantitative studies of germ plasm and germ cells during early embryogenesis of Xenopus laevis. J. Embryol. Exp. Morphol. 33, 57–74.

Wilczynska A, Aigueperse C, Kress M, Dautry F & Weil D (2005) The translational regulator CPEB1 provides a link between dcp1 bodies and stress granules. *J. Cell Sci.* 118, 981–992.

Wilczynska A, Git A, Argasinska J, Belloc E & Standart N (2016) CPEB and miR-15/16 Co-Regulate Translation of Cyclin E1 mRNA during Xenopus Oocyte Maturation. *PLoS One* 11, e0146792.

Wilk K, Bilinski S, Dougherty MT & Kloc M (2005) Delivery of germinal granules and localized RNAs via the messenger transport organizer pathway to the vegetal cortex of Xenopus oocytes occurs through directional expansion of the mitochondrial cloud. *Int. J. Dev. Biol.* 49, 17–21.

Wormington M (1994) Unmasking the role of the 3’ UTR in the cytoplasmic polyadenylation and translational regulation of maternal mRNAs. *BioEssays* 16, 533–535.

Wylie CC & Heasman J (1976) The formation of the gonadal ridge in Xenopus laevis. I. A light and transmission electron microscope study. *J Embryol Exp Morphol* 35, 125–138.

Xie J, Lee J-A, Kress TL, Mowry KL & Black DL (2003) Protein kinase A phosphorylation modulates transport of the polypyrimidine tract-binding protein. *Proc. Natl. Acad. Sci. U. S. A.* 100, 8776–8781.

Xiong, H., Li, Q., Chen, R., Liu, S., Lin, Q., Xiong, Z., Jiang, Q., Guo, L (2016) A multi-step miRNA-mRNA regulatory network construction approach identifies gene signatures associated with endometrioid endometrial carcinoma. Genes (Basel). 7. doi:10.3390/genes7060026

Yamaguchi T, Kataoka K, Watanabe K & Orii H (2014) Restriction of the Xenopus DEADSouth mRNA to the primordial germ cells is ensured by multiple mechanisms. *Mech. Dev.* 131, 15–23.

Yamaguchi T, Taguchi A, Watanabe K & Orii H (2013) Germes is involved in translocation of germ plasm during development of Xenopus primordial germ cells. *Int. J. Dev. Biol.* 57, 439–443.

Yartseva V & Giraldez AJ (2015) The maternal-to-zygotic transition during vertebrate development: a model for reprogramming. *Curr Top Dev Biol* 113, 191–232.

Yasuo H & Lemaire P (2001) Generation of the germ layers along the animal-vegetal axis in Xenopus laevis. *Int. J. Dev. Biol.* 45, 229–235.

Yi B, Ozerova M, Zhang G-X, Yan G, Huang S & Sun J (2015) Post-Transcriptional Regulation of Endothelial Nitric Oxide Synthase Expression by Polypyrimidine Tract-Binding Protein 1. *Arterioscler. Thromb. Vasc. Biol.* 35, 2153–2160.

Yi, R., Qin, Y., Macara, I.G., Cullen, B.R., (2003). Exportin-5 mediates the nuclear export of pre-microRNAs and short hairpin RNAs. Genes Dev. 17, 3011–3016. doi:10.1101/gad.1158803

Yoon, Srikantan S, G.M (2012) MS2-TRAP (MS2-tagged RNA affinity purification): Tagging RNA to identify associated miRNAs. Methods 58, 81–87. doi:10.1016/J.YMETH.2012.07.004

Zhou Y & King M Lou (2004) Sending RNAs into the future: RNA localization and germ cell fate. *IUBMB Life* 56, 19–27.

Zhou Y & King ML (1996) RNA transport to the vegetal cortex of Xenopus oocytes. *Dev Biol* 179, 173–183.

## ABBREVIATIONS

| | |
|---|---|
| % | percentage |
| A | Adenine |
| AP | Alkaline phosphatase |
| APS | Ammonium Persulfate |
| ARE | AU-rich elements |
| Aqua dest. | *aqua destillata* |
| BA | Benzyl alcohol |
| BB | Benzyl benzoate |
| Bp | Base pairs |
| BCIP | 5-bromo-4-chloro-3-indolyl-phosphate |
| BMB | Boehringer Mannheim blocking reagent |
| BSA | Bovine serum albumin |
| C | Cytosine |
| °C | Degrees Celsius |
| cDNA | Copy DNA |
| CoMo | Control morpholino |
| CPE | Cytoplasmic polyadenylation element |
| C-terminus | Carboxy-terminus |
| Cys | Cysteine |
| DAPI | 4',6-Diamidino-2-Phenylindole |
| dATP | Deoxyadenosine triphosphate |
| dCTP | Deoxycytosine triphosphate |
| $ddH_2O$ | Double distilled water |
| dGTP | Deoxyguanosine triphosphate |
| $dH_2O$ | Distilled water |
| Dig | Digoxigenine |
| DMSO | Dimethylsulphoxid |
| DNA | Deoxyribonucleic acid |
| DNase | Deoxyribonuclease |
| dNTP | Deoxynucleotide triphosphate |
| dT | Deoxythymidine |
| DTT | Dithiothreitol |
| dTTP | Deoxythymidine triphosphate |
| *E. coli* | *Escherichia coli* |
| e.g | *exempli gratia* |

| | |
|---|---|
| EDTA | Ethylendiamin-tetra-acetic acid |
| EGTA | Ethylenglycole-bis(2-aminoethylether)-N,N'- tetraacetate |
| Et al. | *et alii* |
| EtBr | Ethidium bromide |
| EtOH | Ethanol |
| FCS | Fetal calf serum |
| Fig. | Figure |
| fw | Forward |
| g | Gram |
| G | Guanine |
| Gln | Glycine |
| H | Hour |
| hCG | Human chorionic gonadotropin |
| $H_2O$ | Water |
| His | Histidine |
| Ig | Immunoglobulin |
| IPTG | Isopropyl-thio-galactoside |
| K | Lysine |
| k | Kilo |
| kb | Kilo base pairs |
| KO | Knock-out |
| KD | Knock-down |
| kD | Kilodalton |
| l | Liter |
| LB | Luria-Bertani |
| LE | Localization element |
| M | Molar |
| mA | Milliampere |
| MAB | maleic acid buffer |
| MEM | MOPS-EGTA-MgSO4 buffer |
| MEMFA | MOPS-EGTA-MgSO4 formaldehyde buffer |
| mg | Milligram |
| MgCl2 | Magnesium chloride |
| min | Minute |
| ml | Milliliter |
| mm | Millimeter |
| mM | Millimolar |
| mRNA | Messenger RNA |

| | |
|---|---|
| miR | microRNA |
| MO | Morpholino |
| µg | Microgram |
| µl | Microliter |
| µm | Micrometer |
| µM | Micromolar |
| n | Nano |
| nr | Number |
| NaAC | Sodium acetate |
| NBT | Nitro-blue-tetrazolium |
| ng | Nanogram |
| nm | Nanometer |
| nM | Nanomolar |
| N-terminus | Amino-terminus |
| ORF | Open reading frame |
| PAGE | Polyacrylamide gel electrophoresis |
| PBS | Phosphate buffered saline |
| PCR | Polymerase chain reaction |
| PFA | Paraformaldehyde |
| pH | *potentium hydrogenium* |
| % | Percentage |
| Pol | Polymerase |
| P | Primer |
| Pro | Proline |
| PVDF | Polyvinylidene difluoride |
| qRT-PCR | Quantitative real-time RT-PCR |
| RBP | RNA binding protein |
| rev | Reverse |
| RNA | Ribonucleic acid |
| RNase | Ribonuclease |
| RNP | Ribonucleoprotein |
| rpm | Rounds per minute |
| RT | Room temperature |
| RT | Reverse transcriptase |
| RT-PCR | Reverse transcription-PCR |
| S | Serine |
| s | Second |
| SDS | Sodium dodecyl sulfate |

| | |
|---|---|
| SSC | Standard sodium citrate |
| st | Stage |
| T | Thymine |
| T | Threonine |
| TAE | Tris-Acetate-EDTA |
| Taq | *Thermus aquaticus* |
| TBE | Tris-Borate-EDTA |
| TBS(T) | Tris-buffered saline (with Tween) |
| Temp. | Temperature |
| UTR | Untranslated region |
| UV | Ultra violet light |
| V | Volume |
| v/v | Volume to volume |
| w/v | Weight to volume |
| wt | Wild type |
| WMISH | Whole mount in situ hybridization |
| x | Multiple |
| X-Gal | 5-Bromo-4-chloro-3-indoxyl-D- galactopyranoside |

## SUPPLEMENT

**Figure S1. Cross-species experiment showing initiation of zygotic transcription at stage 26.** *X. laevis* oocytes were fertilized either with *X. laevis* (A) or *X. tropicalis* (B) spermatozoa and embryos were collected at the indicated stages. Total mRNA was extracted, reverse transcribed and the cDNA was amplified with gene and species-specific primers, to distinguish between maternal and zygotic pools of transcripts. In this experiment another set of primers was used leading to amplicons of 200bp for *X. l * X.l* and 600 bp for *X. l * X. t*. This additional set of primers supports the result obtained previously. The bands corresponding to a molecular weight of approx. 600 nucleotides shows the zygotic pool of transcripts, whereas the band running at 200 nucleotides identifies with the maternally provided pools of transcripts. Transcripts from hybrid embryos, *X.l * X.t* were also amplified with both sets of primers, as indicated for stage 8 and stage 47. Ornithine decarboxilase (*Odc*) served as a house keeping gene control. The blurred band running lowest on the gel corresponds to primers.

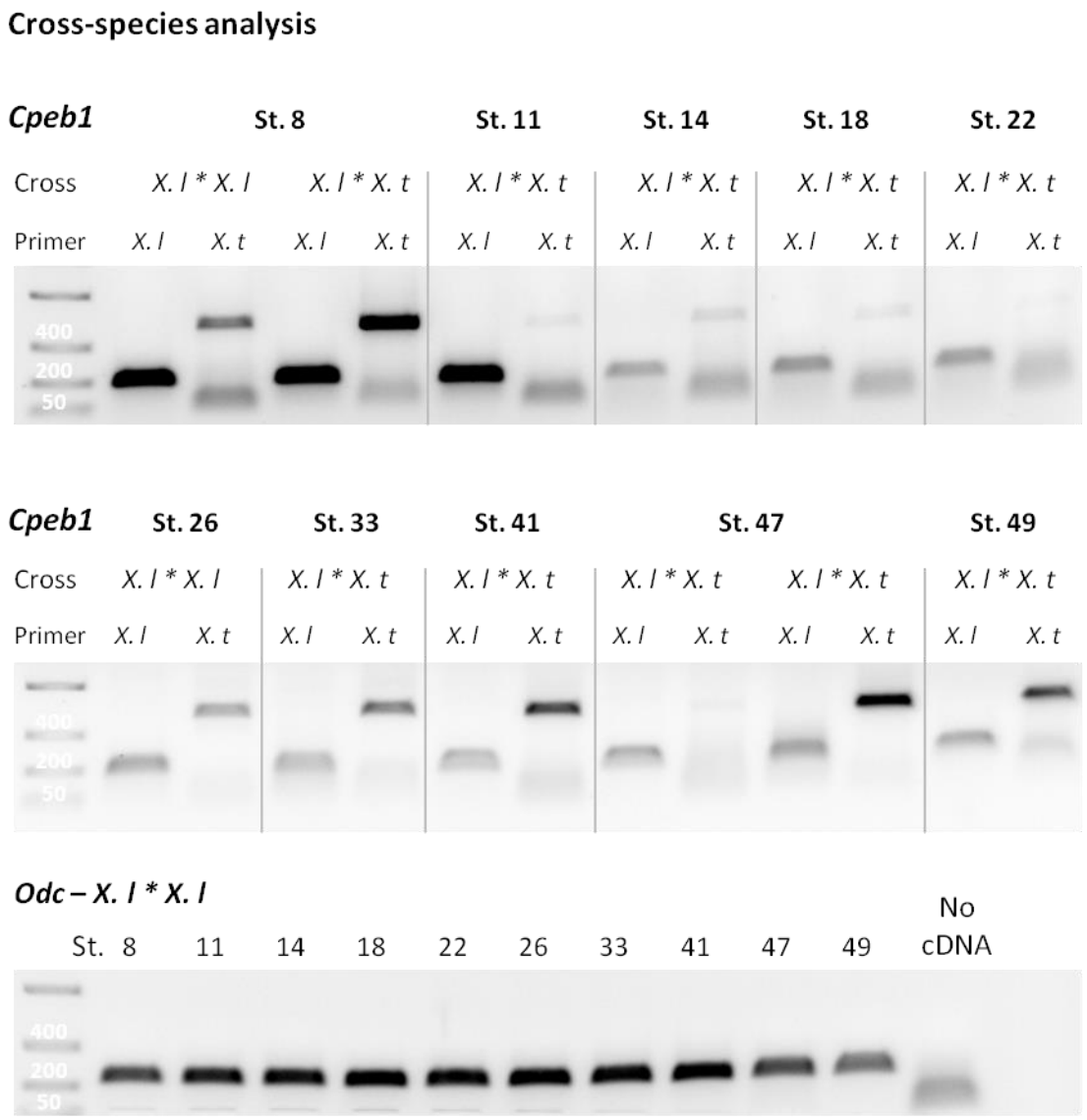

**Figure S2. Subfragment 1b (nucleotides 1 to 139 of *cpeb1*_3UTR) is efficiently protected in the soma by TPMO_2 similarly to Sfr_1 (nucleotides 74 to 139 of of *cpeb1*_3UTR).** TPMOs protect transcripts from miRNA mediated degradation by impeding RISC complex binding to the miRNA target site. Fr_1-139 reporter transcripts (450 ng) were injected vegetally in both blastomeres of two-cell stage embryos with one of the TPMOs (250 µM), both of the TPMOs (250 µM each) or alone serving as a positive control. Tailbud embryos were analyzed for endodermal distribution of the reporter by probing against *gfp* in WMISH. Representative embryos are shown for each of the categories: weak, moderate and strong depletion. Quantification of somatic depletion of Fr_1.b alone or in the presence of TPMOs. N=2 biological replicates.

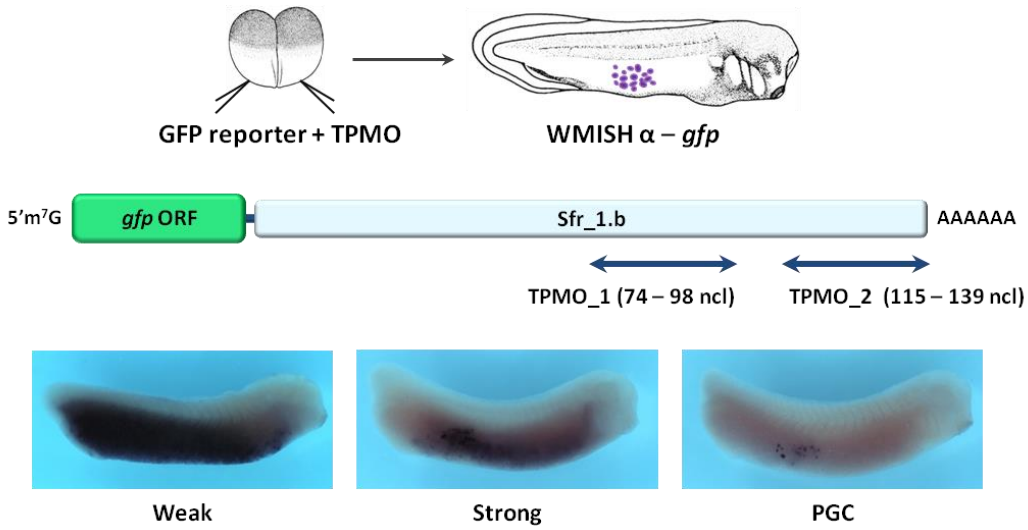


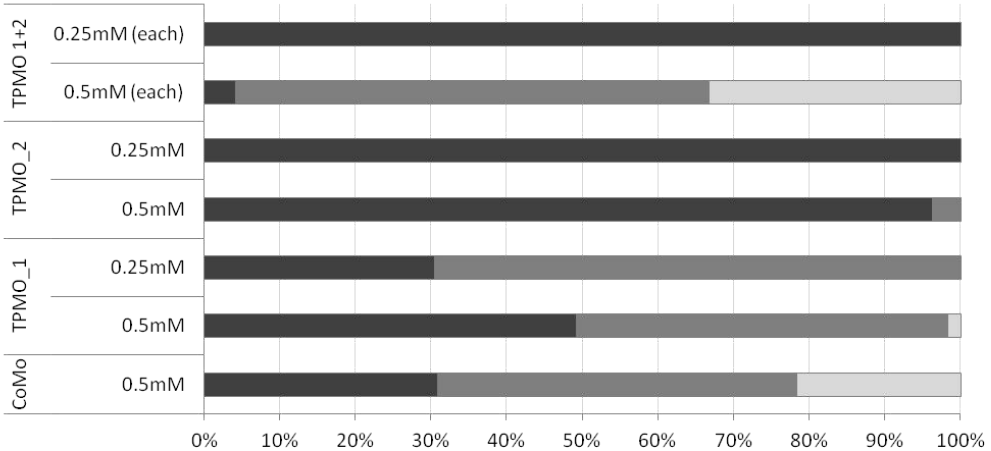


| | CoMo | TPMO_1 | | TPMO_2 | | TPMO 1+2 | |
|---|---|---|---|---|---|---|---|
| | 0.5mM | 0.5mM | 0.25mM | 0.5mM | 0.25mM | 0.5mM (each) | 0.25mM (each) |
| Weak Clearance | 37 | 28 | 7 | 78 | 41 | 1 | 9 |
| Strong Clearance | 57 | 28 | 16 | 3 | 0 | 15 | 0 |
| PGC | 26 | 1 | 0 | 0 | 0 | 8 | 0 |

**Figure S3. Whole mount immuno-fluorescence against CPEB1 and DAZL.** Whole mount immunostaining was carried out on tailbud embryos against CPEB1 and DAZL, serving as a germline specific positive control. Antibodies: mouse α-DAZL detected with Alexa 633 α-mouse; rabbit α-CPEB1 detected with Alexa 488 α-rabbit. Pictures were taken with a 25x objective. Scale bar = 100 µM.

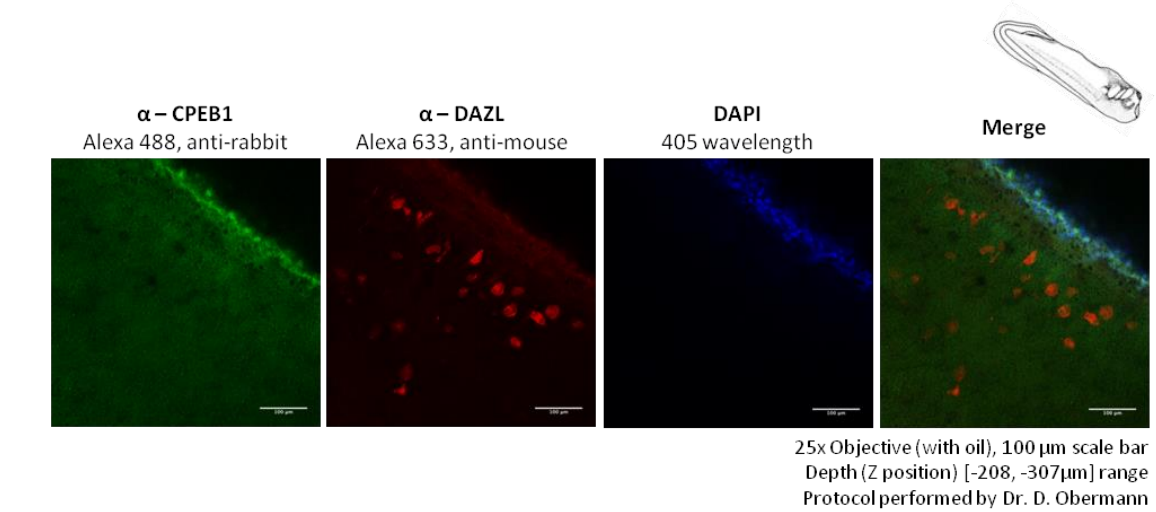


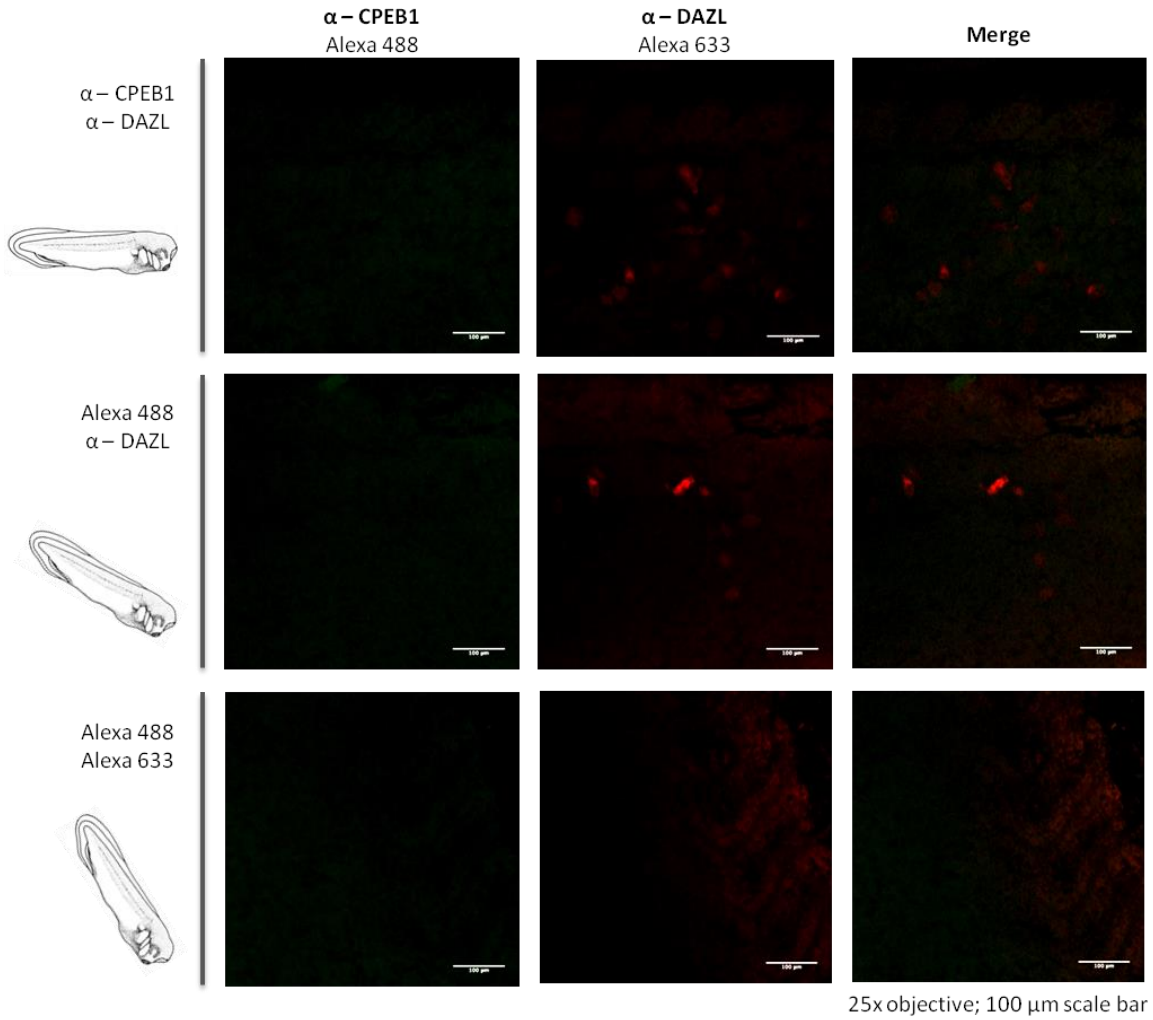

**Figure S4. Whole Mount Immuno-fluorescence against CPEB1, DAZL and GFP_dnd1-LE.** Whole mount immunostaining was carried out on tailbud embryos against CPEB1 and DAZL, serving as a germline specific positive control. Antibodies: mouse α-DAZL detected with Alexa 633 α-mouse; rabbit α-CPEB1 detected with Alexa 488 α-rabbit. Pictures were taken with a 25x objective. Scale bar = 100 µM.

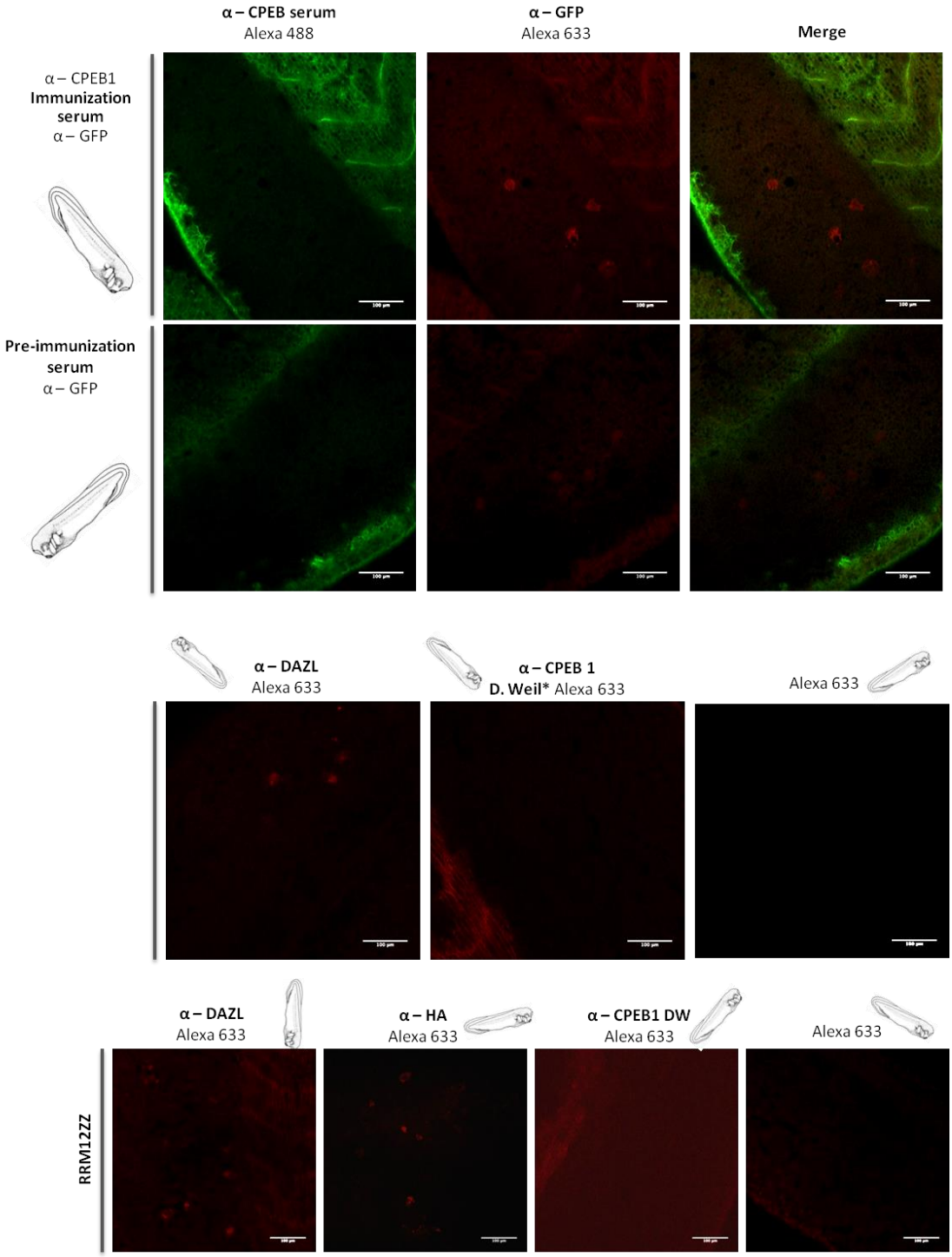

**Figure S5. Depiction of IP experimental outcome and protein expression control.** A. Embryos stage 2 and stage VI oocytes were injected with mRNAs coding for F-GFP, F-CPEB1 and F-Ptbp1 at a concentration of 300ng/µL, thus with approx. 2.4 ng/embryo and 1.2 ng/oocyte. For protein preparation, 200 oocytes after 24h incubation time and 100 embryos stage 13 were flash frozen and used for IP. The protein samples were divided for a test western blot and mass spectrometric analysis. B. Input and IP samples for each condition were loaded onto 12% SDS-PAGE gels, blotted on nitrocellulose membrane and probed for the flag-epitope. The three proteins are present at the expected molecular weights and were successfully pulled down.

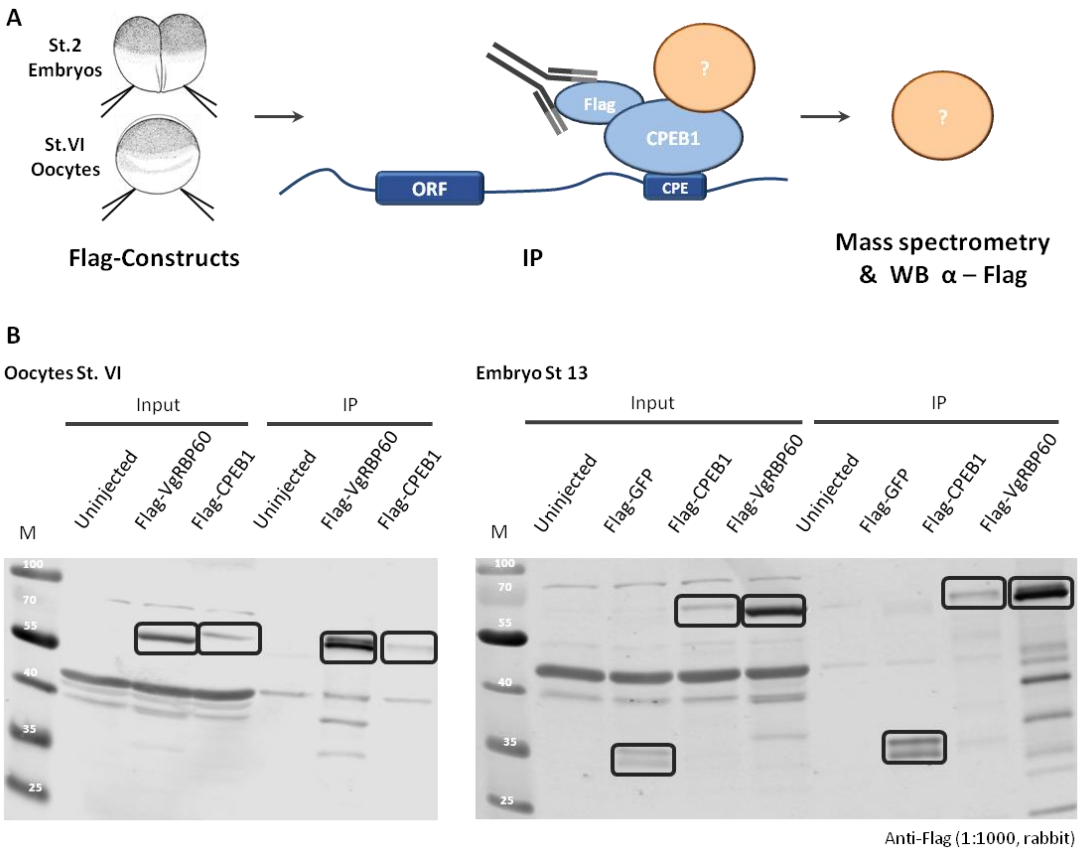

**Table S1. Protein amounts pulled down for endogenously expressed proteins and for the flag-tagged versions.** The UniProt accession, the molecular weight in Daltons (MW Da) and calculated amounts in both femtomoles (fmol) and nanograms (ng) are given.

| | | | Oocytes VI | | | | Embryos St. 13 | | | | | |
|---|---|---|---|---|---|---|---|---|---|---|---|---|
| | | | F-CPEB1 | | F-VgRBP60 | | F-CPEB1 | | F-VgRBP60 | | F-GFP | |
| | UniProt Accession | MW Da | Fmol | Ng | Fmol | Ng | Fmol | Ng | Fmol | Ng | Fmol | Ng |
| **F-GFP** | - | 28350 | - | - | - | - | - | - | - | - | 928.15 | 26.31 |
| **F-CPEB1** | - | 64111 | 269.74 | 17.29 | - | - | 193.03 | 12.38 | - | - | - | - |
| **CPEB1_a** | Q91572 | 63574 | 217.56 | 13.83 | 149.61 | 9.51 | 753.78 | 47.92 | - | - | - | - |
| **CPEB1_b** | Q52KN7 | 63601 | 294.45 | 18.73 | 280.9 | 17.87 | - | - | - | - | - | - |
| **F-VgRBP60** | - | 61530 | - | - | 880.13 | 54.15 | - | - | 3318.7 | 204.2 | - | - |
| **HnRNP related transport protein VgRBP60** | Q9PTS5 | 59838 | - | - | 242.35 | 14.5 | 56.41 | 3.38 | 434.99 | 26.03 | - | - |
| **VgRBP60** | Q42R55 | 51939 | - | - | - | - | - | - | 19.89 | 1.03 | - | - |

## Supplementary Tables for Mass Spectrometry

**Table S2. Selected top CPEB1 candidates for the embryo sample.** The described stringency thresholds applied. Moreover, the fold change to Ptbp1 is above 5.

| Embryos | | | | | | | | | | | | | | |
|---|---|---|---|---|---|---|---|---|---|---|---|---|---|---|
| Top CPEB1 candidates | | | | | | | | | | | | | | |
| UniProt Accession | gene name | IEP | Mw Da | uninjected | FLAG-GFP | FLAG-CPEB1 | FLAG-Ptbp1 | F-GFP/Uninjected | F-CPEB1/uninjected | F-Ptbp1/uninjected | F-CPEB1/F-GFP | F-Ptbp1/F-GFP | F-CPEB1/F-Ptbp1 | F-Ptbp1/F-CPEB1 |
| Q7ZYG2 | cstf1 | 6.16 | 49323 | | | 9.80 | | Div0 | Div0 | Div0 | Div0 | Div0 | Div0 | 0.00 |
| Q7ZYU9 | tuba1a | 4.76 | 50863 | | | 5.85 | | Div0 | Div0 | Div0 | Div0 | Div0 | Div0 | 0.00 |
| O42226 | eif4a3-b | 6.37 | 47460 | | | 6.66 | | Div0 | Div0 | Div0 | Div0 | Div0 | Div0 | 0.00 |
| Q7ZYV9 | sympk | 5.36 | 135193 | 0.42 | | 90.74 | 3.40 | 0.00 | Div0 | 8.06 | Div0 | Div0 | 26.66 | 0.04 |
| Q5M779 | mrpl11 | 10 | 20699 | 0.56 | 0.69 | 15.83 | 1.62 | 1.23 | 28.18 | 2.89 | 22.98 | 2.35 | 9.76 | 0.10 |
| Q68F38 | vac14 | 5.74 | 90001 | 2.23 | 6.35 | 63.49 | 4.09 | 2.85 | 28.44 | 1.83 | 9.99 | 0.64 | 15.51 | 0.06 |
| Q5XGZ1 | cpsf3 | 4.99 | 78949 | 0.74 | 0.55 | 12.75 | 1.25 | 0.75 | 17.32 | 1.70 | 22.98 | 2.25 | 10.21 | 0.10 |
| Q9W799 | cpsf2 | 4.81 | 89842 | 0.85 | 0.45 | 23.03 | 0.99 | 0.53 | 27.22 | 1.17 | 51.28 | 2.21 | 23.25 | 0.04 |
| O57683 | sf3b1 | 6.48 | 146956 | 17.66 | 13.15 | 115.52 | 20.54 | 0.74 | 6.54 | 1.16 | 8.79 | 1.56 | 5.62 | 0.18 |
| Q6GR45 | eif6 | 4.44 | 27110 | 5.56 | 4.20 | 41.33 | 5.47 | 0.75 | 7.43 | 0.98 | 9.85 | 1.30 | 7.56 | 0.13 |
| Q6AZR6 | xrcc6 | 5.92 | 69897 | 1.96 | 1.81 | 51.83 | 1.49 | 0.92 | 26.38 | 0.76 | 28.58 | 0.82 | 34.75 | 0.03 |
| Q6GNS3 | nmd3 | 6.83 | 59181 | 0.56 | 0.47 | 20.16 | | 0.84 | 36.15 | 0.00 | 42.78 | 0.00 | Div0 | 0.00 |
| Q7SYT0 | eef1a2 | 9.34 | 50805 | | | 47.36 | | Div0 | Div0 | Div0 | Div0 | Div0 | Div0 | 0.00 |
| Q6GQC3 | tuba8 | 5.11 | 51809 | | | 5.74 | | Div0 | Div0 | Div0 | Div0 | Div0 | Div0 | 0.00 |
| Q8AVF0 | | 7.38 | 61713 | 0.81 | | 62.85 | | 0.00 | 78.05 | 0.00 | Div0 | Div0 | Div0 | 0.00 |

| | | | | | | | | | | | | | | |
|---|---|---|---|---|---|---|---|---|---|---|---|---|---|---|
| Q5XGZ6 | LOC495107 | 6.22 | 64113 | 0.39 | 0.91 | 11.09 | | 2.35 | 28.58 | 0.00 | 12.16 | 0.00 | Div0 | 0.00 |
| Q7ZTM1 | ppil2 | 8.88 | 59742 | 0.45 | 0.91 | 10.93 | 1.21 | 2.02 | 24.18 | 2.68 | 11.97 | 1.33 | 9.03 | 0.11 |
| Q6NU40 | chtf18 | 6.02 | 113964 | 3.79 | 2.99 | 121.19 | | 0.79 | 31.97 | 0.00 | 40.51 | 0.00 | Div0 | 0.00 |
| Q6DCM0 | aaas | 6.34 | 58150 | 0.22 | 0.26 | 7.81 | | 1.20 | 35.60 | 0.00 | 29.76 | 0.00 | Div0 | 0.00 |
| Q6GNR4 | cltc | 5.4 | 193142 | 1.68 | | 25.17 | | 0.00 | 14.99 | 0.00 | Div0 | Div0 | Div0 | 0.00 |
| Q90WN3 | prkaca | 9.01 | 40648 | | | 12.18 | | Div0 | Div0 | Div0 | Div0 | Div0 | Div0 | 0.00 |

**Table S.3. Selected top Ptbp1 candidates for the embryo sample.** The described stringency thresholds applied. Moreover, the fold change to CPEB1 is above 2.

| Embryos | | | | | | | | | | | | | | |
|---|---|---|---|---|---|---|---|---|---|---|---|---|---|---|
| Top Ptbp1 Candidates with coverage above 40% | | | | | | | | | | | | | | |
| UniProt Accession | gene name | IEP | Mw Da | uninjected | FLAG-GFP | FLAG-CPEB1 | FLAG-Ptbp1 | F-GFP/Uninjected | F-CPEB1/uninjected | F-Ptbp1/uninjected | F-CPEB1/F-GFP | F-Ptbp1/F-GFP | F-CPEB1/F-Ptbp1 | F-Ptbp1/F-CPEB1 |
| Q2TAV5 | ilf3 | 8.73 | 98752 | | | | 40.72 | Div0 | Div0 | Div0 | Div0 | Div0 | 0.00 | Div0 |
| H1A8Z1 | RRM1 | 6.32 | 91749 | | | | 9.29 | Div0 | Div0 | Div0 | Div0 | Div0 | 0.00 | Div0 |
| Q6DEB0 | pdha1 | 7.69 | 45195 | 0.66 | 1.39 | | 110.42 | 2.11 | 0.00 | Div0 | 0.00 | 79.47 | 0.00 | Div0 |
| Q6AX83 | lars | 6.65 | 135303 | 1.32 | 1.96 | 6.59 | 68.71 | 1.48 | 5.00 | 52.11 | 3.37 | 35.14 | 0.10 | 10.43 |
| Q6GPP0 | wdr70 | 5.83 | 69615 | 2.17 | 2.62 | 4.89 | 59.29 | 1.21 | 2.26 | 27.37 | 1.86 | 22.59 | 0.08 | 12.13 |
| Q9PSI1 | | 8.22 | 43918 | 2.93 | 2.63 | 7.81 | 38.37 | 0.90 | 2.66 | 13.08 | 2.97 | 14.59 | 0.20 | 4.92 |
| Q68EU5 | tia1 | 7.66 | 43320 | 0.75 | | 2.64 | 9.68 | 0.00 | 3.50 | 12.83 | Div0 | Div0 | 0.27 | 3.66 |
| Q640J5 | hnrnph3 | 5.87 | 37248 | 1.59 | 1.34 | 3.36 | 10.96 | 0.85 | 2.12 | 6.91 | 2.50 | 8.15 | 0.31 | 3.26 |
| Q32NK0 | myef2 | 9.58 | 71995 | 1.23 | 1.33 | 3.07 | 9.62 | 1.08 | 2.50 | 7.84 | 2.32 | 7.25 | 0.32 | 3.13 |
| Q66KI6 | pum1 | 6.36 | 128227 | 0.35 | | 3.83 | 8.34 | 0.00 | 10.99 | 23.96 | Div0 | Div0 | 0.46 | 2.18 |
| Q5U5A8 | LOC495316 | 6.56 | 121641 | 2.08 | 3.52 | 3.50 | 19.38 | 1.69 | 1.68 | 9.30 | 0.99 | 5.50 | 0.18 | 5.54 |
| Q6GQD0 | ncbp1-b | 5.85 | 93005 | | | | 13.87 | Div0 | Div0 | Div0 | Div0 | Div0 | 0.00 | Div0 |
| Q9PT63 | ckap5 | 8.03 | 229988 | 3.51 | 6.98 | 12.77 | 169.27 | 1.99 | 3.64 | 48.20 | 1.83 | 24.25 | 0.08 | 13.25 |

**Table S.4. Selected top CPEB1 and Ptbp1 common candidates for the embryo sample.** The stringency thresholds are the pulled down amount (>5ng) and sequence coverage (>40%).

| Embryos | | | | | | | | | | | | | |
|---|---|---|---|---|---|---|---|---|---|---|---|---|---|
| Top CPEB1 and Ptbp1 Common Candidates | | | | | | | | | | | | | |
| UniProt Accession | gene name | IEP | Mw Da | uninjected | FLAG-GFP | FLAG-CPEB1 | FLAG-Ptbp1 | F-GFP/Uninjected | F-CPEB1/uninjected | F-Ptbp1/uninjected | F-CPEB1/F-GFP | F-Ptbp1/F-GFP | F-CPEB1/F-Ptbp1 | F-Ptbp1/F-CPEB1 |
| Q8AVV2 | eif4a2 | 9.02 | 30765 | | | 11.07 | 4.57 | Div0 | Div0 | Div0 | Div0 | Div0 | 2.42 | 0.41 |
| Q6EE38 | | 10.9 | 26891 | | | 8.71 | 2.90 | Div0 | Div0 | Div0 | Div0 | Div0 | 3.00 | 0.33 |
| Q7ZXB4 | ptbp1 | 9.3 | 59471 | | | 3.65 | 11.36 | Div0 | Div0 | Div0 | Div0 | Div0 | 0.32 | 3.11 |
| Q1JQ73 | elavl1-a | 9.05 | 37427 | | | 1.69 | 8.34 | Div0 | Div0 | Div0 | Div0 | Div0 | 0.20 | 4.94 |

**Table S.5. Selected top candidates for the oocyte series.** The stringency thresholds previously described apply.

**Oocytes**

**Top CPEB1 candidates**

| UniProt Accession | gene name | IEP | Mw Da | uninjected | FLAG-CPEB1 | FLAG-Ptbp1 | F-CPEB1/uninjected | F-Ptbp1/uninjected | F-CPEB1/F-Ptbp1 | F-Ptbp1/F-CPEB1 |
|---|---|---|---|---|---|---|---|---|---|---|
| A3KMT2 | dapl1-a | 10.5 | 12584 | | 7.39 | | Div0 | Div0 | Div0 | 0.00 |
| O93400 | actb | 5.15 | 42109 | | 21.65 | | Div0 | Div0 | Div0 | 0.00 |
| Q4QR39 | psmc6 | 7.27 | 44433 | | 10.98 | | Div0 | Div0 | Div0 | 0.00 |
| Q6AZV2 | gcdh | 8.26 | 48969 | 8.61 | Div0 | 6.72 | 48.36 | 0.78 | 61.99 | 0.02 |
| Q9W799 | cpsf2 | 4.81 | 89842 | 0.87 | 6.47 | 1.59 | 7.47 | 1.84 | 4.06 | 0.25 |
| Q7ZYV9 | sympk | 5.36 | 135193 | 2.43 | 27.95 | 12.01 | 11.51 | 4.94 | 2.33 | 0.43 |
| Q2NLA5 | LOC734179 | 6.92 | 88254 | 2.30 | 17.20 | 2.05 | 7.50 | 0.89 | 8.38 | 0.12 |
| Q6PF26 | qars | 6.76 | 88269 | 4.15 | 27.46 | 3.04 | 6.62 | 0.73 | 9.03 | 0.11 |

**Top Ptbp1 Candidates**

| UniProt Accession | gene name | IEP | Mw Da | uninjected | FLAG-CPEB1 | FLAG-Ptbp1 | F-CPEB1/uninjected | F-Ptbp1/uninjected | F-CPEB1/F-Ptbp1 | F-Ptbp1/F-CPEB1 |
|---|---|---|---|---|---|---|---|---|---|---|
| Q5U5C2 | vars | 7.13 | 142176 | 51.63 | 21.53 | 206.80 | 0.42 | 4.01 | 0.10 | 9.61 |
| Q5U259 | elavl1-b | 8.82 | 36236 | | 1.36 | 6.10 | Div0 | Div0 | 0.22 | 4.50 |
| Q7ZY29 | esrp1 | 5.95 | 77339 | | 0.68 | 7.76 | Div0 | Div0 | 0.09 | 11.34 |
| Q5U528 | gtpbp10 | 9.17 | 42409 | 0.97 | 0.74 | 34.67 | 0.75 | 35.57 | 0.02 | 47.16 |
| Q9YGP5 | rbpms | 9.01 | 21733 | | | 9.57 | Div0 | Div0 | 0.00 | Div0 |
| Q5XHI1 | mrpl3 | 9.76 | 38395 | 0.54 | | 28.70 | 0.00 | 53.28 | 0.00 | Div0 |
| Q6DJE0 | sec23b | 6.23 | 84057 | 0.83 | 1.15 | 6.57 | 1.38 | 7.92 | 0.17 | 5.73 |

**Top CPEB1 and Ptbp1 candidates**

| UniProt Accession | gene name | IEP | mwDa | uninjected | FLAG-CPEB1 | FLAG-Ptbp1 | F-CPEB1/uninjected | F-Ptbp1/uninjected | F-CPEB1/F-Ptbp1 | F-Ptbp1/F-CPEB1 |
|---|---|---|---|---|---|---|---|---|---|---|
| A2BD83 | paf1 | 4.29 | 59776 | | 5.66 | 5.12 | Div0 | Div0 | 1.11 | 0.90 |
| Q5FWY4 | mmcm6 | 4.95 | 93552 | | 6.18 | 6.92 | Div0 | Div0 | 0.89 | 1.12 |
| Q7SZ11 | | 7.64 | 38517 | 0.29 | 4.01 | 4.10 | 13.79 | 14.12 | 0.98 | 1.02 |